UNIVERSIDAD EUROPEA DE MADRID

ESCUELA DE ARQUITECTURA, INGENIERÍA Y DISEÑO

DEGREE IN AEROSPACE ENGINEERING

FINAL PROJECT DEGREE REPORT

AIRFOIL AND WING NUMERICAL ANALYSIS FOR THE IMPROVEMENT OF AN UAV DESIGN

MARÍA DEL MAR ARENAS PÉREZ

YEAR 2022-2023

.

TITLE: AIRFOIL AND WING NUMERICAL ANALYSIS FOR THE IMPROVEMENT OF AN UAV DESIGN

AUTHOR: MARÍA DEL MAR ARENAS PÉREZ

SUPERVISOR: DANIEL GONZÁLEZ JUÁREZ

DEGREE OR COURSE: AEROSPACE ENGINEERING IN AIRCRAFTS

DATE: 9TH December 2022

.

.

ABSTRACT

As far as aviation is concerned, there are several airfoils and wings according the properties needed for the aircraft to fly with the best qualities and conditions possible, then this project is made in order to analyze and calculate the proper airfoil and wing for a purpose in specific.

The mentioned purpose is to create an UAV properly to help in saving lives in the strait of Gibraltar, as there are so many people trying to cross it to hopeful have a better life than they had in their birth countries.

The intended function for this UAV is to supervise these people in the dinghies through the ISR (Intelligence, Surveillance and Reconnaissance) system, and in case they needed help a drop-down boat would be launched to them while the rescue services from Cruz Roja arrives.

The way to approach this project is to realize a comparative of lift and moment coefficients of the chosen NACA 2412 obtained by three different ways:

- Analytical general solution from Joukowsky transformation.
- Numerical modeling by finite elements in Ansys Fluent.
- Scale model impressed in 3D with its consequently wind tunnel test at Universidad Europea de Madrid, using different speed ranges and angles of attack in order to obtain the lift experimental curve Cl-α.

Next is to extrapolate the results from the airfoil analysis to the possible application of mentioned airfoil to an unmanned aerial vehicle, analyzing the effect that could take the entire structure to the lift and drag generated.

This prototype is being analyzed by the finite element method via Ansys, to contrarrest the obtained values with the airfoil analysis and with the complete UAV in order to obtain the possible existent correlations between both cases (unmanned aerial vehicle and only the airfoil).

Finally is the designing of the UAV. Catia is an useful tool to carry this job. From the wing design that was carried before, the rest of the aircraft is design proportionally, starting with the fuselage, tail and next the study of the propellers in order to have the best autonomy.

The result from the UAV Catia design is introduced in Ansys to check its aerodynamic properties, to later show how profitable it is to the mentioned purpose of the project.

Keywords: NACA 2412, wind tunnel, Ansys, UAV, drone.

.

RESUMEN

En lo que respecta a la aviación, hay muchos perfiles aerodinámicos y alas de acuerdo con las propiedades necesarias para que la aeronave vuele con las mejores cualidades y condiciones posibles, por lo que este proyecto se realiza para analizar y calcular el perfil aerodinámico y el ala adecuados para un propósito específico.

El propósito mencionado es crear un UAV para ayudar a salvar vidas en el estrecho de Gibraltar, ya que hay muchas personas que intentan cruzarlo con la esperanza de tener una vida mejor que la que tenían en sus países de origen.

La función prevista para este UAV es supervisar a estas personas en los botes a través del sistema ISR (Inteligencia, Vigilancia y Reconocimiento), y en caso de que necesitaran ayuda se les lanzaría un barco desplegable mientras llegan los servicios de rescate de Cruz Roja.

La forma de empezar este proyecto consiste en realizar una comparativa de los coeficientes de sustentación y de momentos de un perfil NACA 2412 obtenidos por 3 métodos distintos:

- Mediante la solución analítica general a partir de la transformación de Joukowsky
- Mediante una modelización numérica por elementos finitos en el ANSYS FLUENT.
- Mediante un modelo a escala impreso en 3D con un posterior ensayo en el túnel de viento de la Universidad Europea de Madrid, a distintos rangos de velocidades y ángulos de ataque para obtener la curva de sustentación experimental Cl-α.

Por otro lado, se extrapolan los resultados del análisis del perfil solo, a la posible aplicación de ese mismo perfil a un vehículo no tripulado, analizando el posible efecto que tenga el resto de la estructura a la sustentación y el arrastre.

Este modelo se analizará mediante métodos numéricos de Elementos finitos vía ANSYS, para contrarrestar los valores obtenidos en el análisis del ala sola, con el vehículo no tripulado al completo, y obtener las posibles correlaciones existentes entre ambos casos (vehículo completo y ala sola).

Finalmente está el diseño del UAV. Catia es una herramienta útil para llevar a cabo este trabajo. A partir del diseño del ala que se realizó anteriormente, el resto de la aeronave se diseña proporcionalmente, comenzando por el fuselaje, la cola y luego el estudio de las hélices para tener la mejor autonomía.

El resultado del diseño del UAV realizado en Catia se introduce en ANSYS para comprobar sus propiedades aerodinámicas, para posteriormente mostrar lo rentable que es para el propósito mencionado del proyecto.

Palabras clave: NACA 2412, túnel viento, ANSYS, UAV, dron.

.

ACKNOWLEDGEMENTS

I am very grateful for all the support I received through all these years during college, but specially to my family that raised me and always believed in me even though sometimes lost the hope, I owe them everything.

I want to thank my classmates making a good environment in class instead of a competence, they always offered their help when a task was tough, or in the period exams, without them I would not have come this far.

All the professor that encouraged me and taught me and transmitted all the passion they feel to the aviation field, I will always remember them. I want to give a shout out to my tutor Daniel that accepted my project without hesitation and helped me in the wind tunnel test along Alberto.

These have been very delightful years where I met incredible people and they are part of me now. Hopefully everyone of them goes well in their professional and personal lives.

.

Contents

.

.

Figures

.

.

.

Tables

.

Chapter 1. INTRODUCTION

UAV stands for Unmanned Aerial Vehicle; its meaning following the encyclopaedia is "powered, aerial vehicle that does not carry a human operator, uses aerodynamic forces to provide vehicle lift, can fly autonomously or be piloted remotely, can be expendable or recoverable, and can carry a lethal or nonlethal payload"[1]

It exists for a wide range of objectives in the aviation field. Commonly known for its military missions from the several countries air forces, as sending confidential information or fighting in dangerous situations. [2]

This time the mission of the UAV that has been designed is completely the opposite as mentioned before. It has been created to help people to cross the stretch of Gibraltar with the help of an ISR system.

As there is no information publicly because of its military principal functions, a study for the airfoil and wing has been made to search the most adequate final one. It was necessary to search the most aerodynamic airfoils as this mission requires.

Exist many different types of airfoil then a study is made from the commercial NACA airfoils to later create the wing design and implement the mentioned wing in a UAV. The UAV is also designed to make sure it complies with the project mission.

The aim of the project is to realize a comparative of lift and moment coefficients of the chosen NACA 2412 obtained by three different ways of analytical general solution from Joukowsky transformation, numerical modeling by finite elements in Ansys Fluent and scale model impressed in 3D with its consequently wind tunnel test at Universidad Europea de Madrid, using different speed ranges and angles of attack in order to obtain the lift experimental curve Cl-α

Next is to extrapolate the results from the airfoil analysis to the possible application of mentioned airfoil to an unmanned aerial vehicle, analysing the effect that could take the entire structure to the lift and drag generated.

This prototype is being analysed by the finite element method vía Ansys, to contrarrest the obtained values with the airfoil analysis and with the complete UAV in order to obtain the possibles existent correlations between both cases (UAV and only the airfoil).

The main objectives of this project are:

- Obtaining the lift coefficient from an analytical way.
- Obtaining the lift coefficient from a numerical way with the finite element method.
- Obtaining the lift coefficient from an experimental way in wind tunnel test with a prototype scale.
- Values comparative and validation range along the airfoil data, Ansys CFD and wind tunnel tests.
- Real application of the required UAV.

.

Chapter 2. BACKGROUND, STATE OF THE ART

The UAVs are used for many different missions, the most common is for military issues. The objective for this project is to use UAV to the opposite missions that uses the air forces. The mentioned aim is to save people from the sea, specifically from the stretch of Gibraltar.

Nowadays the people in charge for this purpose are the rescue services, but their vigilance are not as effective as possible due to meteorologic conditions, for example. With this UAV the supervision could be able during the whole time and their message transmission would be instantaneously. Also, it will count with diurnal and nocturnal sensors to locate the people. [3]

There is some UAV also in charge of people from the narcotraffic, as they are able to send the material with no impediment but the radars. Now the national police have requested to use one of the UAV extracted from the narcotraffic people to combat their objective and have this new object working in their side.

Therefore, if the judiciary and law enforcement bodies realized that implementing this tool to fight against this issue is helpful, then also might have their vision in using these UAV for other purposes, as search and rescue people. [4]

Also the UAVs used for the narcotraffic are little and with low endurance plus they need a person to control them, therefore this UAV will be more effective and it has a higher endurance, service ceiling and range, self-sufficient (except when the batteries has to be charged and fill the fuel tank) among other qualities.

.

Chapter 3. THEORETICAL BASIS FOR THE THEORETICAL LIFT COEFFICIENT ESTIMATION.

Aerodynamics are the part from fluid mechanics that follow the study between the body and the fluids around it. In this case, the air is the chosen fluid, and the study will be done with a wide range of different speeds.[5]

It is important to take into account that the best aerodynamic efficiency takes place the higher the altitude and speed are because of the decrease of the pressure.

As the aircraft must overcome its weight and produce more lift to counteract and therefore it can fly, (mentioned amount of lift is produced mostly by its wings), it is necessary to introduce the forces that exits in every aircraft:

- Lift: is the amount of force that the aircraft must produce in order to fly. As mentioned before, the wings are the ones that create most of this lift force. This is due to the variation of pressures that are produced between the upper and low surfaces of the wing.

- Drag: this force is opponent to the movement of the aircraft through the air and must be counteracted with the thrust produced with the engines of the aircraft. As the speed is increased, the drag also gets higher, therefore it always is going to be a positive force with a parabolic result in its graphs.

- Weight: it is produced due to the gravitational force, as every body that has a mass it is attracted to the earth. The weight is compound by all the elements on the aircraft, like its structure, engines, wings, etc. To do the calculations, the centre of mass is chosen in order to have a stabilized aircraft while flying.

- Thrust: it is the component that produces a propulsive force and therefore, counteract the drag and impulse the aircraft forward while it operates. The thrust is produced by the engines of the aircraft, and it can be located on the nose, wings or the end of the airplane. [6]

In the next figure is represented graphically the principal forces that occur in every aircraft along its different components.

This guide is to visualize how the forces act in the aircraft at a determine angle of attack. Also it marks the way that flight path and relative wind go.

.
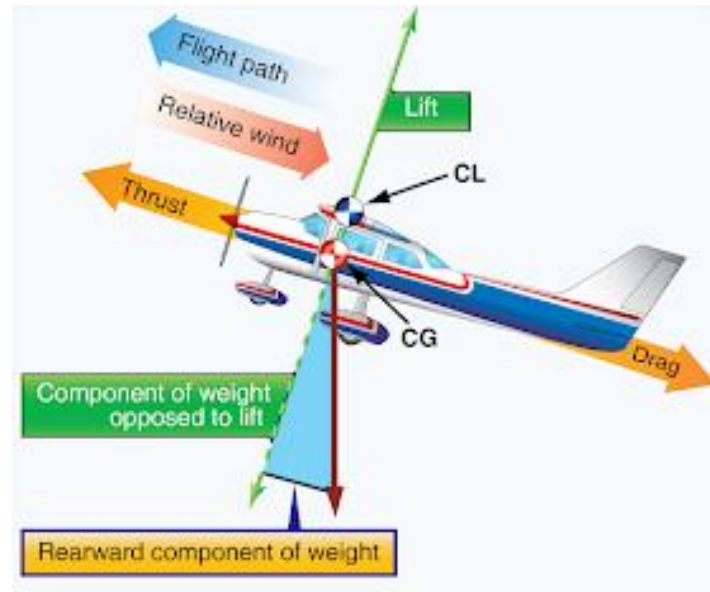
Figure 1 The principal forces of the aircraft 7

In order to determine the best proper aerodynamic airfoil for the design of the wing, it is necessary to have the knowledge of the following basic concepts:

1. Aerodynamic centre: it is defined as the point where the angle of attach is independent from the aerodynamic moment, and also, as the font says "its presence is plotted in all standard NACA wind tunnel test graphs, where its consequence can be seen as the pitching moment curve that is constant over almost the entire α-sweep range. If the slope of the lift curve, Clα, and the pitching moment of the quarter chord, Cmαc/4, are known, the aerodynamic centre can be computed". [8]

$$\frac{dCM}{dCL} = 0$$

   That is the reason why it is considered necessary to test the final wing made in scale into the wind tunnel. These step and results are better explained in the following points.

2. Pitching moment: it is the aerodynamic centre of the airfoil although it is needed to be read at the quart chord of the airfoil behind the leading edge to have a better stabilization and control of the final wing. [9]

$$Cm = \frac{M}{qSc}$$

17

.

3. Centre of pressure is the point where all the pressures of the body are sum up and equals to zero. As the lift coefficient increases, the pressure of centre tends to go forward in the leading direction of the aircraft. [10]

$$x_{Cp} = \frac{C}{4} \cdot \left[1 + \frac{\pi}{Cl} \cdot (A_1 - A_2) \right]$$

A1 and A2 will be determined in the following chapter 4.

4. Chord: it is a line that unify the leading edge point and its curvature centre with the trailing edge point of the airfoil. It is used to calculate with better prediction the pitching moment. [11]

In the next figure is represented graphically the chord section:
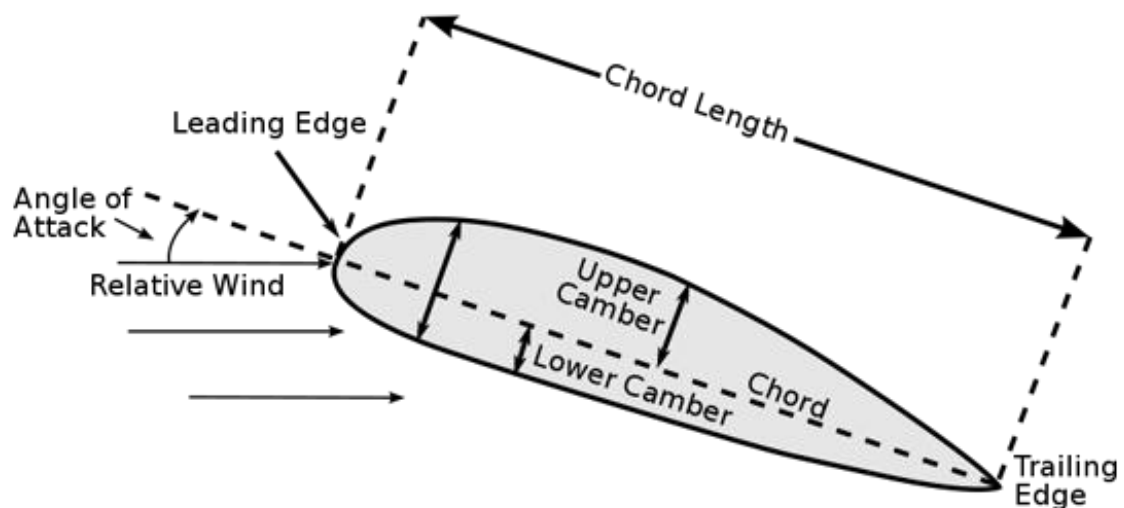
Figure 2 Chord representation graphically 12

5. Lift Coefficient: it is the product that relates the lift according to the density of the air at the altitude which the body is flying with the speed and surface of the wing. It is a dimensionless quantity, and it helps to identify the lift the wing has through the variables of shape, inclination and the flow that has around the airfoil. [13]

$$Cl = \frac{2L}{\rho S u^2}$$

.

6. Drag Coefficient: it is a dimensionless unit that indicates the aerodynamic drag that suffers the airfoil through a determined conditions as it is related with the speed, the flow that happens through the surface of the wing, the density of the air and the position that the object is found. Its formula is similar to the lift coefficient. [14]

$$Cd = \frac{2D}{\rho S u^2}$$

To carry out the analysis of the different airfoil, it is indispensable to find out its lift coefficient and drag coefficient.

Next is to introduce some adequate NACA airfoil for the project purpose wing in the Wolfram Mathematica program, that will be compound from 4 digits and resolve its unknowns' variables as the lift and drag coefficients, and adding the aerodynamic centre moment, leading edge coefficient, aerodynamic centre and centre of pressure.

The study of the airfoil will be done with the results from the variables found mentioned before, and from that point with the chosen NACA airfoil, the wing design will be carried out.

.

Chapter 4. CL VALUES PREDICTION TO ANY 4 DIGITS. NACA 2412 APPLICATION.

NACA refers to the National Advisory Committee for Aeronautics, and it is the most used series of airfoil in the aviation field.

Exit many types of NACA, 4 digits or 5 digits are the most famous and commonly employed. For this project the study is being made for the NACA of 4 digits because it is easy to calculate as well as it presents good results concerning stall conditions. [15]

Next is represented mathematically the calculation of the 4 digits NACA airfoil with examples at the next points.

4.1 General equations to the middle chord to any 4 digit. NACA MPTT

The digits from a 4 digit NACA profile are read as:

- 1st digit: It is the chord percentage curvature - For a symmetrical profile the M equals to 0.
- 2nd digit: It is the position of maximum bend in tenths of the chord.
- 3rd and 4th digit: They are the maximum thickness in percentage of the chord.

In general, the NACA profiles are divided in two sections. They can be extended to the next unit expression:

- **SECTION 1 - 0 <= X/c <= P/10**

$$\frac{z1}{c} = \frac{M}{P^2} \cdot \left[\frac{2P}{10} \cdot \left(\frac{x}{c} \right) - \left(\frac{x}{c} \right)^2 \right]$$

- **SECTION 2 - P/10 <= x/c <= 1**

$$\frac{z2}{c} = \frac{M}{(10 - P)^2} \cdot \left[\left(1 - \frac{2P}{10} \right) + \frac{2P}{10} \cdot \left(\frac{x}{c} \right) - \left(\frac{x}{c} \right)^2 \right]$$

.

The following drawing shows the different elements existent on a NACA airfoil, standing our the leading edge and trailing edge is situated, along the measures that are used regarding the maximum thickness and maximum camber of the airfoil.
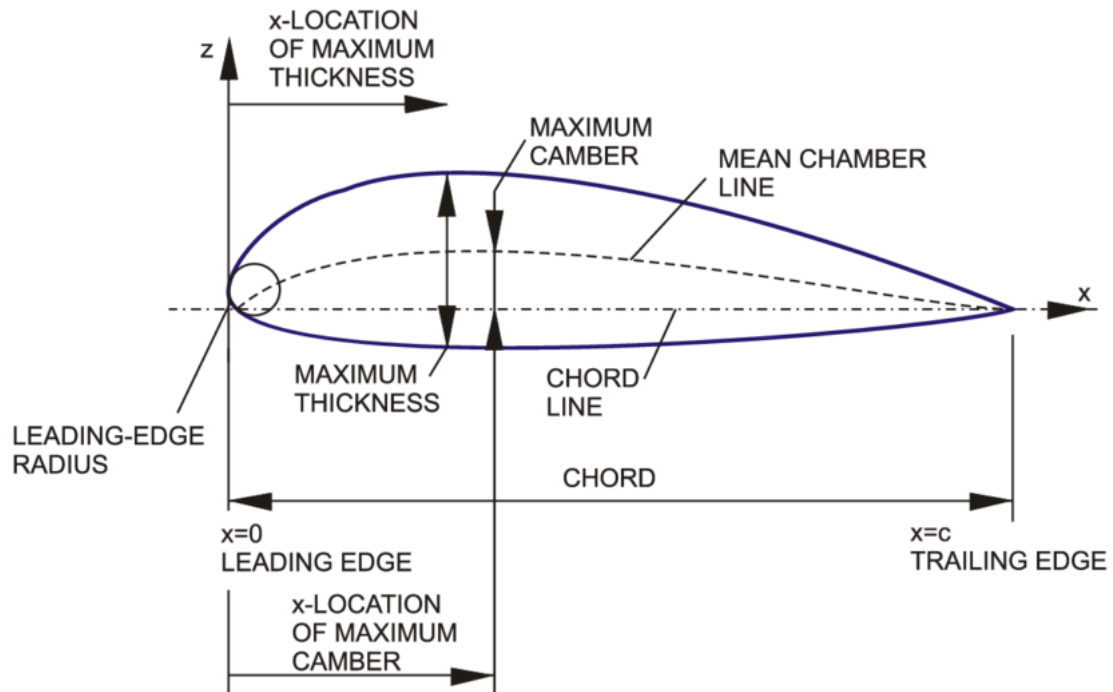
Figure 3 NACA drawing explanation 16

.

4.2 Theoretical lift coefficient procurement.

In order to obtain the coefficients of theoretical lift, the chord derivatives must be integrated in function of the θ variable. This variable corresponds to the angular variable defined in C/2.

By the derivation of the expressions, the following equations are achieved:

- First chord section derivation:

$$\frac{D}{Dx}\left(\frac{z1}{c}\right) = \frac{D}{Dx}\left(\frac{M}{P^2} \cdot \left[\frac{2P}{10} \cdot \left(\frac{x}{c}\right) - \left(\frac{x}{c}\right)^2\right]\right)$$

$$\frac{D}{Dx}\left(\frac{z1}{c}\right) = \frac{M}{P^2} \cdot \left[\frac{2P}{10} \cdot \left(\frac{1}{c}\right) - 2\left(\frac{x}{c}\right)\left(\frac{1}{c}\right)\right]$$

$$\frac{D}{Dx}\left(\frac{z1}{c}\right) = \frac{M}{P \cdot c \cdot 5} - \frac{2M \cdot x}{P^2 \cdot c^2}$$

- Second chord section derivation:

$$\frac{D}{Dx}\left(\frac{z2}{c}\right) = \frac{D}{Dx}\left(\frac{M}{(10-P)^2} \cdot \left[\left(1 - \frac{2P}{10}\right) + \frac{2P}{10} \cdot \left(\frac{x}{c}\right) - \left(\frac{x}{c}\right)^2\right]\right)$$

$$\frac{D}{Dx}\left(\frac{z2}{c}\right) = \frac{M}{(10-P)^2} \cdot \left[\frac{2P}{10} \cdot \left(\frac{1}{c}\right) - 2 \cdot \left(\frac{x}{c}\right) \cdot \left(\frac{1}{c}\right)\right]$$

$$\frac{D}{Dx}\left(\frac{z2}{c}\right) = \frac{2M \cdot P}{10c \cdot (10-P)^2} - \frac{2M \cdot x}{c^2 \cdot (10-P)^2}$$

Executing the following variable change:

$$x = \frac{c}{2} \cdot \left(1 - Cos(\theta)\right)$$

.

The substitution is realized in the next equation:

$$\frac{D}{Dx}\left(\frac{z1}{c}\right) = \frac{M}{P \cdot c \cdot 5} - \frac{2M}{P^2 \cdot c^2} \cdot \frac{c}{2} \cdot \left(1 - Cos(\theta)\right)$$

$$\frac{D}{Dx}\left(\frac{z1}{c}\right) = \frac{M}{P \cdot c}\left(\frac{1}{5} - \frac{1}{P} \cdot \left(1 - Cos(\theta)\right)\right)$$

$$\frac{D}{Dx}\left(\frac{z1}{c}\right) = \frac{M}{P \cdot c}\left(\frac{1}{5} - \frac{1}{P} + \frac{Cos(\theta)}{P}\right)$$

$$\frac{D}{Dx}\left(\frac{z1}{c}\right) = \frac{M}{P \cdot c}\left(\frac{1}{5} - \frac{1}{P} + \frac{Cos(\theta)}{P}\right)$$

$$\frac{D}{Dx}(z1) = \frac{M}{P}\left(\frac{1}{5} - \frac{1}{P} + \frac{Cos(\theta)}{P}\right)$$

In an analogous path, the second chord derivative is carried out:

$$\frac{D}{Dx}\left(\frac{z2}{c}\right) = \frac{2M \cdot P}{10c \cdot (10 - P)^2} - \frac{2M}{c^2 \cdot (10 - P)^2} \cdot \frac{c}{2} \cdot \left(1 - Cos(\theta)\right)$$

$$\frac{D}{Dx}\left(\frac{z2}{c}\right) = \frac{M \cdot P}{5c \cdot (10 - P)^2} - \frac{M}{c \cdot (10 - P)^2} \cdot \left(1 - Cos(\theta)\right)$$

$$\frac{D}{Dx}\left(\frac{z2}{c}\right) = \frac{M}{c \cdot (10 - P)^2}\left(\frac{P}{5} - 1 + Cos(\theta)\right)$$

$$\frac{D}{Dx}(z2) = \frac{M}{(10 - P)^2}\left(\frac{P}{5} - 1 + Cos(\theta)\right)$$

.

The continuous step is to substitute the integration limits in each section. For the first section:

$$0 \leq \frac{x}{c} \leq \frac{P}{10}$$

Taking into account that the adimensional variable x/c goes from 0 to 1, the variable θ goes from 0 to π.

$$x = \frac{c}{2} \cdot (1 - Cos(\theta))$$

$$\frac{x}{c} = \frac{1}{2} \cdot (1 - Cos(\theta))$$

$$\frac{P}{10} = \frac{1}{2} \cdot (1 - Cos(\theta))$$

$$\frac{P}{5} = 1 - Cos(\theta)$$

$$Cos(\theta) = 1 - \frac{P}{5}$$

In consequence the angle that separates the first section from the second section is:

$$\theta 1 = ArcCos\left(1 - \frac{P}{5}\right)$$

Therefore the integration limits are:

- Tramo 1:

$$0 \leq \theta \leq ArcCos\left(1 - \frac{P}{5}\right)$$

- Tramo 2:

$$ArcCos\left(1 - \frac{P}{5}\right) \leq \theta \leq \pi$$

.

Once the values from the integration limits are obtained, the values A0, A1 and A2 will be defined:

$$A_0 = \alpha - \frac{1}{\pi} \int_0^\pi \frac{dz}{dx} d\theta$$

$$A_n = \frac{2}{\pi} \int_0^\pi \frac{dz}{dx} \cdot \cos\cos(n \cdot \theta) \cdot d\theta$$

Applying the A0 value, the next result is achieved:

$$A_0 = \alpha - \frac{1}{\pi} * \left(\int_0^{ArcCos\left(1-\frac{P}{5}\right)} \frac{d(z1)}{dx} \cdot d\theta + \int_{ArcCos\left(1-\frac{P}{5}\right)}^{\pi} \frac{d(z2)}{dx} \cdot d\theta \right)$$

$$A_0 = \alpha - \frac{1}{\pi} * \left(\int_0^{ArcCos\left(1-\frac{P}{5}\right)} \frac{M}{P}\left(\frac{1}{5} - \frac{1}{P} + \frac{Cos(\theta)}{P}\right) \cdot d\theta + \int_{ArcCos\left(1-\frac{P}{5}\right)}^{\pi} \frac{M}{(10-P)^2}\left(\frac{P}{5} - 1 + Cos(\theta)\right) \cdot d\theta \right)$$

$$A_0 = \alpha - \frac{1}{\pi} * \left(\frac{M}{P} \int_0^{ArcCos\left(1-\frac{P}{5}\right)} \left(\frac{1}{5} - \frac{1}{P} + \frac{Cos(\theta)}{P}\right) \cdot d\theta + \frac{M}{(10-P)^2} \int_{ArcCos\left(1-\frac{P}{5}\right)}^{\pi} \left(\frac{P}{5} - 1 + Cos(\theta)\right) \cdot d\theta \right)$$

$$A_0 = \alpha - \frac{1}{\pi} * \left(\frac{M}{P} \int_0^{ArcCos\left(1-\frac{P}{5}\right)} \left(\frac{1}{5} - \frac{1}{P} + \frac{Cos(\theta)}{P}\right) \cdot d\theta + \frac{M}{(10-P)^2} \int_{ArcCos\left(1-\frac{P}{5}\right)}^{\pi} \left(\frac{P}{5} - 1 + Cos(\theta)\right) \cdot d\theta \right)$$

$$A_0 = \alpha - \frac{1}{\pi} * \frac{M}{P} \cdot \left(\left(\frac{1}{5} - \frac{1}{P}\right)\theta - \frac{Sin(\theta)}{P} \right)_0^{ArcCos\left(1-\frac{P}{5}\right)} - \frac{1}{\pi} \cdot \frac{M}{(10-P)^2} \left(\left(\frac{P}{5} - 1\right) \cdot \theta - Sin(\theta) \right)_{ArcCos\left(1-\frac{P}{5}\right)}^{\pi}$$

25

.

In a kindred path, the values A1 and A2 are also obtained

$$A_1 = \frac{2}{\pi} * \left(\int_0^{ArcCos\left(1-\frac{P}{5}\right)} \frac{M}{P}\left(\frac{1}{5} - \frac{1}{P} + \frac{Cos(\theta)}{P}\right) Cos(\theta) \cdot d\theta + \int_{ArcCos\left(1-\frac{P}{5}\right)}^{\pi} \frac{M}{(10-P)^2}\left(\frac{P}{5} - 1 + Cos(\theta)\right) \cdot Cos(\theta) \cdot d\theta \right)$$

$$A_2 = \frac{2}{\pi} * \left(\int_0^{ArcCos\left(1-\frac{P}{5}\right)} \frac{M}{P}\left(\frac{1}{5} - \frac{1}{P} + \frac{Cos(\theta)}{P}\right) Cos(2\theta) \cdot d\theta + \int_{ArcCos\left(1-\frac{P}{5}\right)}^{\pi} \frac{M}{(10-P)^2}\left(\frac{P}{5} - 1 + Cos(\theta)\right) \cdot Cos(2\theta) \cdot d\theta \right)$$

Finally, to obtain the lift coefficient Cl, the following expression is used:

$$C_L = 2 \cdot \pi \cdot \left(A_0 + \frac{A_1}{2} \right)^{17}$$

By substituting the expressions, the Cl is obtained in the 4 digits NACA profile parameters function, as well as the angle of attack:

$$C_L = 2 \cdot \pi \cdot \left(\alpha - \frac{1}{\pi} * \left(\frac{M}{P} \int_0^{ArcCos\left(1-\frac{P}{5}\right)} \left(\frac{1}{5} - \frac{1}{P} + \frac{Cos(\theta)}{P}\right) \cdot d\theta + \frac{M}{(10-P)^2} \int_{ArcCos\left(1-\frac{P}{5}\right)}^{\pi} \left(\frac{P}{5} - 1 + Cos(\theta)\right) \cdot d\theta \right) \right.$$

$$\left. + \frac{1}{2} \left(\frac{2}{\pi} * \left(\int_0^{ArcCos\left(1-\frac{P}{5}\right)} \frac{M}{P}\left(\frac{1}{5} - \frac{1}{P} + \frac{Cos(\theta)}{P}\right) Cos(\theta) \cdot d\theta + \int_{ArcCos\left(1-\frac{P}{5}\right)}^{\pi} \frac{M}{(10-P)^2}\left(\frac{P}{5} - 1 + Cos(\theta)\right) \cdot Cos(\theta) \cdot d\theta \right) \right) \right)$$

In equal procedure, by substituting the coefficients A0, A1 and A2 the following aerodynamic coefficients are acquired:

- Moment coefficient in C/4 (theoretical position in the aerodynamic centre):

$$Cm,_{\frac{C}{4}} = \frac{\pi}{4} \cdot (A_2 - A_1)$$

- Theoretical position of pressure centre:

$$x_{Cp} = \frac{C}{4} \cdot \left[1 + \frac{\pi}{Cl} \cdot (A_1 - A_2) \right]$$

- Moment coefficient at leading edge:

$$Cm,_{Le} = -\left(\frac{CL}{4} + \frac{\pi}{4} \cdot (A_1 - A_2) \right)$$

.

4.3   Theoretical modelation to the 4 digits NACA profiles.

Due to the ability of being able to parametric every theoretical estimation from a 4 digit NACA profile, it has been chosen the programming of mentioned variables in the Wolfram Mathematica Software.

By way of application of the chosen NACA, the following profile, the following results are achieved:

- NACA 1410

DATOS PARA EL PERFIL NACA 1410

α (Ángulo de Ataque) = 0 °

C (cuerda) = 1 m

Ecuaciones del perfil:

$z1/c = 0.0625 \left(\dfrac{0.8\,x}{c} - \dfrac{1.\,x^2}{c^2} \right)$

$z2/c = 0.0277778 \left(0.2 + \dfrac{0.8\,x}{c} - \dfrac{1.\,x^2}{c^2} \right)$

PASO 1: DERIVADAS

$d(z1/c)/dx = \dfrac{0.05}{c} - \dfrac{0.125\,x}{c^2}$

$d(z2/c)/dx = \dfrac{0.0222222}{c} - \dfrac{0.0555556\,x}{c^2}$

PASO 2: CAMBIO DE VARIABLE

$x = \dfrac{1}{2}\,c\,(1 - Cos[\theta])$

PASO 3: SUSTITUIR EN LAS DERIVADAS, Y ARREGLAR

$d(z1)/dx = -0.0125 + 0.0625\,Cos[\theta]$

$d(z2)/dx = -0.00555556 + 0.0277778\,Cos[\theta]$

PASO 4: LIMITES DE INTEGRACION DE LA VARIABLE θ

I1: $\theta = [0\ ;\ 1.36944\ ]$ rad

I2: $\theta = [\ 1.36944\ ,\ \pi\ ]$ rad

PASO 5: INTEGRALES

$A0 = \alpha - 1/\pi \cdot (\int_{0}^{\theta1}(-0.0125+0.0625\,Cos[\theta])\cdot d\theta + \int_{\theta1}^{\pi}(-0.00555556+0.0277778\,Cos[\theta])\cdot d\theta) = -0.00224644$

$A1 = 2/\pi \cdot (\int_{0}^{\theta1}(-0.0125+0.0625\,Cos[\theta])\cdot Cos(\theta)\cdot d\theta + \int_{\theta1}^{\pi}(-0.00555556+0.0277778\,Cos[\theta])\cdot Cos(\theta)\cdot d\theta) = 0.0407476$

$A2 = 2/\pi \cdot (\int_{0}^{\theta1}(-0.0125+0.0625\,Cos[\theta])\cdot Cos(2\theta)\cdot d\theta + \int_{\theta1}^{\pi}(-0.00555556+0.0277778\,Cos[\theta])\cdot Cos(2\theta)\cdot d\theta) = 0.00693064$

$A0 = -0.00224644$

$A1 = 0.0407476$

$A2 = 0.00693064$

PASO 6: RESULTADOS

Cl (coef. sust) $= 2 \cdot \pi \cdot (A0 + A1/2) = 0.113897$

Cm,ac (coef. momentos centro aerod.) $= \pi/4 \cdot (A2-A1) = -0.0265598$

Cm,le (coef. momentos borde ataque) $= -[Cl/4 + \pi/4 \cdot (A1-A2)] = -0.0550341$

X,ca (centro aerodinamico) $= c/4 = 0.25$ m

X,cp (centro presiones) $= c/4 \cdot (1 - (\pi/Cl) * (A1-A2)) = 0.0168099$ m

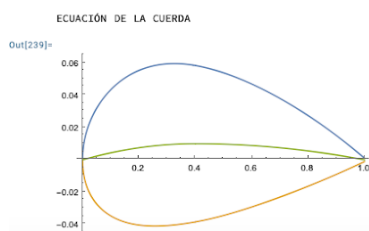ECUACIÓN DE LA CUERDA

Out[239]=

Figure 4 Characteristics of NACA 1410

.

- NACA 2412

DATOS PARA EL PERFIL NACA 2412

α (Ángulo de Ataque) = 0 °

C (cuerda) = 1 m

Ecuaciones del perfil:

$$z_1/c = 0.125 \left(\frac{0.8\,x}{c} - \frac{1.\,x^2}{c^2} \right)$$

$$z_2/c = 0.0555556 \left(0.2 + \frac{0.8\,x}{c} - \frac{1.\,x^2}{c^2} \right)$$

PASO 1: DERIVADAS

$$d(z_1/c)/dx = \frac{0.1}{c} - \frac{0.25\,x}{c^2}$$

$$d(z_2/c)/dx = \frac{0.0444444}{c} - \frac{0.111111\,x}{c^2}$$

PASO 2: CAMBIO DE VARIABLE

$$x = \frac{1}{2}\,c\,(1 - \cos[\theta])$$

PASO 3: SUSTITUIR EN LAS DERIVADAS, Y ARREGLAR

$d(z_1)/dx = -0.025 + 0.125 \cos[\theta]$

$d(z_2)/dx = -0.0111111 + 0.0555556 \cos[\theta]$

PASO 4: LIMITES DE INTEGRACION DE LA VARIABLE θ

I1: $\theta = [0 ; 1.36944]$ rad

I2: $\theta = [1.36944, \pi]$ rad

PASO 5: INTEGRALES

$A_0 = \alpha - 1/\pi \cdot \left(\int_0^{\theta_1} (-0.025 + 0.125 \cos[\theta]) \cdot d\theta + \int_{\theta_1}^{\pi} (-0.0111111 + 0.0555556 \cos[\theta]) \cdot d\theta \right) = -0.00449289$

$A_1 = 2/\pi \cdot \left(\int_0^{\theta_1} (-0.025 + 0.125 \cos[\theta]) \cdot \cos(\theta) \cdot d\theta + \int_{\theta_1}^{\pi} (-0.0111111 + 0.0555556 \cos[\theta]) \cdot \cos(\theta) \cdot d\theta \right) = 0.0814951$

$A_2 = 2/\pi \cdot \left(\int_0^{\theta_1} (-0.025 + 0.125 \cos[\theta]) \cdot \cos(2\theta) \cdot d\theta + \int_{\theta_1}^{\pi} (-0.0111111 + 0.0555556 \cos[\theta]) \cdot \cos(2\theta) \cdot d\theta \right) = 0.0138613$

$A_0 = -0.00449289$

$A_1 = 0.0814951$

$A_2 = 0.0138613$

PASO 6: RESULTADOS

Cl (coef. sust) = $2 \cdot \pi \cdot (A_0 + A_1/2)$ = 0.227795

Cm,ac (coef. momentos centro aerod.) = $\pi/4 \cdot (A_2 - A_1)$ = -0.0531195

Cm,le (coef. momentos borde ataque) = $-[Cl/4 + \pi/4 \cdot (A_1 - A_2)]$ = -0.110068

X,ca (centro aerodinamico) = c/4 = 0.25 m

X,cp (centro presiones) = $c/4 \cdot (1 - (\pi/Cl) * (A_1 - A_2))$ = 0.0168099 m

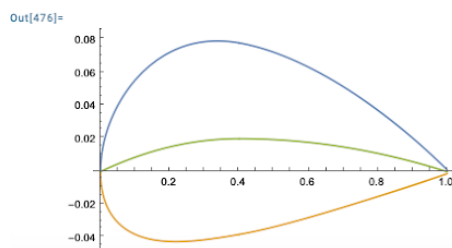ECUACIÓN DE LA CUERDA

Figure 5 Characteristics of NACA 2412

28

.

- NACA 4324

DATOS PARA EL PERFIL NACA 4424

α (Ángulo de Ataque)= 0 °

C (cuerda) = 1 m

Ecuaciones del perfil:

$$z1/c = 0.25 \left(\frac{0.8\,x}{c} - \frac{1.\,x^2}{c^2} \right)$$

$$z2/c = 0.111111 \left(0.2 + \frac{0.8\,x}{c} - \frac{1.\,x^2}{c^2} \right)$$

PASO 1: DERIVADAS

$$d(z1/c)/dx = \frac{0.2}{c} - \frac{0.5\,x}{c^2}$$

$$d(z2/c)/dx = \frac{0.0888889}{c} - \frac{0.222222\,x}{c^2}$$

PASO 2: CAMBIO DE VARIABLE

$$x = \frac{1}{2}\,c\,(1-\cos[\theta])$$

PASO 3: SUSTITUIR EN LAS DERIVADAS, Y ARREGLAR

$d(z1)/dx = -0.05 + 0.25\cos[\theta]$

$d(z2)/dx = -0.0222222 + 0.111111\cos[\theta]$

PASO 4: LIMITES DE INTEGRACION DE LA VARIABLE θ

I1: $\theta = [0 ; 1.36944]$ rad

I2: $\theta = [1.36944 , \pi]$ rad

PASO 5: INTEGRALES

$A0 = \alpha - 1/\pi \cdot (\int_0^{\theta 1}(-0.05+0.25\cos[\theta])\cdot d\theta + \int_{\theta 1}^{\pi}(-0.0222222+0.111111\cos[\theta])\cdot d\theta) = -0.00898577$

$A1 = 2/\pi \cdot (\int_0^{\theta 1}(-0.05+0.25\cos[\theta])\cdot\cos(\theta)\cdot d\theta + \int_{\theta 1}^{\pi}(-0.0222222+0.111111\cos[\theta])\cdot\cos(\theta)\cdot d\theta) = 0.16299$

$A2 = 2/\pi \cdot (\int_0^{\theta 1}(-0.05+0.25\cos[\theta])\cdot\cos(2\theta)\cdot d\theta + \int_{\theta 1}^{\pi}(-0.0222222+0.111111\cos[\theta])\cdot\cos(2\theta)\cdot d\theta) = 0.0277226$

$A0 = -0.00898577$

$A1 = 0.16299$

$A2 = 0.0277226$

PASO 6: RESULTADOS

Cl (coef. sust) = $2\cdot\pi\cdot(A0+A1/2) = 0.45559$

Cm,ac (coef. momentos centro aerod.) = $\pi/4\cdot(A2-A1) = -0.106239$

Cm,le (coef. momentos borde ataque) = $-[Cl/4 + \pi/4\cdot(A1-A2)] = -0.220136$

X,ca (centro aerodinamico) = $c/4 = 0.25$ m

X,cp (centro presiones) = $c/4\cdot(1-(\pi/Cl)*(A1-A2)) = 0.0168099$ m

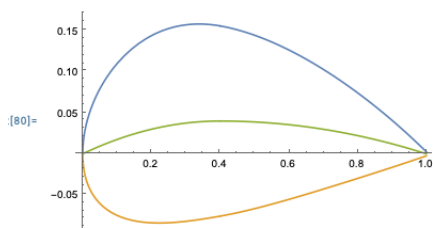ECUACIÓN DE LA CUERDA

:[80]=

Figure 6 Characteristics of NACA 4324

29

.

- NACA 4418

DATOS PARA EL PERFIL NACA 4418

α (Ángulo de Ataque)= 0 °

C (cuerda) = 1 m

Ecuaciones del perfil:

$$z1/c = 0.25 \left(\frac{0.8\,x}{c} - \frac{1.\,x^2}{c^2} \right)$$

$$z2/c = 0.111111 \left(0.2 + \frac{0.8\,x}{c} - \frac{1.\,x^2}{c^2} \right)$$

PASO 1: DERIVADAS

$$d(z1/c)/dx = \frac{0.2}{c} - \frac{0.5\,x}{c^2}$$

$$d(z2/c)/dx = \frac{0.0888889}{c} - \frac{0.222222\,x}{c^2}$$

PASO 2: CAMBIO DE VARIABLE

$$x = \frac{1}{2}\,c\,(1 - \cos[\theta])$$

PASO 3: SUSTITUIR EN LAS DERIVADAS, Y ARREGLAR

$d(z1)/dx = -0.05 + 0.25\cos[\theta]$

$d(z2)/dx = -0.0222222 + 0.111111\cos[\theta]$

PASO 4: LIMITES DE INTEGRACION DE LA VARIABLE θ

I1: θ = [0 ; 1.36944] rad

I2: θ = [1.36944 , π] rad

PASO 5: INTEGRALES

$A0 = \alpha - 1/\pi \cdot \left(\int_{0}^{\theta 1}(-0.05+0.25\cos[\theta]) \cdot d\theta + \int_{\theta 1}^{\pi}(-0.0222222+0.111111\cos[\theta]) \cdot d\theta \right) = -0.00898577$

$A1 = 2/\pi \cdot \left(\int_{0}^{\theta 1}(-0.05+0.25\cos[\theta]) \cdot \cos(\theta) \cdot d\theta + \int_{\theta 1}^{\pi}(-0.0222222+0.111111\cos[\theta]) \cdot \cos(\theta) \cdot d\theta \right) = 0.16299$

$A2 = 2/\pi \cdot \left(\int_{0}^{\theta 1}(-0.05+0.25\cos[\theta]) \cdot \cos(2\theta) \cdot d\theta + \int_{\theta 1}^{\pi}(-0.0222222+0.111111\cos[\theta]) \cdot \cos(2\theta) \cdot d\theta \right) = 0.0277226$

$A0 = -0.00898577$

$A1 = 0.16299$

$A2 = 0.0277226$

PASO 6: RESULTADOS

Cl (coef. sust) = $2 \cdot \pi \cdot (A0 + A1/2)$ = 0.45559

Cm,ac (coef. momentos centro aerod.) = $\pi/4 \cdot (A2 - A1)$ = -0.106239

Cm,le (coef. momentos borde ataque) = $-[Cl/4 + \pi/4 \cdot (A1 - A2)]$ = -0.220136

X,ca (centro aerodinamico) = $c/4$ = 0.25 m

X,cp (centro presiones) = $c/4 \cdot (1 - (\pi/Cl) * (A1 - A2))$ = 0.0168099 m

ECUACIÓN DE LA CUERDA
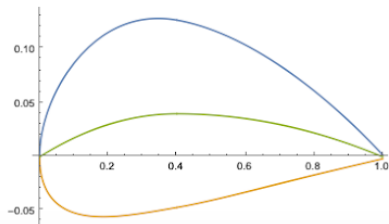
Out[318]=

Figure 7 Characteristics of NACA 4418

.

- NACA 6412

DATOS PARA EL PERFIL NACA 6412

α (Ángulo de Ataque) = 0 º

C (cuerda) = 1 m

Ecuaciones del perfil:

$$z1/c = 0.375 \left(\frac{0.8\, x}{c} - \frac{1.\, x^2}{c^2} \right)$$

$$z2/c = 0.166667 \left(0.2 + \frac{0.8\, x}{c} - \frac{1.\, x^2}{c^2} \right)$$

PASO 1: DERIVADAS

$$d(z1/c)/dx = \frac{0.3}{c} - \frac{0.75\, x}{c^2}$$

$$d(z2/c)/dx = \frac{0.133333}{c} - \frac{0.333333\, x}{c^2}$$

PASO 2: CAMBIO DE VARIABLE

$$x = \frac{1}{2}\, c\, (1 - \cos[\theta])$$

PASO 3: SUSTITUIR EN LAS DERIVADAS, Y ARREGLAR

$d(z1)/dx = -0.075 + 0.375\, \cos[\theta]$

$d(z2)/dx = -0.0333333 + 0.166667\, \cos[\theta]$

PASO 4: LIMITES DE INTEGRACION DE LA VARIABLE θ

I1: $\theta = [\, 0\, ;\, 1.36944\,]$ rad

I2: $\theta = [\, 1.36944\, ,\, \pi\,]$ rad

PASO 5: INTEGRALES

$A0 = \alpha - 1/\pi \cdot (\int_0^{\theta 1} (-0.075 + 0.375\, \cos[\theta]) \cdot d\theta + \int_{\theta 1}^{\pi} (-0.0333333 + 0.166667\, \cos[\theta]) \cdot d\theta) = -0.0134787$

$A1 = 2/\pi \cdot (\int_0^{\theta 1} (-0.075 + 0.375\, \cos[\theta]) \cdot \cos(\theta) \cdot d\theta + \int_{\theta 1}^{\pi} (-0.0333333 + 0.166667\, \cos[\theta]) \cdot \cos(\theta) \cdot d\theta) = 0.244485$

$A2 = 2/\pi \cdot (\int_0^{\theta 1} (-0.075 + 0.375\, \cos[\theta]) \cdot \cos(2\theta) \cdot d\theta + \int_{\theta 1}^{\pi} (-0.0333333 + 0.166667\, \cos[\theta]) \cdot \cos(2\theta) \cdot d\theta) = 0.0415838$

$A0 = -0.0134787$

$A1 = 0.244485$

$A2 = 0.0415838$

PASO 6: RESULTADOS

Cl (coef. sust) $= 2 \cdot \pi \cdot (A0 + A1/2) = 0.683385$

Cm,ac (coef. momentos centro aerod.) $= \pi/4 \cdot (A2 - A1) = -0.159359$

Cm,le (coef. momentos borde ataque) $= -[Cl/4 + \pi/4 \cdot (A1 - A2)] = -0.330205$

X,ca (centro aerodinamico) $= c/4 = 0.25$ m

X,cp (centro presiones) $= c/4 \cdot (1 - (\pi/Cl) * (A1 - A2)) = 0.0168099$ m
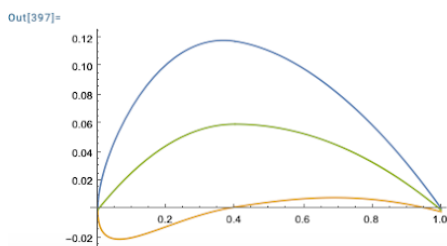
ECUACIÓN DE LA CUERDA

Out[397]=

Figure 8 Characteristics of NACA 6412
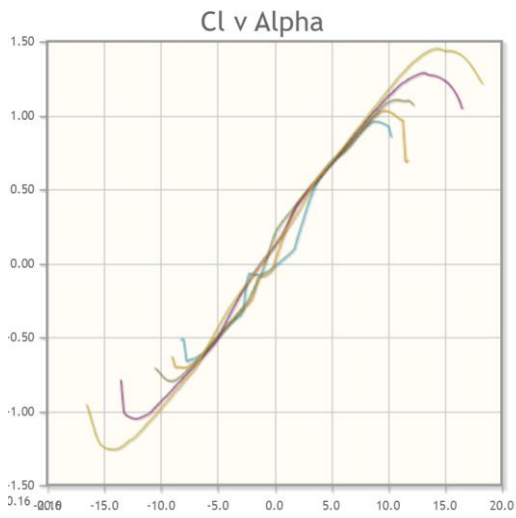
.

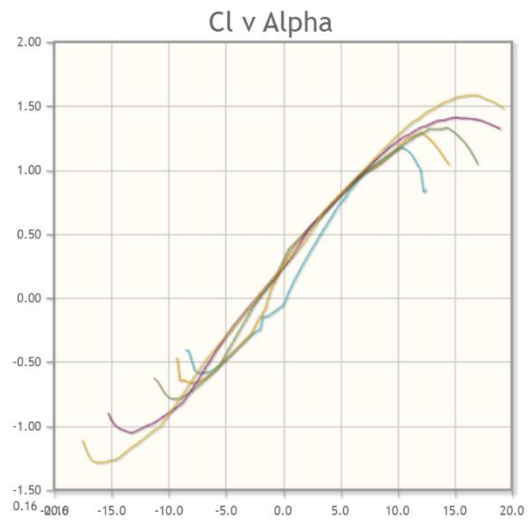*Figure 9 Cl vs Alpha curve of NACA 1410 18*

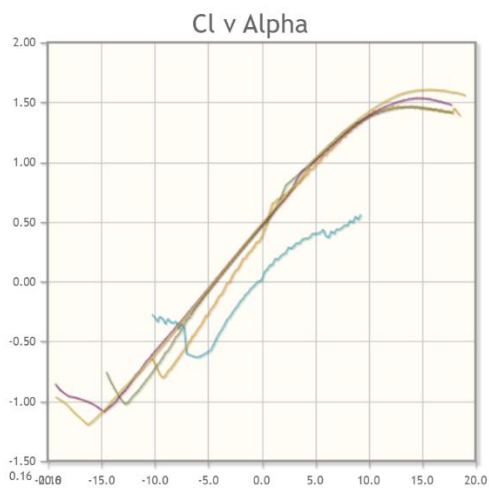*Figure 10 Cl vs Alpha curve of NACA 2412 19*

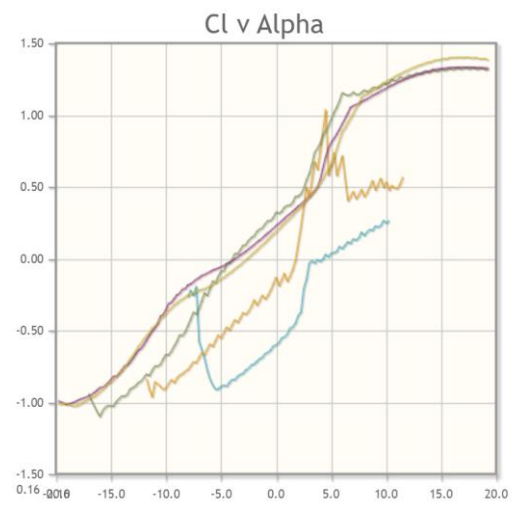*Figure 11 Cl vs Alpha curve of NACA 4418 20*

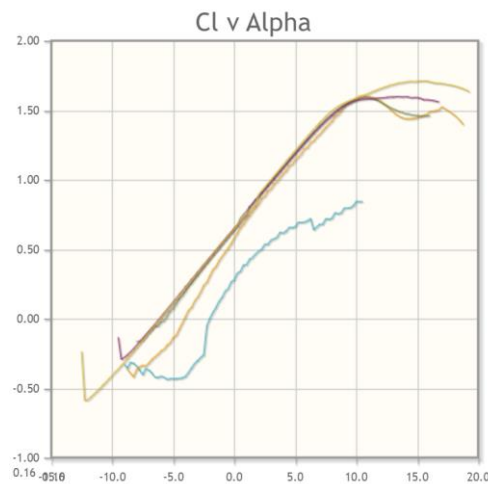*Figure 12 Cl vs Alpha curve of NACA 4424 21*

32

.

Figure 13 Cl vs Alpha curve of NACA 6412 22

As far as the Cl-Alpha curves is concerned, it is shown that the more stabilized and therefore will have better qualities in flight, will be the NACA 2412. Although it is not the one that generates more lift, the other conditions tend to decline for NACA 2412 to be the most appropriate option.

In the next table is shown all the results given by the elaborate calculation from Wolfram Mathematica:

NACA	CL	CM,ac	CM,le	X,ca (m)	X,cp (m)
1410	0,113897	-0,0265598	-0,0550341	0,25	0,0168099
2412	0,227795	-0,0531195	-0,110068	0,25	0,0168099
4418	0,45559	-0,106239	-0,220136	0,25	0,0168099
4424	0,45559	-0,106239	-0,220136	0,25	0,0168099
6412	0,683385	-0,159359	-0,330205	0,25	0,0168099

Table 1 Recording of studied NACAs information

Although as high is the M number and therefore also is its CL, it is important to take into account that the moment coefficients of aerodynamic centre and leading edge must be as central as possible.

Also, it is essential to observe their CL/Alpha curve and corroborate the best airfoil to have the better lift according to its proportions, then the final decision is to take one of the NACA airfoil with the number of M and P at its lower, then in consequence the NACA 2412 is the selected for the preliminary wing design and consequently the preliminary UAV design.

The source code where the calculation shown before has been made is added to the Annex A of this document.

.

Chapter 5.   3D MODELING NACA 2412.

In order to be able to run the CFD simulation on Ansys Fluent, the first step is to design the wing in Catia, to later export this file in .igs to Ansys.

The measures of the wing are 7,8 meters of length and 1,6 meters of chord. The shape of the airfoil is made from the information of the position of the points extracted from the NACA airfoil generator data on internet [23]

Continuing with the study, it is properly to design the real wing and the scale wing. This last wing is for printing on a 3D printer to later wind tunnel test it and prove its efficiency.

5.1 Design of the real wing

The final NACA airfoil is 2412 as mentioned in the previous points, then the process is to introduce the points in Catia and unify them with curvilinear lines. It has to be in this shape because of the better aerodynamic efficiency of the wing.

Once the shape of the profile wing is made, the chord is created. The final chord is 1,6 meters.

The final step to create the wing in Catia is to decide the length, in this case will be 7,8 meters.

Now the wing is created, we import the document in the format .igs due to it is the one Ansys can read. The wing design was made in Catia because of the three dimensions. In other programs such as AutoCAD the object is only created in two dimensions and Ansys can not run the correct simulation in these conditions.

The next figures shows the final real wing In Catia as well as the sketch that represents the three views plus the isometrical view.
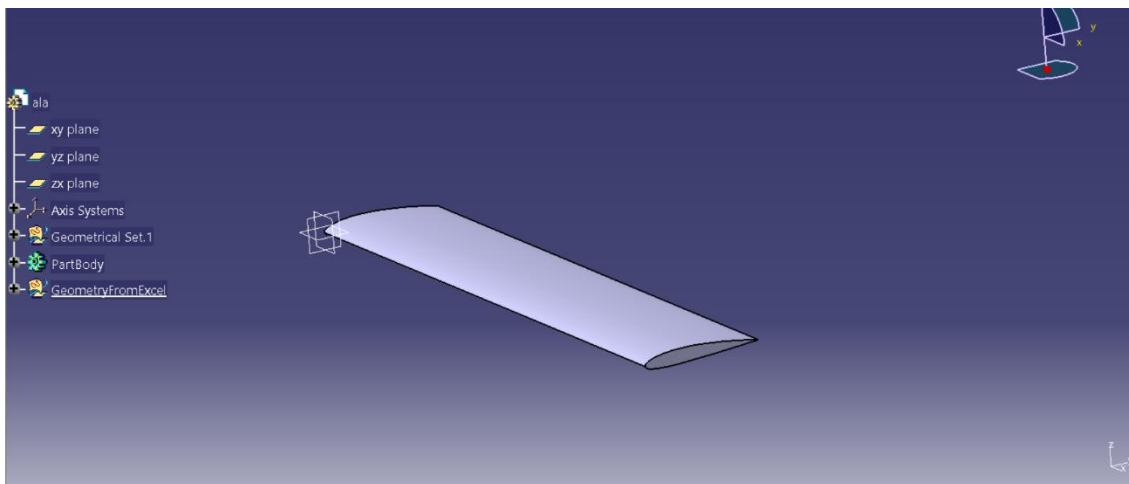

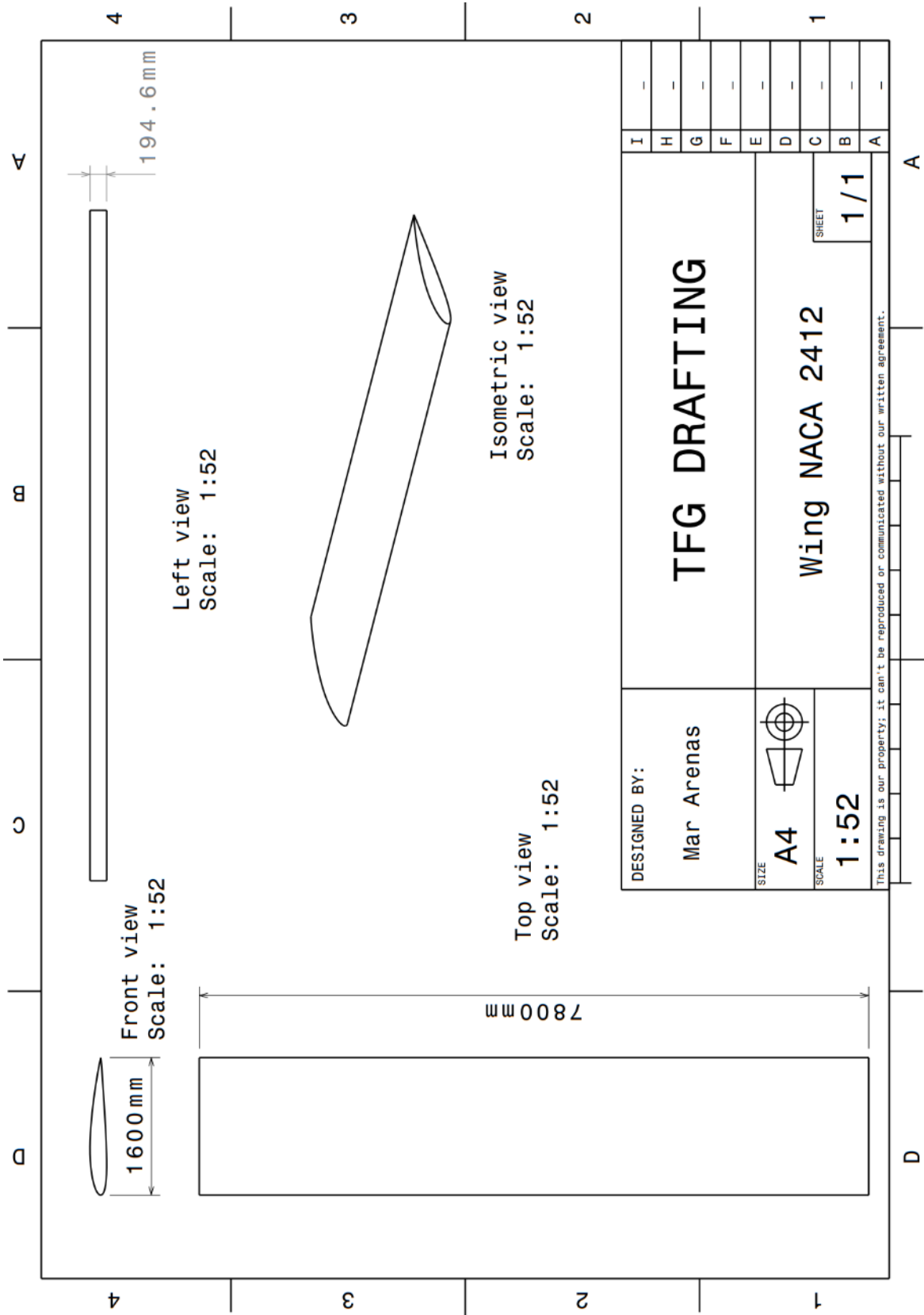*Figure 14 Isometrical view of the real wing made in Catia*

34

Figure 15 Sketch of the three views and isometrical view with their corresponding unit of the real wing made in Catia

.

5.2 Design of the scale wing

The scale wing was made by taking the previous design of the real wing in Catia and rearrange its dimensions. The scale respecting the real wing is 1:100
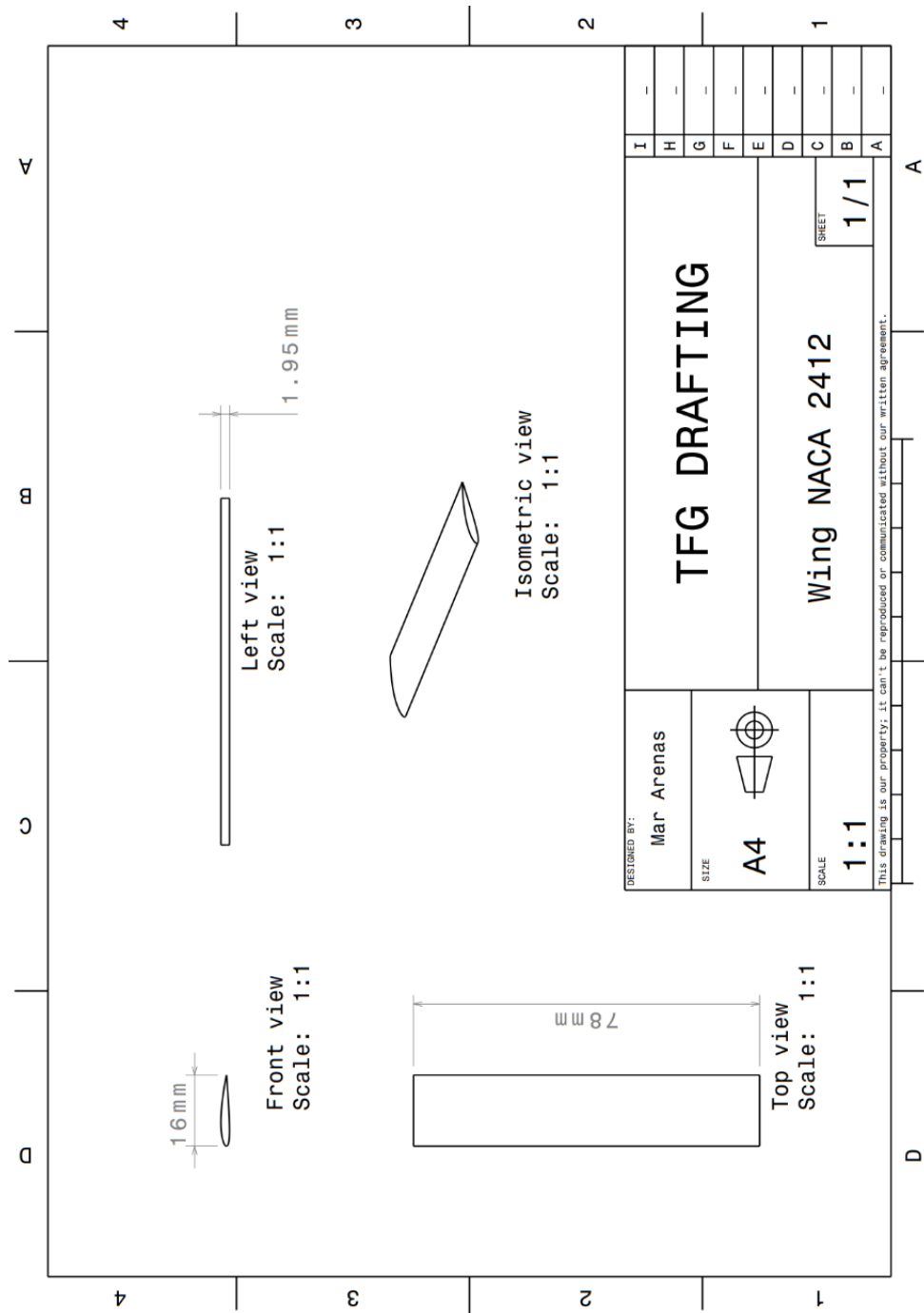

Figure 16 Sketch of the three views and isometrical view with their corresponding unit of the wing with scale 1:100 made in Catia

.

5.3 Printing of the scale wing

As printing the scale wing is concerned, it has been carried out thanks to a 3D printer. The material chosen was PLA in wood colour, to see properly the surface of the wing.

The temperature has risen up to 230 degrees Celsius, and it lasts around 4 days and 17 hours in total.

Concerning the structure, two holes through the entire wing had been created in order to reinforce its frame for the wind tunnel test.

In previous years projects the wing had been broken due to the high capacity wind that the wind tunnel is capable of, therefore to have a complete study and a wide range of results from the wind tunnel, two bars were introduced in the wing through these mentioned holes with the help of screws and washers.

In the following photos are shown every step of the printing, as well as creating the pieces in the 3D printer (where appears the structure of the wing).
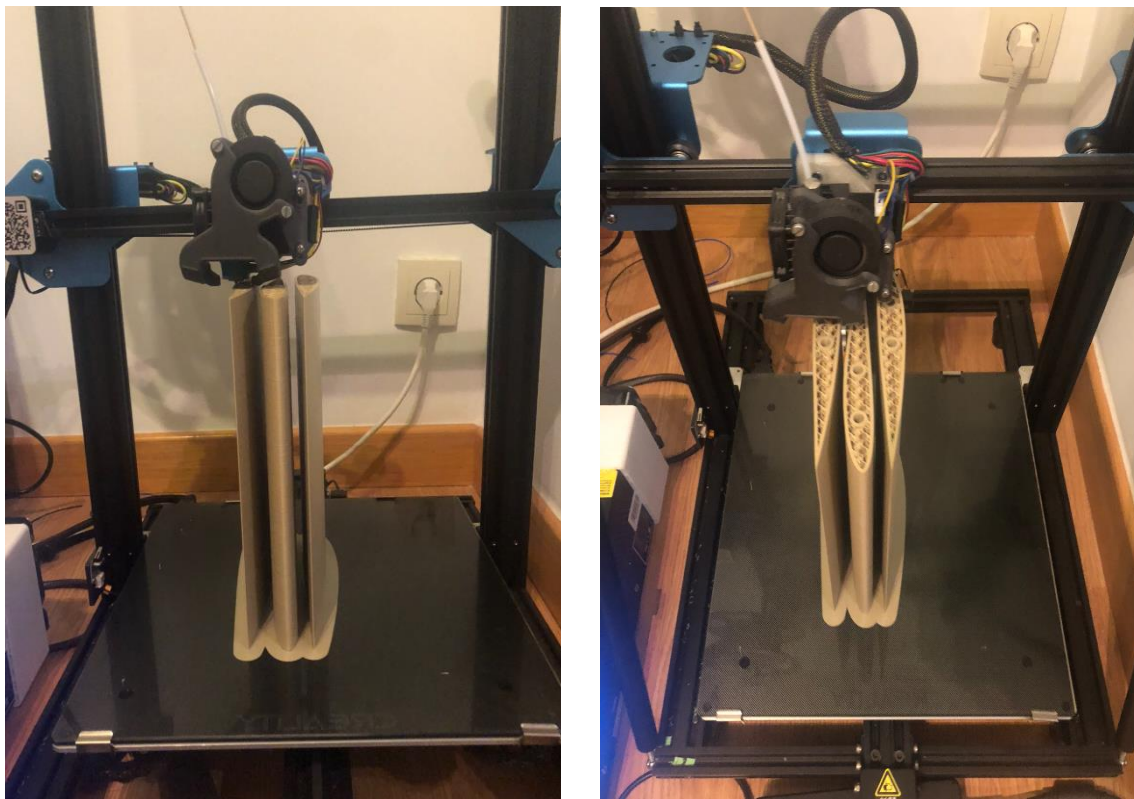

Figure 17 printing process of the scale wing in the 3D printer part 1

.

As printing is concerned, the whole wing in one piece was not able to be created due to the dimensions of the 3D printer, then it had to be divided into three parts of 26 milometers each one. The total measures of the parts sum 78 milometers, the desired dimensions.

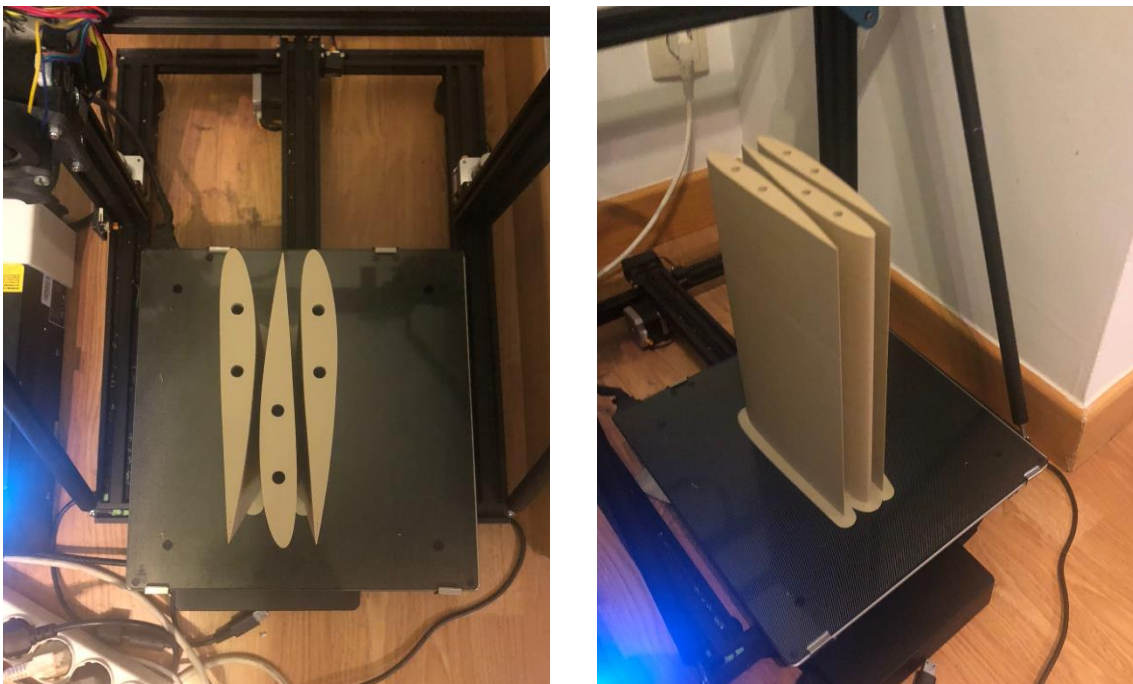*Figure 18 printing process of the scale wing in the 3D printer part 2*

Figure 19 printing process of the scale wing in the 3D printer part 3

.

The next pictures show the final parts of the scale wing plus the bars, therefore goes the sticking of the pieces to unify the whole object.

The sticking process is made with epoxy resin due to its properties, since only is needing a few minutes to rearrange the parts and then passed around 24 hours, the resistance has good quality.

Figure 20 sticking process of the scale wing plus introducing the bars

As it can be seen, the epoxy resin was added on the profile parts of the different elements to have better adhesion.

Once passed the necessary hours and prove every part is well added and sticked to their side's elements, some marks have to be signed on the wing. These marks are done with the help of a template situated in the laboratory where the wind tunnel is located, and its function is to tag the wing where the dynamometers are situated in the wind tunnel.

In total there is three dynamometers therefore the number of marks is the same. In the marks a hole is created to introduce some anchorage rings to later adjust them at the end of the dynamometers.

These mentioned attachments are put into the wing with the help of a blowtorch and pliers.
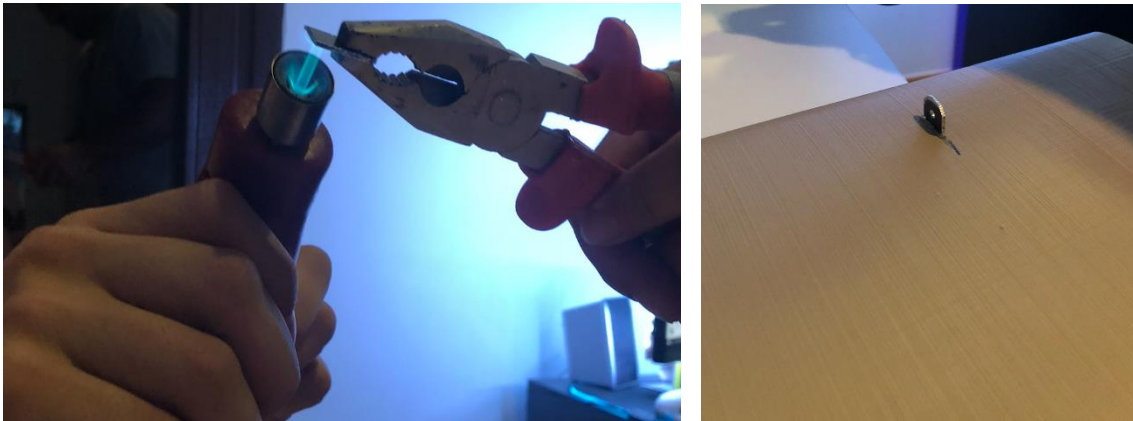
.

Figure 21 process of the heating of the anchorage ring with the help of blowtorch and pliers and anchorage ring introduced in the wing

Figure 22 Final scale wing with every anchorage ring introduced

.

Final scale wing is presented below with the bars introduced throughout the wing with screws and washers, plus the three anchorage rings.
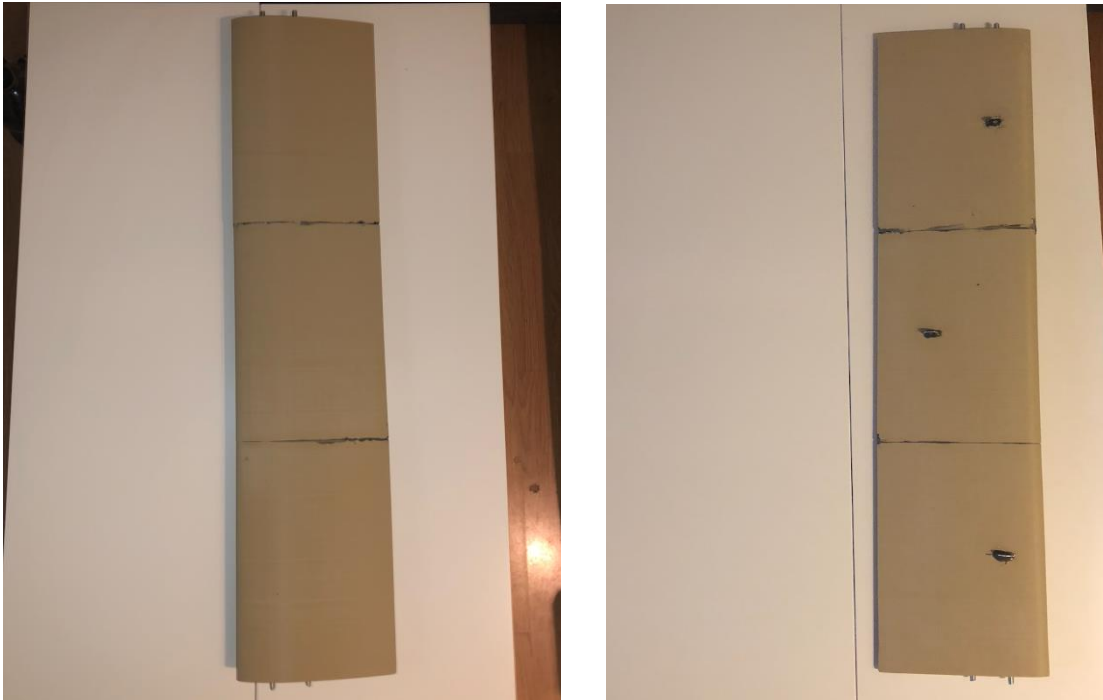

Figure 23 upside and downside view of the final scale wing

Finally, as the epoxy resin turns out black, in order to have an aesthetic wing, a full painting in black is done. It was needed around 10 minutes for the upside part and 10 more minutes for the downside part to have the work done and 24 hours to be completely ready for the wind tunnel test.

It hardly affects the aerodynamic efficiency of the wing due to one layer of painting was applied.

Figure 24 upside and downside view of the final scale wing painted in black

.

Chapter 6. NACA AIRFOIL 2412 CFD ANALYSIS IN ANSYS FLUENT.

To accomplish the CFD simulation analysis in Ansys Fluent was necessary to import the wing design in Catia to Ansys in the file called igs. The simulation in Ansys was made with the scale wing (1:100) and the real wing.

As the scale wing was printed, there will be a wind tunnel test to later compare their results and analyse their properties.

6.1   CFD simulation on scale wing.

To run properly the CFD simulation, it is needed to prepare the wing in Ansys Workbench. The geometry must be created.
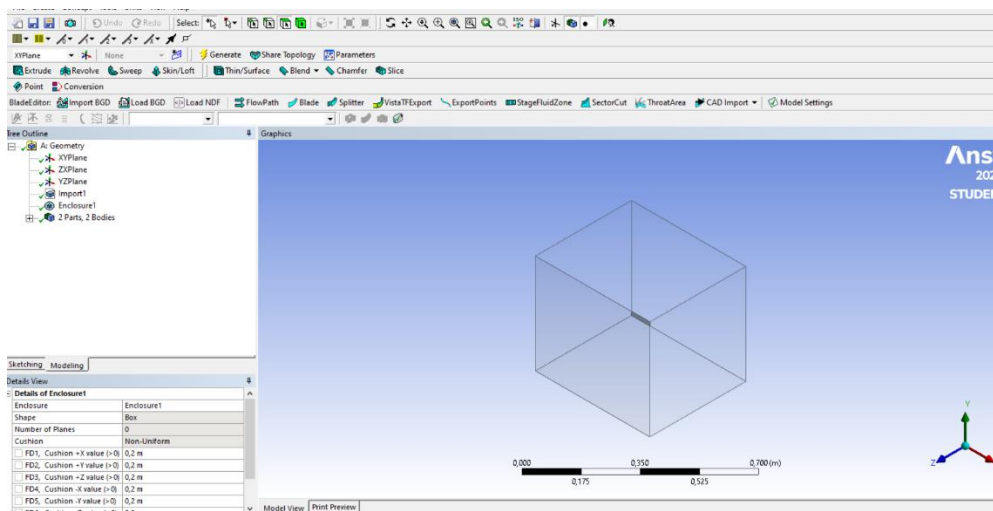
Figure 25 geometry of the scale wing in Ansys Workbench part 1
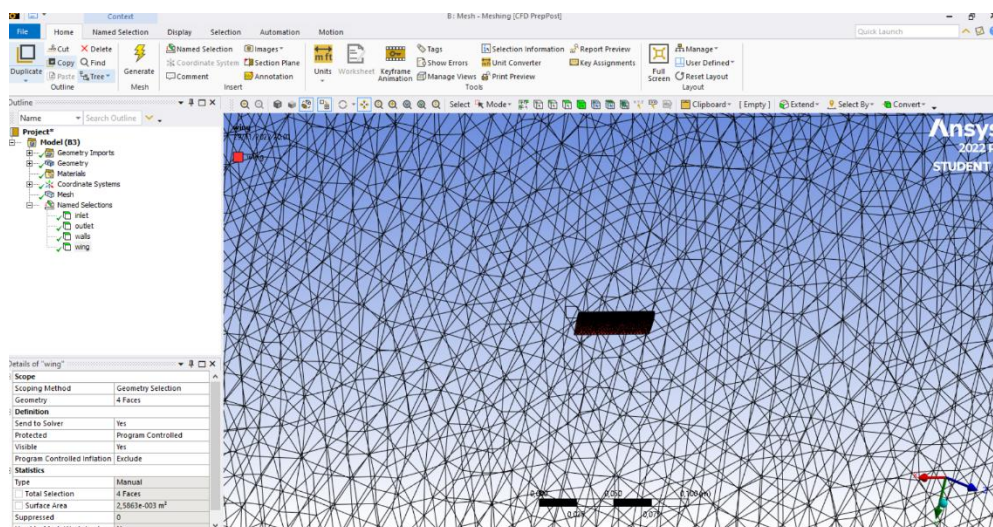
Figure 26 geometry of the scale wing in Ansys Workbench part 2

.

As doing the simulation, apart from abstracting the lift and drag results, also show some pictures about how the flow interacts with the surface of the wing. There were done so many calculations, therefore below are shown some pictures of some of them.
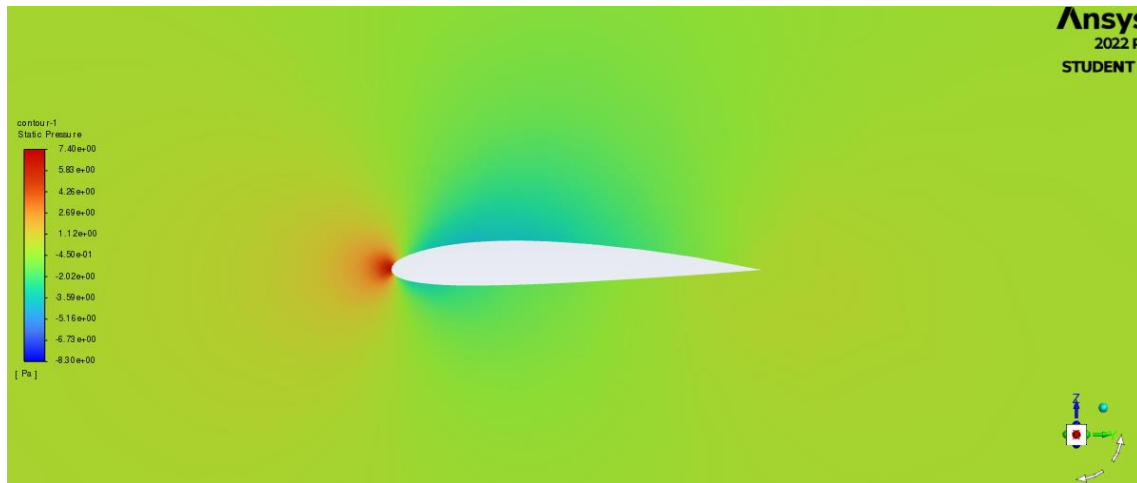

Figure 27 contour of static pressure at 3.7 m/s and 0 of AoA of scale wing
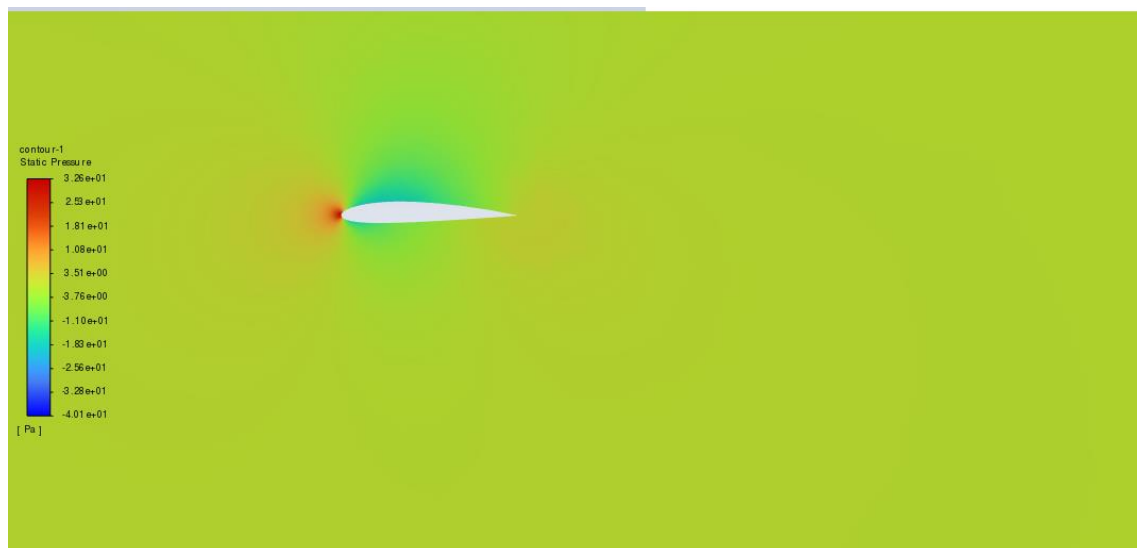

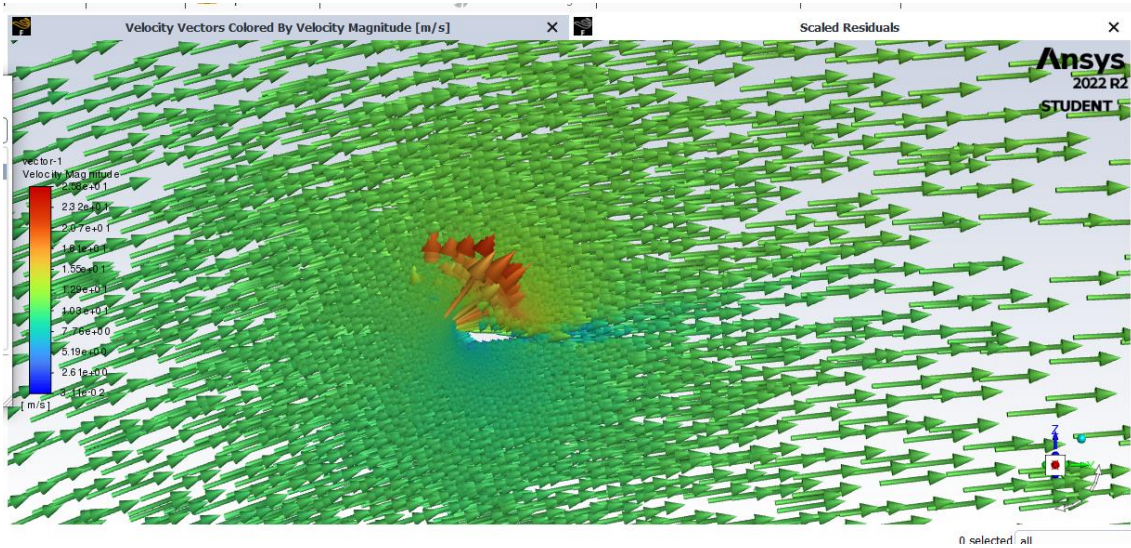*Figure 28 contour of static pressure at 7.78 m/s and 0 of AoA of scale wing*

.

Figure 29 contour of velocity vectors at 11.6 m/s and 15 of AoA of scale wing
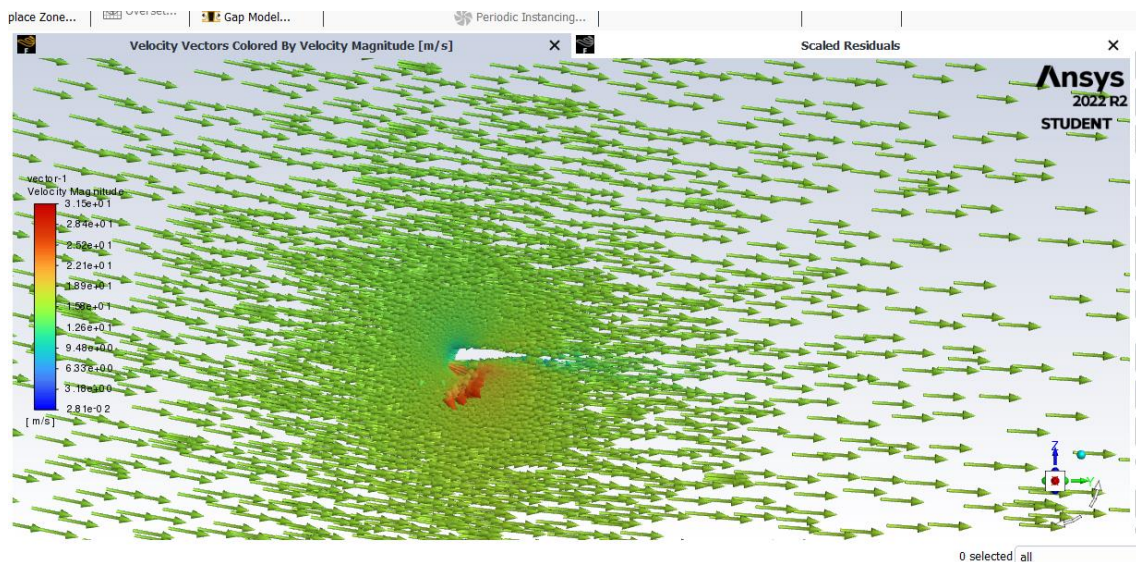

Figure 30 contour of velocity vectors at 15.6 m/s and -9 of AoA of scale wing

The range of angles of attack were determined by the wind tunnel testing possible angles of attack, as there is a template in the laboratory at the university that helps in the guidance of the position of the wing.

Also, the speeds chosen were in consequence of the power of the wind tunnel because of their specific manner to determine their velocities. The test was run to be able to resist the power up to 40% of the wind tunnel, therefore the CFD simulation input data was run according to the wind tunnel test, that later will be described in chapter 7.

.

6.2 Comparatives to different speed ranges and Alpha values.

The speeds used are 3.7 m/s, 7.78 m/s, 11.6 m/s and 15.6 m/s with a range of -15 to 15 degrees of angles of attack. The topic measured in the CFD was lift and drag. Then the numerical analysis is done to be able to obtain the lift coefficient, drag coefficient, and Cl/Cd data.

Velocity (m/s)	Alpha	Lift	Drag	Cl	Cd	Cl/Cd
3.7	-15	-0.006	0.0058	-0.557284143	0.538708005	-1.034482759
	-12	-0.0591	0.0039	-5.489248805	0.362234693	-15.15384615
	-9	-0.0628	0.0032	-5.832907359	0.297218209	-19.625
	-6	-0.0036	0.0018	-0.334370486	0.167185243	-2
	-3	-0.00014	0.001	-0.013003297	0.09288069	-0.14
	0	0.002	0.0011	0.185761381	0.102168759	1.818181818
	3	0.0046	0.0016	0.427251176	0.148609105	2.875
	6	0.008	0.0029	0.743045523	0.269354002	2.75862069
	9	0.0103	0.0047	0.956671111	0.436539245	2.191489362
	12	0.0092	0.006	0.854502352	0.557284143	1.533333333
	15	0.0099	0.008	0.919518835	0.743045523	1.2375

Table X:

Table 2 data obtained from the CFD simulation at 3.7 m/s of scale wing

Velocity (m/s)	Alpha	Lift	Drag	Cl	Cd	Cl/Cd
7.78	-15	-0.032	0.027	-0.672232751	0.567196384	-1.185185185
	-12	-0.033	0.0204	-0.693240025	0.428548379	-1.617647059
	-9	-0.028	0.012	-0.588203657	0.252087282	-2.333333333
	-6	-0.016	0.006	-0.336116376	0.126043641	-2.666666667
	-3	-0.00031	0.0028	-0.006512255	0.058820366	-0.110714286
	0	0.001	0.0029	0.021007273	0.060921093	0.344827586
	3	0.021	0.0054	0.441152743	0.113439277	3.888888889
	6	0.037	0.011	0.777269119	0.231080008	3.363636364
	9	0.048	0.0203	1.008349127	0.426447652	2.36453202
	12	0.0507	0.029	1.065068765	0.609210931	1.748275862
	15	0.046	0.038	0.96633458	0.798276392	1.210526316

Table X:

Table 3 Data obtained from the CFD simulation at 7.78 m/s of scale wing

.

Velocity (m/s)	Alpha	Lift	Drag	Cl	Cd	Cl/Cd
11.6	-15	-0.073	0.06	-0.689283148	0.56697532	-1.215719844
	-12	-0.075	0.044	-0.708167618	0.415781902	-1.70321896
	-9	-0.063	0.027	-0.594860799	0.255138894	-2.33151751
	-6	-0.037	0.013	-0.349362692	0.122844653	-2.84393894
	-3	-0.00067	0.004	-0.006326297	0.037798355	-0.16736965
	0	0.0051	0.024	0.048155398	0.226790128	0.21233463
	3	0.048	0.01	0.453227276	0.094495887	4.796264591
	6	0.08	0.024	0.755378793	0.226790128	3.3307393
	9	0.108	0.044	1.01976137	0.415781902	2.452635302
	12	0.114	0.066	1.07641478	0.623672853	1.725928546
	15	0.104	0.086	0.981992431	0.812664626	1.208361234

Table 4 Data obtained from the CFD simulation at 11.6 m/s of scale wing

Velocity (m/s)	Alpha	Lift	Drag	Cl	Cd	Cl/Cd
15.6	-15	-0.133	0.116	-0.694914426	0.606090778	-1.146551724
	-12	-0.13	0.08	-0.679239665	0.41799364	-1.625
	-9	-0.11	0.048	-0.574741255	0.250796184	-2.291666667
	-6	-0.068	0.022	-0.355294594	0.114948251	-3.090909091
	-3	-0.0013	0.007	-0.006792397	0.036574443	-0.185714286
	0	0.044	0.0076	0.229896502	0.039709396	5.789473684
	3	0.087	0.018	0.454568083	0.094048569	4.833333333
	6	0.1517	0.042	0.792620439	0.219446661	3.611904762
	9	0.197	0.08	1.029309338	0.41799364	2.4625
	12	0.209	0.12	1.092008384	0.62699046	1.741666667
	15	0.191	0.156	0.997959815	0.815087597	1.224358974

Table 5 Data obtained from the CFD simulation at 15.6 m/s of scale wing

To visualize the results, some graphics were made in Excel about its lift coefficient and drag coefficient combined with their correspondent angle of attack in order to obtain the following graphics:

- Cl vs Alpha
- Cd vs Alpha
- Cl vs Cd
- Cl/Cd vs Alpha

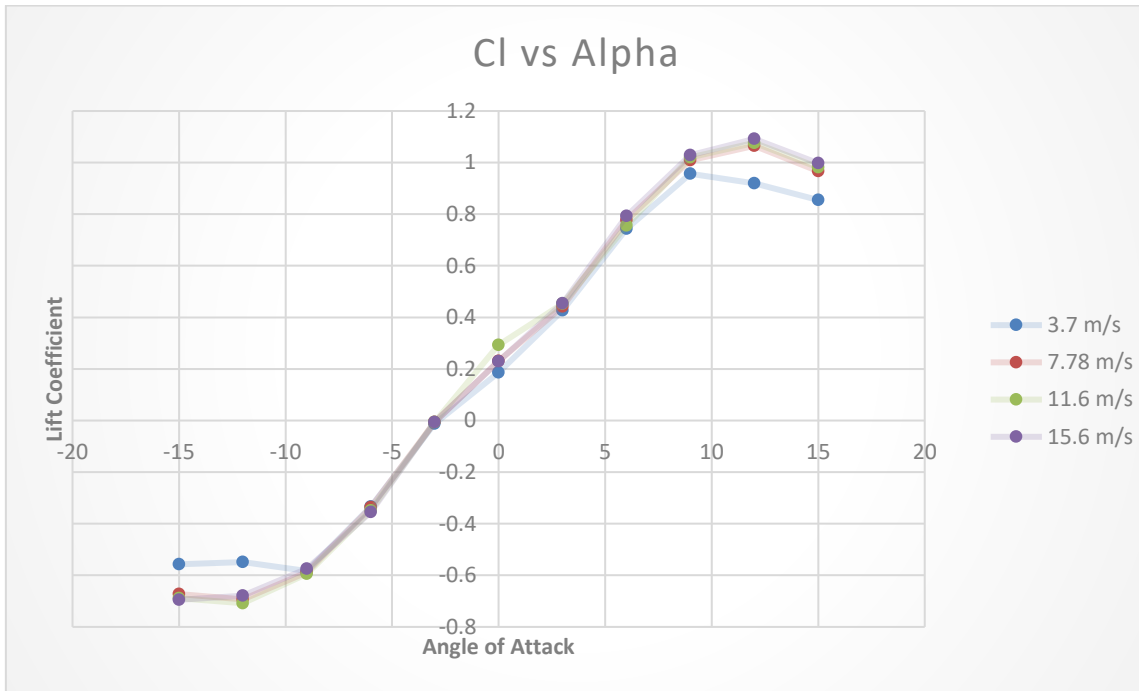The following images show the results for the different wide of angles of attack and their speeds.

.

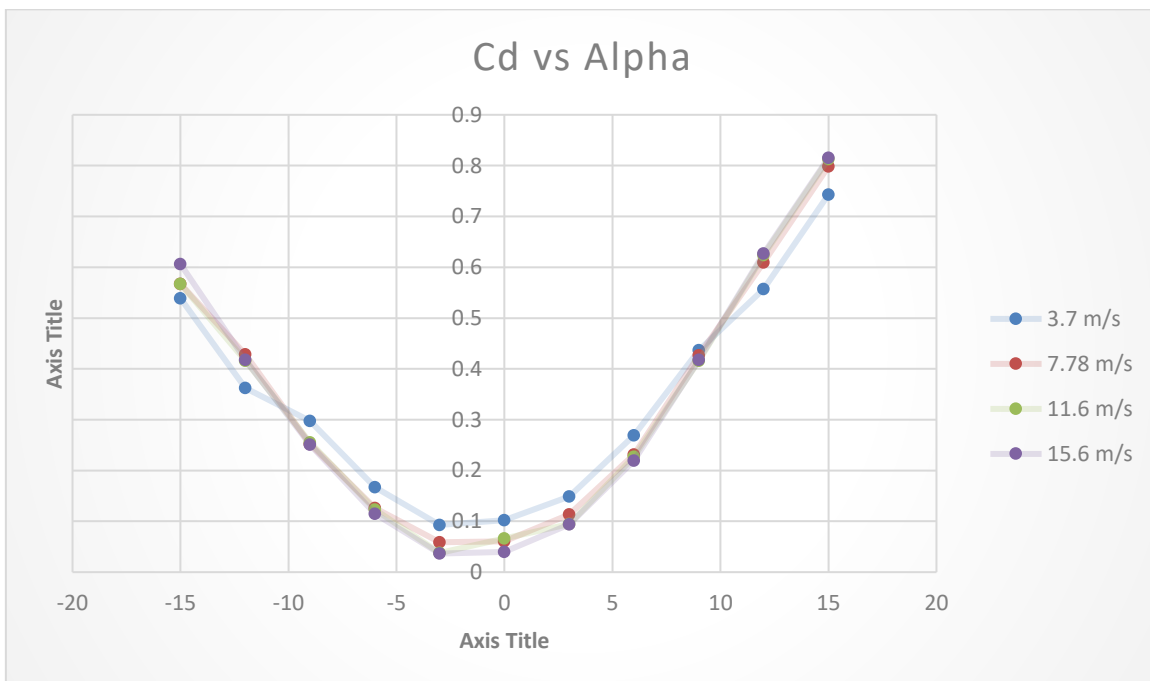*Figure 31 Cl vs Alpha CFD simulation scale wing*

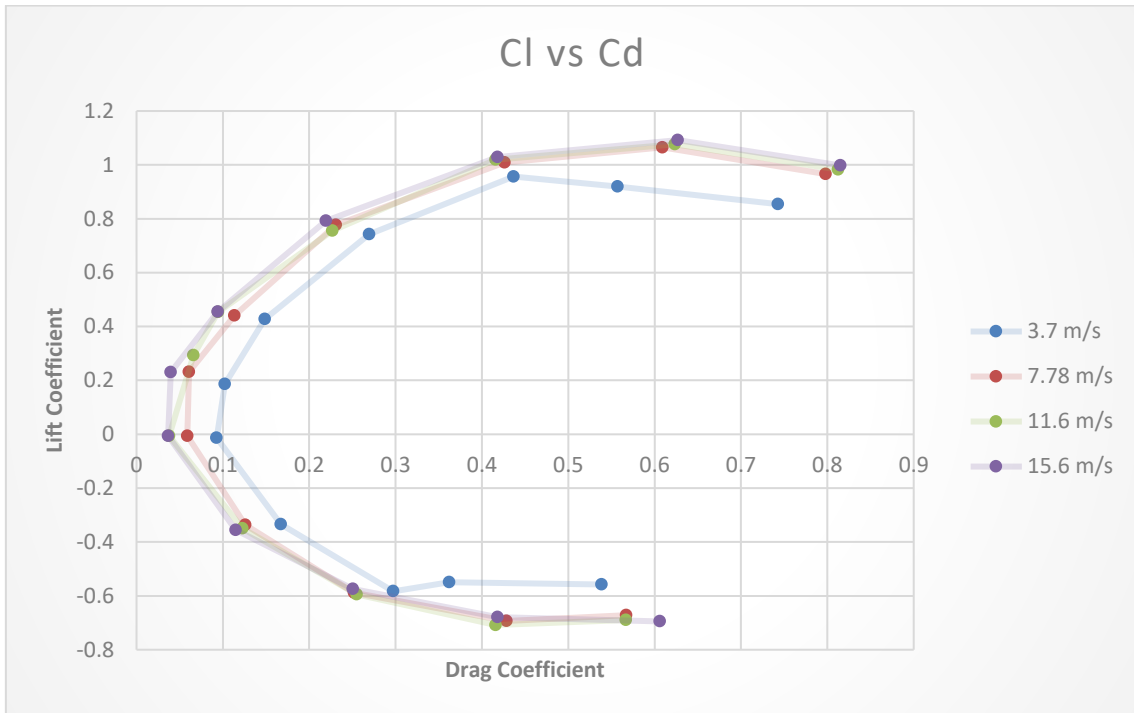*Figure 32 Cd vs Alpha CFD simulation scale wing*

.

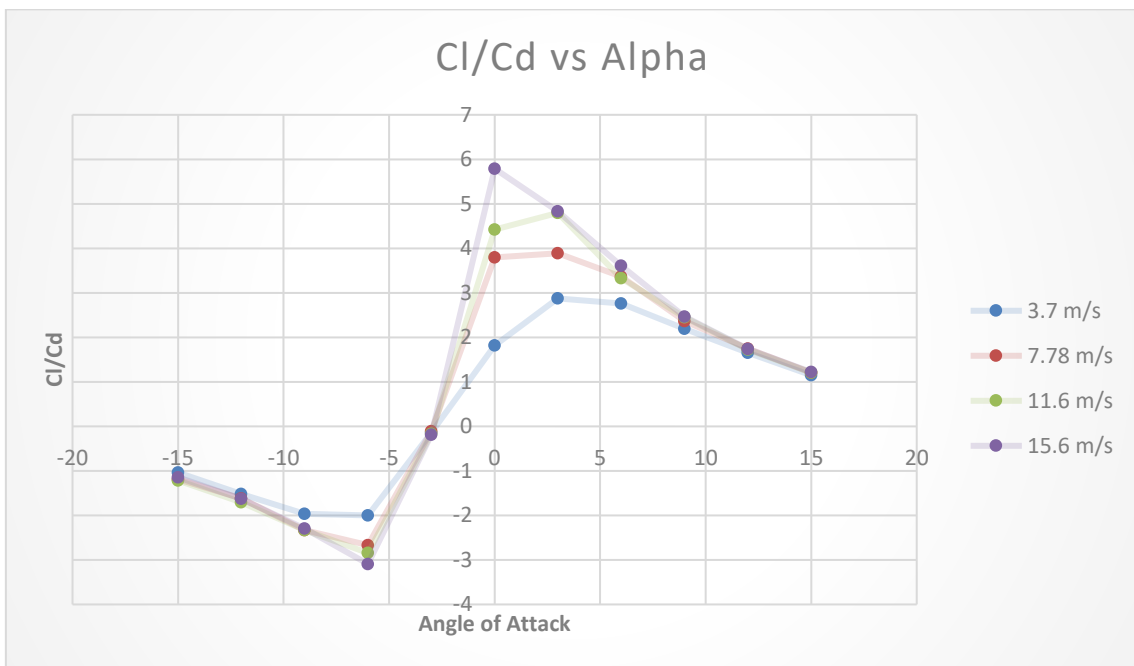*Figure 33 Cl vs Cd CFD simulation scale wing*

Figure 34 Cl/Cd vs Alpha CFD simulation scale wing

.

6.3 CFD simulation on the real wing

For the real wing with the measures of 7,8 meters with a chord of 1,6 meters, the preparation of the geometry was made with the same steps as before with the scale wing.

As so many calculations were made, these images below show the flow around the surface of the wing respecting the static pressure and velocity vectors of a specific angle of attack of 40 degrees.

In this case only was made for the cruising speed because of its dimensions, though at low speeds the data would not be useful enough for our study as it is for its cruising speed.
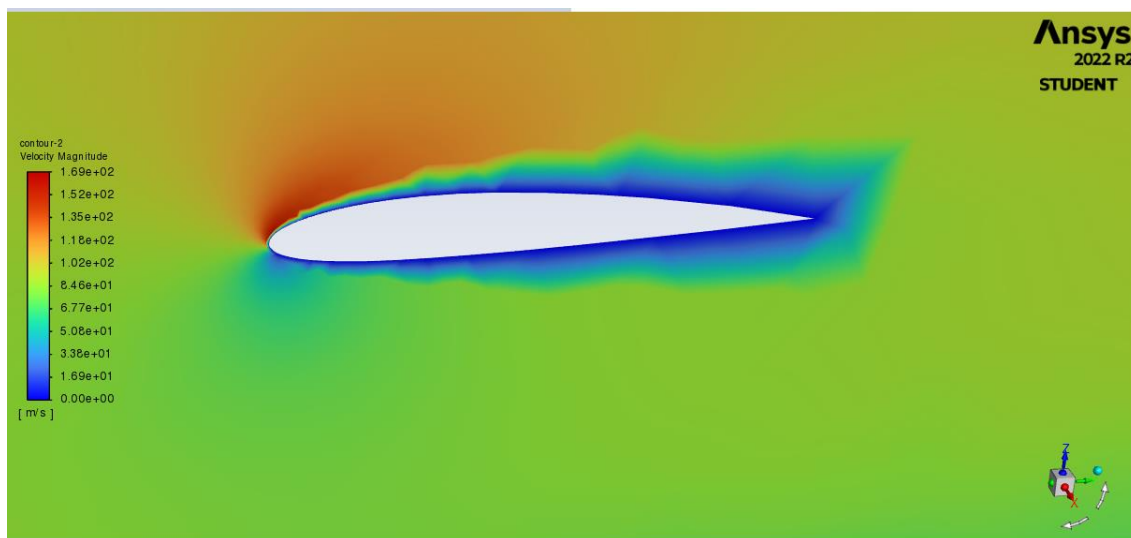
Figure 35 contour of static pressure at 96 m/s and 40 of AoA of the real wing
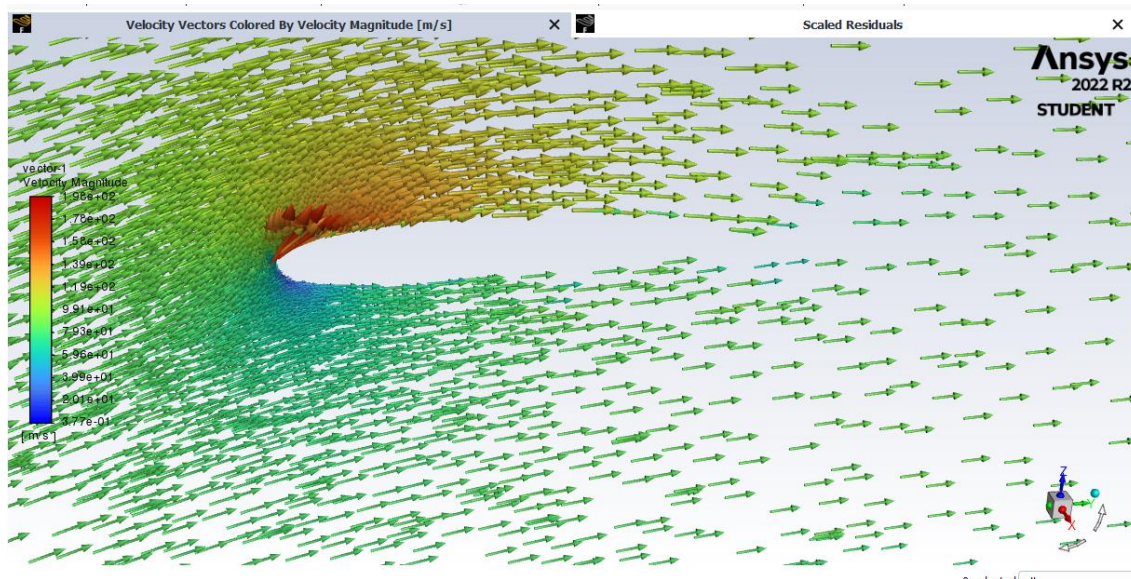
Figure 36 contour of velocity vectors at 96 m/s and 40 of AoA of the real wing

.

Next table show the obtained results from the CFD simulation in Ansys Fluent:

Velocity	Angle	Lift	Drag	Cl	Cd	Cl/Cd
96	-5	9,325.11	867.14	0.24867635	0.02312433	10.7538819
	0	18,005.32	863.30	0.48015484	0.02302201	20.8563352
	5	26,514.97	2,882.40	0.70708503	0.07686602	9.19892867
	10	34,729.17	6,124.48	0.92613638	0.16332384	5.67055245
	15	43,999.02	10,894.81	1.17333912	0.2905361	4.03853129
	20	51,724.38	28,177.84	1.37935412	0.7514294	1.83564034
	25	64,803.18	26,526.21	1.72813169	0.7073848	2.44298677
	30	67,955.09	34,892.11	1.81218491	0.93048152	1.94757755
	35	66,133.12	42,424.72	1.76359772	1.13135657	1.55883457
	40	61,374.81	49,025.38	1.63670609	1.30737889	1.25189882

Table 6 Data for Cl, Cd and Cl/Cd Ansys for the real wing

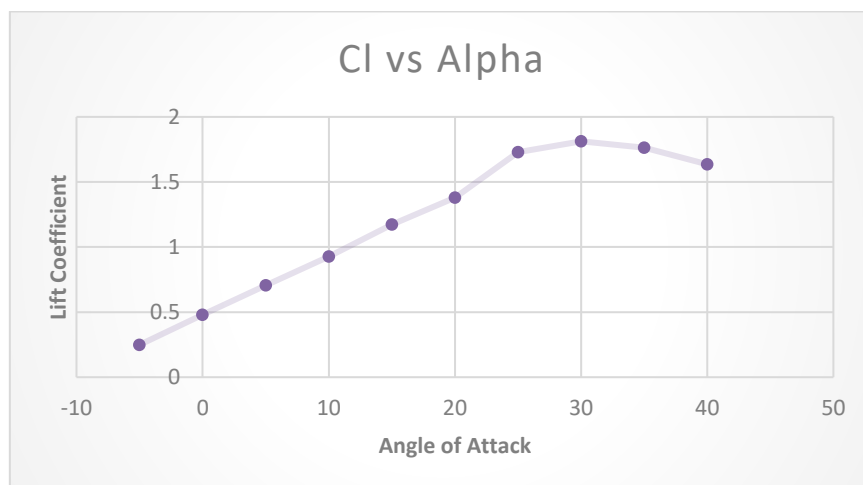Therefore, these results are indicated graphically in the following images:

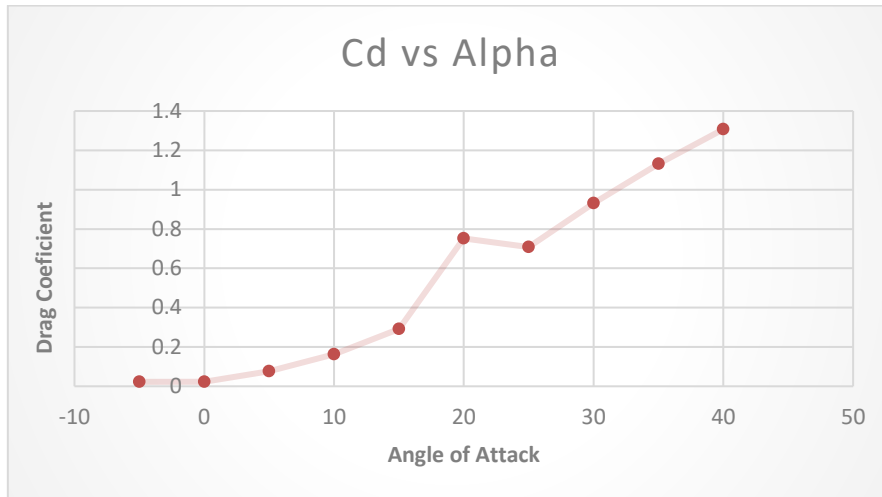*Figure 37 graphic Cl vs Alpha results from Ansys for the real wing*

.

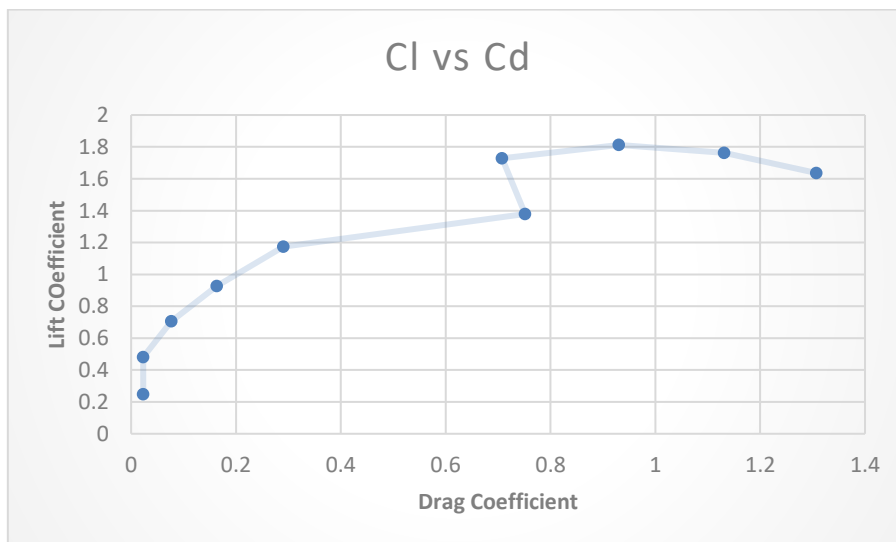*Figure 38 graphic Cd vs Alpha results from Ansys for the real wing*

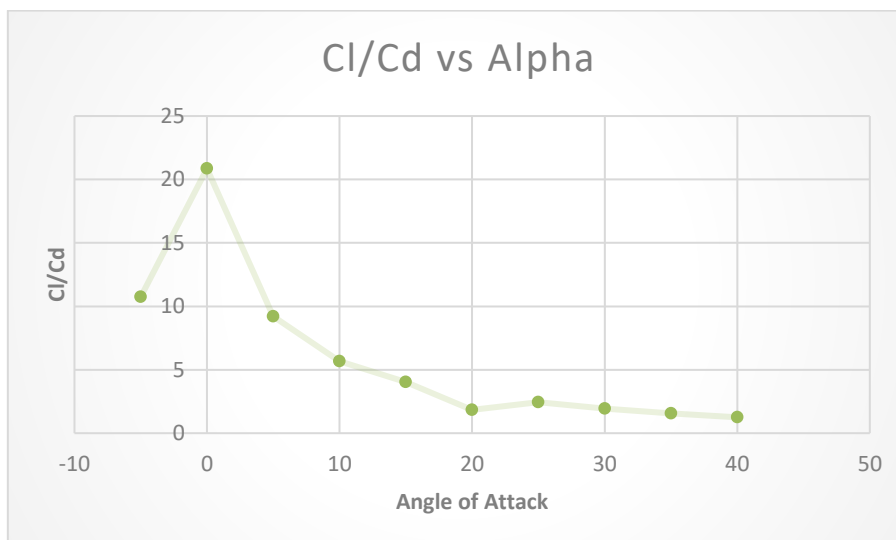*Figure 39 graphic Cl vs Cd results from Ansys for the real wing*

Figure 40 graphic Cl /Cd vs Alpha results from Ansys for the real wing

.

Chapter 7.   WIND TUNNEL TEST OF THE WING

The scale wing is carried to the wind tunnel test located in the Universidad Europea de Madrid to be able to run the test and complete the aerodynamic study.

7.1   Wind tunnel description

Wind tunnel were created as a facility to test the wings before implementing them in the aircraft because if the wings were directly put on this tak would have a higher cost.

The test that are run in the wind tunnel are reliable due to it functioning. The air goes through the surface of the wing and the object that is tested is stated stationary. The dynamometers read its lift and drag forces to later be able to calculate its properties.

The wind tunnel situated in the Universidad Europea de Madrid, following the information from the internet is "closed horizontal axis that occupies a space of 12x5.6 m2, has 2 test chambers, a high speed 0.9 x 0.9 m2 and a los speed one 1.8 x1.8 m2, with a maximum wind speed of 150 and 50 km/h respectively". [24]

The range of velocities that the little chamber can run is shown in the next table:

Power (%)	Speed (m/s)	Speed (km/h)
10	3,7	13,3
20	7,78	28
30	11,6	41,8
40	15,6	56
50	19,33	69
60	23,5	84
70	27,47	98
80	31,31	112
85	32,31	116
88	32,31	116
92	32,31	116

Table 7 Data for the power and speed from the wind tunnel at Universidad Europea de Madrid

In this study the maximum power used to test the scale wing is 40%, due to the vibrations were increasing as high the power was, then to not break the wing the 15.6 m/s speed was the highest studied.

Although the test was run from -15 to 15 degrees of angle of attack with 4 different speeds, that elaborates a complete test for the project.

There were three dynamometers holding the wing and reading the information in three different parts of the wing. The dynamometers were able to read lift and drag at the same time.

.

7.2   Test preparation

Once the wing is situated in the wind tunnel and fasten to the dynamometers, the test is run. In the following images are shown the procedure. Also there was a camera that was helpful to read the velocity and the pressure the wind tunnel had at the moment, plus the information from the program on the computer.
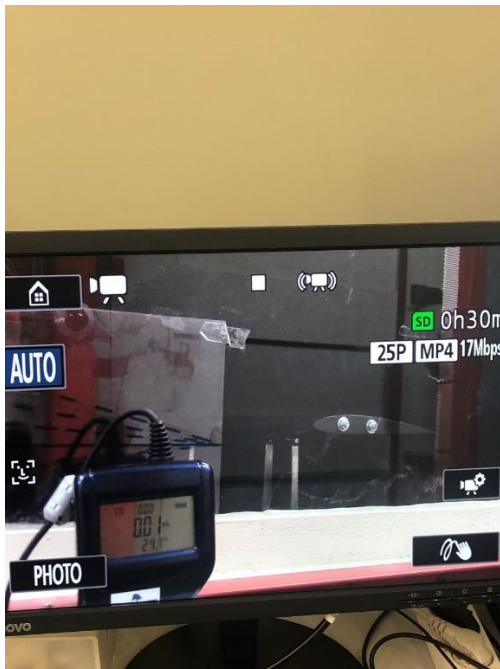

Figure 41 Wind tunnel camera and wing attached to the dynamometers

Figure 42 wing attached to the dynamometers

.

7.3   Final results from the wind tunnel test for the scale wing

The three dynamometers read their only position with lift and drag, Therefore P1 and P2 refers to the same dynamometer located in one side of the wing, the same for P5 and P6. Regarding P3 and P4 was the same dynamometer located in the center of the wing.

Velocity	Alpha	P1l	P3l	P5l	P2d	P4d	P6d
3,7	-15	0,46	-0,26	0,47	0	-0,04	-0,05
	-12	0,14	-0,66	0,44	-0,22	0,23	-0,04
	-9	0,08	-0,2	0,24	-0,33	0,36	-0,24
	-6	0,26	0,05	0,3	0,05	-0,29	0,15
	-3	0,17	-0,17	-0,29	0,02	-0,01	0,11
	0	0,16	0,13	0,08	0,17	0,05	0,2
	3	0,15	0,8	0,54	1,53	-3,02	1,75
	6	-0,66	-0,21	0,59	-0,5	0,45	-0,25
	9	0,23	-0,13	-0,29	0,03	-0,25	0,1
	12	1,28	-0,33	-1,01	0,85	-1,35	0,68
	15	1,59	3,69	0,54	2,66	-5,7	2,82

Table 8 data read from the wind tunnel for 3.7 m/s

Velocity	Alpha	P1l	P3l	P5l	P2d	P4d	P6d
7,78	-15	1,13	-0,05	1,19	-0,41	-0,01	-0,49
	-12	1,09	-0,7	1,42	-0,43	0,31	-0,22
	-9	0,82	-0,38	0,9	-0,57	0,4	-0,4
	-6	0,7	-0,28	1,13	-0,04	-0,32	0,06
	-3	0,33	-0,3	-0,12	-0,03	-0,01	0,04
	0	0,05	0,01	0,51	0,18	0,07	0,15
	3	-0,24	0,6	0,04	1,72	-3,3	1,74
	6	-1,19	-0,43	0,08	-0,04	-0,24	-0,1
	9	0,48	-0,23	-0,32	0,17	-0,96	0,31
	12	0,63	-0,23	-0,96	1,18	-2,61	1,23
	15	0,7	-0,34	0,14	2,83	-7,7	2,77

Table 9 data read from the wind tunnel for 7.78 m/s

.

Velocity	Alpha	P1l	P3l	P5l	P2d	P4d	P6d
11,6	-15	2,59	0,44	0,47	-1,22	0,09	-0,95
	-12	2,99	-0,8	3,27	-0,43	0,53	-0,32
	-9	1,92	-0,76	2,07	-0,89	0,49	-0,52
	-6	1,68	-1,22	2,45	-0,22	-0,26	-0,04
	-3	0,27	-0,79	0,23	-0,1	0,02	-0,06
	0	-0,18	-0,16	-1,19	0,22	0,07	0,14
	3	-0,95	0,07	-1,82	1,93	-3,97	1,9
	6	-1,46	-0,67	-1,79	0,73	-1,45	0,28
	9	-0,37	-0,37	-0,12	0,07	-1,33	0,33
	12	-0,59	-0,77	-1,83	1,28	-5,6	1,91
	15	-0,91	-1,68	-1,01	2,89	-10,52	2,84

Table 10 data read from the wind tunnel for 11.6 m/s

Velocity	Alpha	P1l	P3l	P5l	P2d	P4d	P6d
15,6	-15	5,29	0,72	6	-1,27	0,08	-1,79
	-12	5,21	-1,69	5,92	-1,14	0,59	-0,8
	-9	4,12	-1,47	3,92	-1,37	0,79	-1,05
	-6	3,06	-1,94	4,29	-0,39	-0,14	-0,04
	-3	0,36	-1,6	0,91	-0,14	0,06	-0,14
	0	-1,94	-1,06	-0,32	0,66	0,12	0,03
	3	-4,31	-0,16	-5,57	2,18	-4,26	1,67
	6	-4,25	1,16	-6,53	2,13	-2,32	1,11
	9	-2,19	-0,96	-5,31	0,14	-2,52	0,16
	12	-2,94	-1,77	-5,83	1,88	-10,18	2,09
	15	-3,45	-2,03	-3,83	3,06	-14,46	2,56

Table 11 data read from the wind tunnel for 15.6 m/s

Concerning the numerical analysis, the following tables show the results from the wind tunnel test for each of the speeds chosen:

Velocity	Alpha	Total Lift	Total Drag	Cl	Cd	Cl/Cd
3,7	-15	-0.007	0.0073	-0.650164833	0.67802904	-0.95890411
	-12	-0.006	0.0049	-0.596386913	0.455115383	-1.310408163
	-9	-0.004	0.0025	-0.371522762	0.232201726	-1.6
	-6	-0.004	0.0019	-0.334370486	0.176473312	-1.894736842
	-3	-0.001	0.0007	-0.105883987	0.065016483	-1.628571429
	0	0.0022	0.0014	0.204337519	0.130032967	1.571428571
	3	0.0046	0.0018	0.427251176	0.167185243	2.555555556
	6	0.0093	0.0031	0.863790421	0.28793014	3
	9	0.0096	0.0045	0.891654628	0.417963107	2.133333333
	12	0.0099	0.0072	0.919518835	0.668740971	1.375
	15	0.0082	0.0086	0.761621662	0.798773938	0.953488372

Table 12 numerical analysis from the wind tunnel for 3.7 m/s

.

Velocity	Alpha	Total Lift	Total Drag	Cl	Cd	Cl/Cd
7,78	-15	-0.042	0.073	-0.882305486	1.533530964	-1.738095238
	-12	-0.038	0.0324	-0.798276392	0.680635661	-0.852631579
	-9	-0.023	0.0125	-0.48316729	0.262590918	-0.543478261
	-6	-0.019	0.0023	-0.399138196	0.048316729	-0.121052632
	-3	-0.00039	0.0029	-0.008192837	0.060921093	-7.435897436
	0	0.012	0.0035	0.252087282	0.073525457	0.291666667
	3	0.028	0.0051	0.588203657	0.107137095	0.182142857
	6	0.042	0.0174	0.882305486	0.365526559	0.414285714
	9	0.049	0.0242	1.0293564	0.508376018	0.493877551
	12	0.052	0.0297	1.092378221	0.623916022	0.571153846
	15	0.041	0.0482	0.861298213	1.012550582	1.175609756

Table 13 numerical analysis from the wind tunnel for 7.78 m/s

Velocity	Alpha	Total Lift	Total Drag	Cl	Cd	Cl/Cd
11,6	-15	-0.092	0.042	-0.869362158	0.396882724	-2.19047619
	-12	-0.082	0.031	-0.774866271	0.292937249	-2.64516129
	-9	-0.077	0.022	-0.727618328	0.207890951	-3.5
	-6	-0.058	0.016	-0.548076143	0.151193419	-3.625
	-3	-0.028	0.002	-0.264588483	0.018899177	-14
	0	0.043	0.009	0.406332313	0.085046298	4.777777778
	3	0.051	0.014	0.481929022	0.132294241	3.642857143
	6	0.089	0.029	0.841013392	0.274038072	3.068965517
	9	0.103	0.042	0.973307633	0.396882724	2.452380952
	12	0.118	0.073	1.115051464	0.689819973	1.616438356
	15	0.093	0.092	0.878811747	0.869362158	1.010869565

Table 14 numerical analysis from the wind tunnel for 11.6 m/s

Velocity	Alpha	Total Lift	Total Drag	Cl	Cd	Cl/Cd
15,6	-15	-0.184	0.466	-0.961385371	2.434812951	-0.394849785
	-12	-0.164	0.082	-0.856886961	0.428443481	-2
	-9	-0.139	0.031	-0.726263949	0.161972535	-4.483870968
	-6	-0.041	0.025	-0.21422174	0.130623012	-1.64
	-3	-0.029	0.004	-0.151522694	0.020899682	-7.25
	0	0.049	0.0079	0.256021104	0.041276872	6.202531646
	3	0.095	0.021	0.496367447	0.10972333	4.523809524
	6	0.1486	0.059	0.776423186	0.308270309	2.518644068
	9	0.182	0.092	0.95093553	0.480692686	1.97826087
	12	0.217	0.173	1.133807748	0.903911246	1.25433526
	15	0.183	0.195	0.956160451	1.018859497	0.938461538

Table 15 numerical analysis from the wind tunnel for 15.6 m/s

It is important to take into account that there is needed to do a transformation on the drag force due to the position of the dynamometers. The results have been multiplied for 20/31.5.

In the next graphs shows the final results comparison for all the different speed in the wind tunnel.
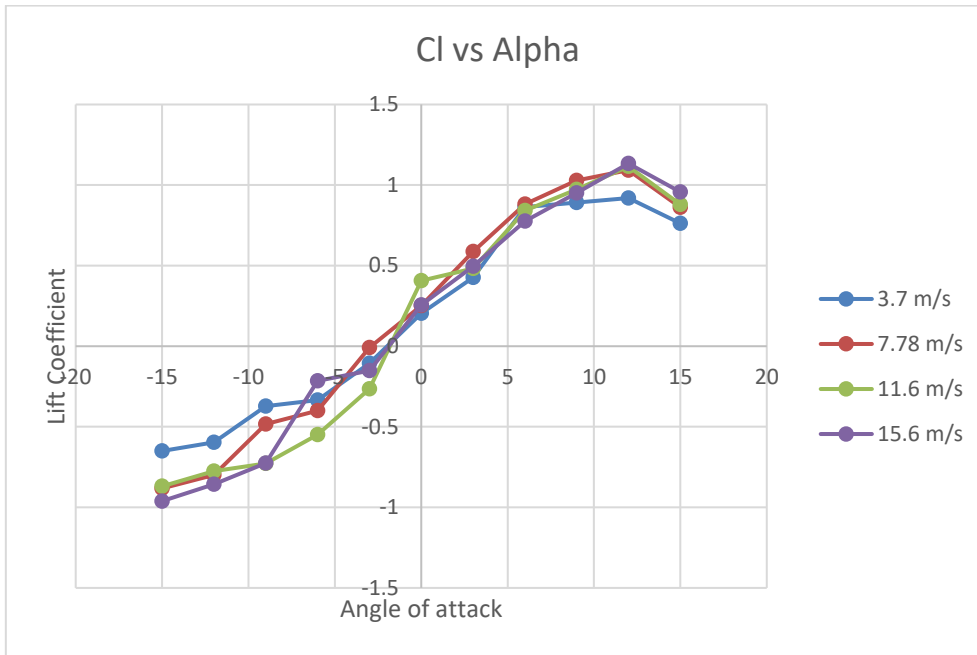
.

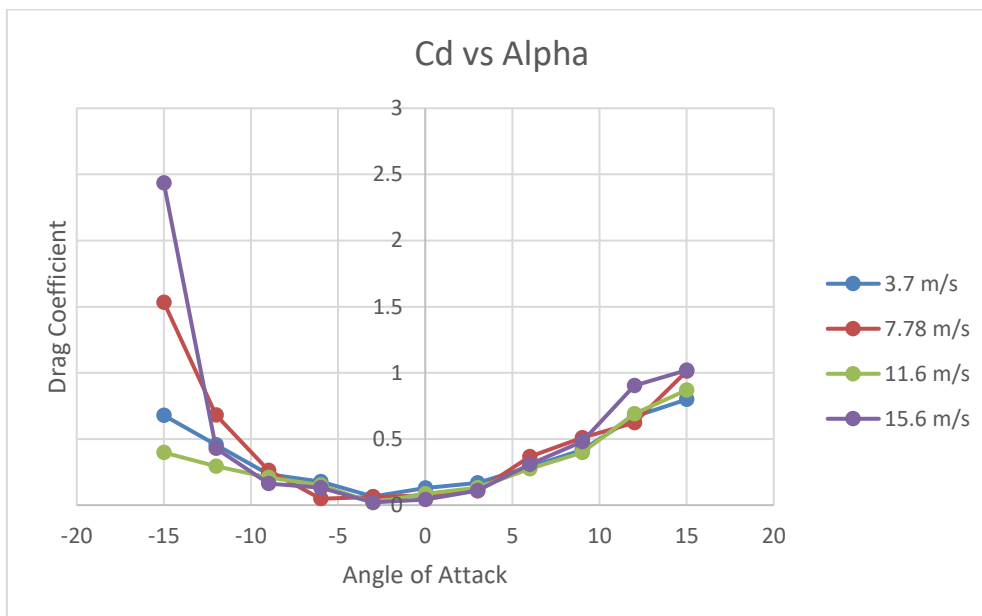*Figure 43 Cl vs Alpha wind tunnel test scale wing*

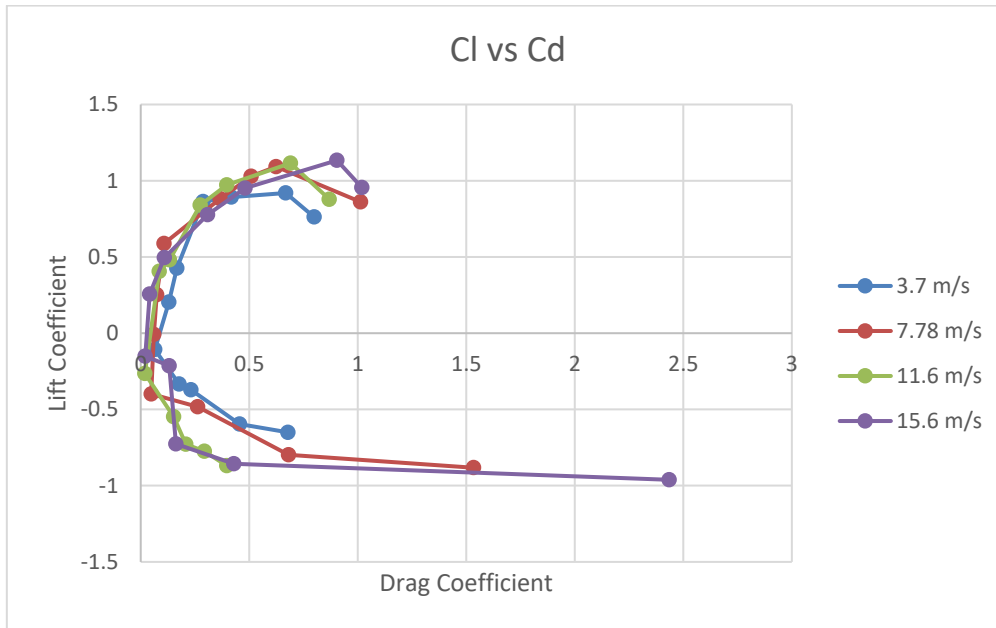*Figure 44 Cd vs Alpha wind tunnel test scale wing*

.

Figure 45 Cl vs Cd wind tunnel test scale wing
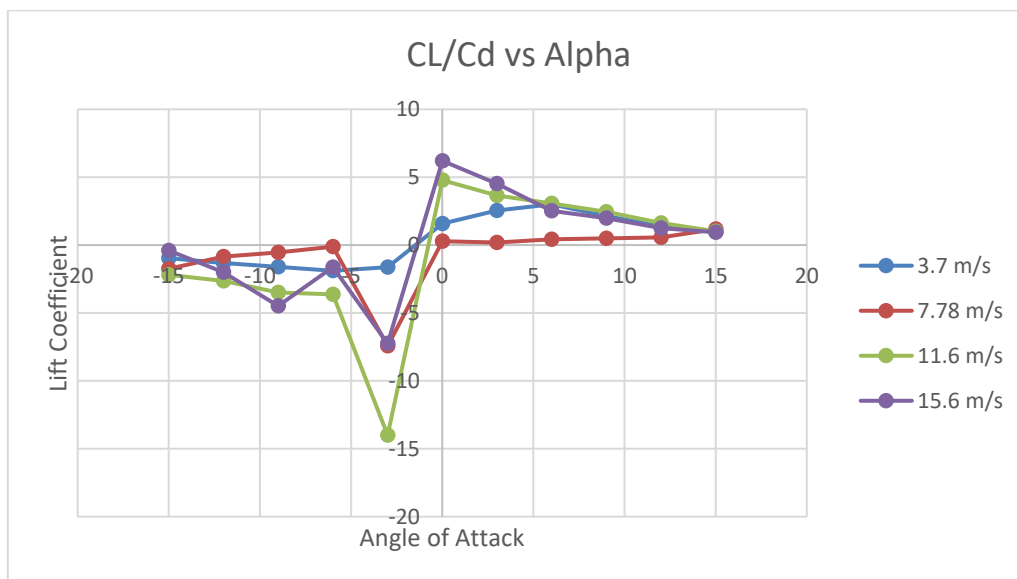

Figure 46 Cl/Cd vs Alpha wind tunnel test scale wing

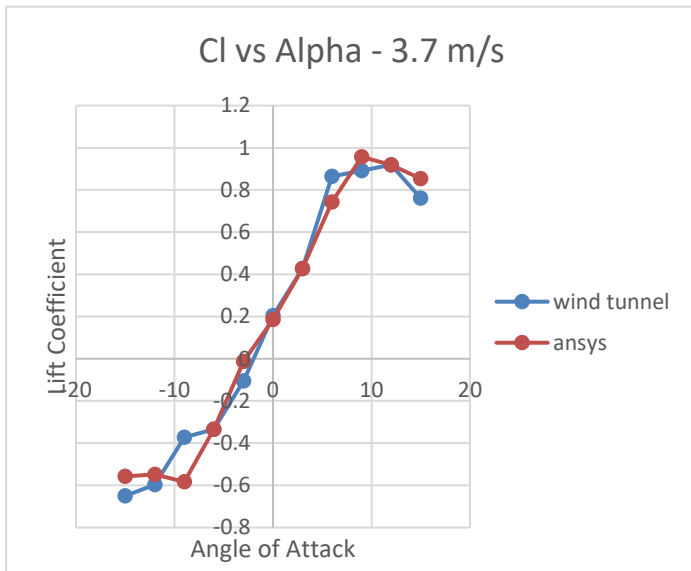# Chapter 8. ANALYTICAL, NUMERICAL AND EXPERIMENTAL COMPARISON

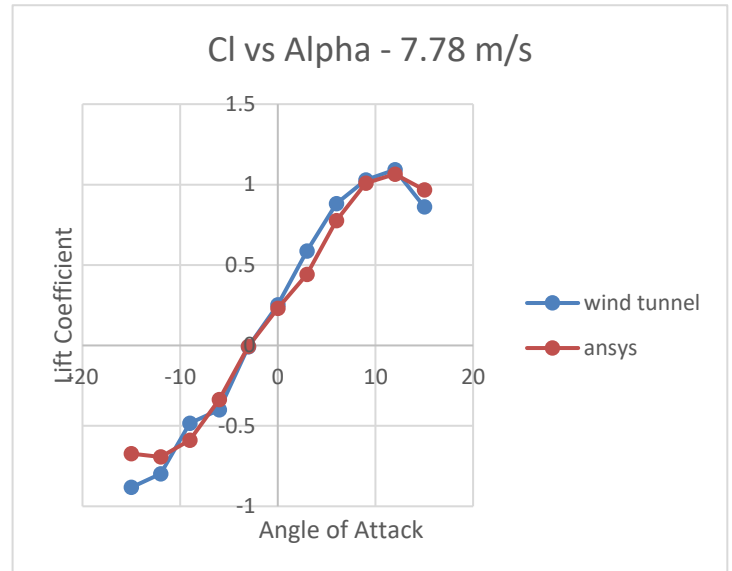*Figure 47 Cl vs Alpha comparison 3.7 m/s scale wing*

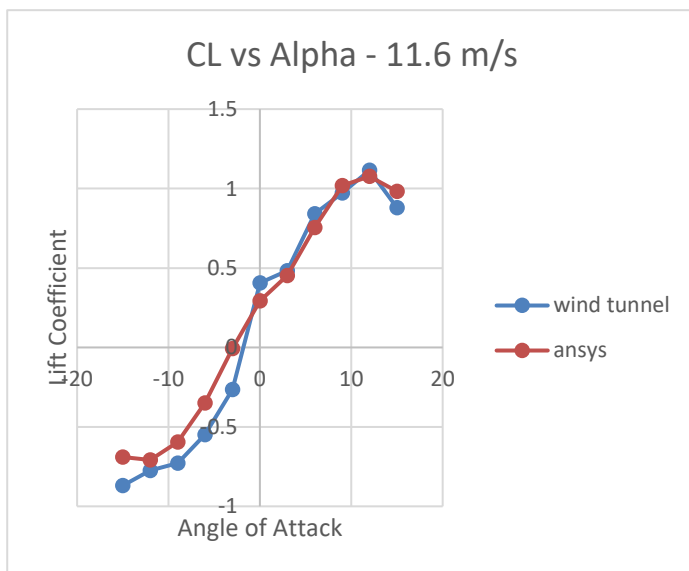*Figure 48 Cl vs Alpha comparison 7.78 m/s scale wing*
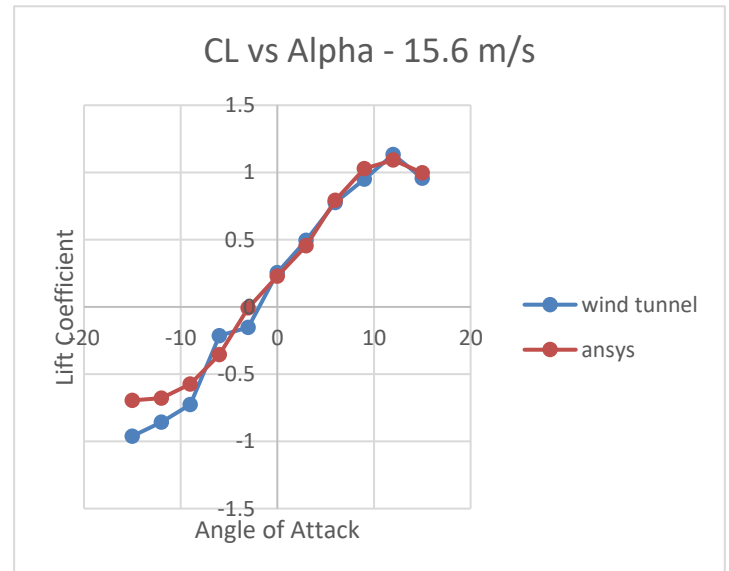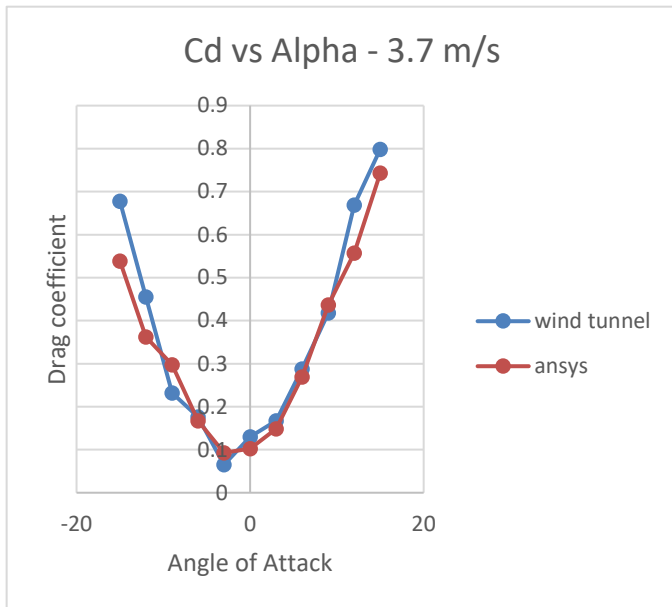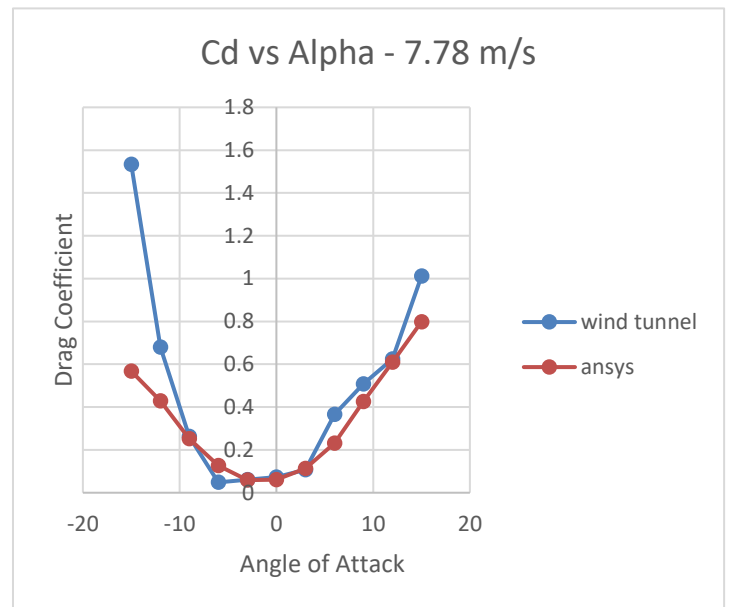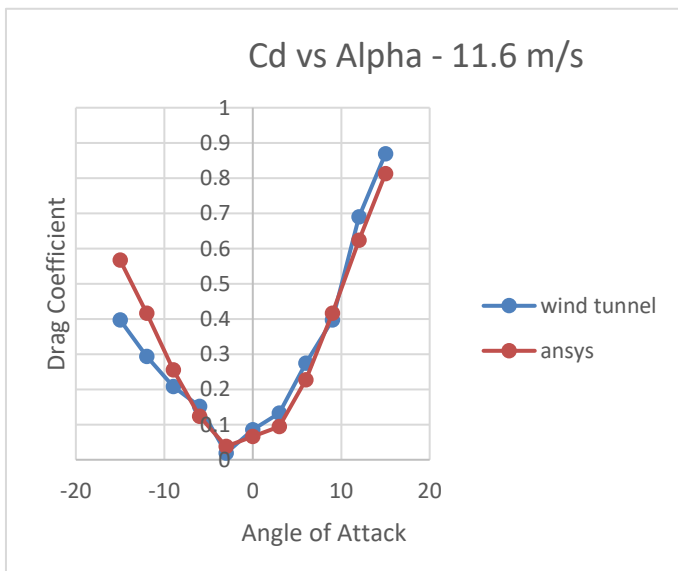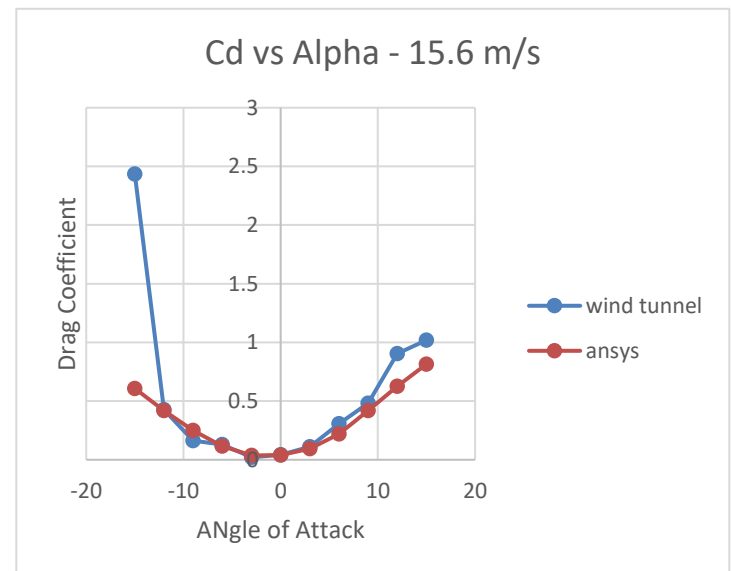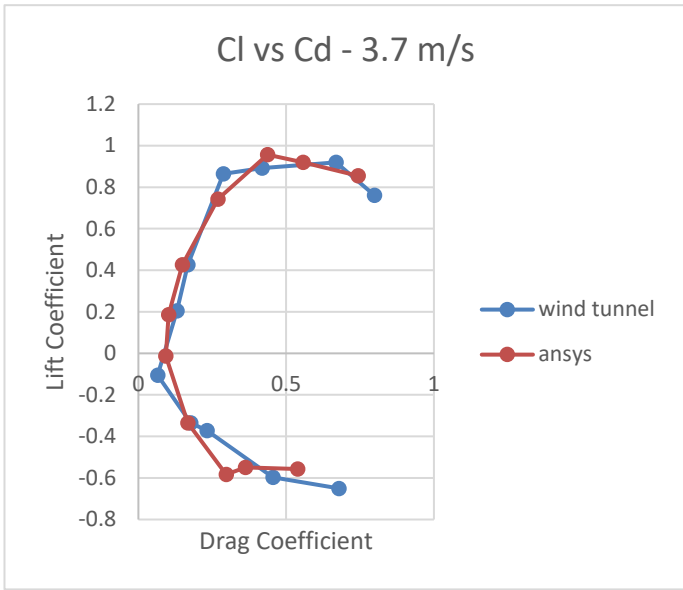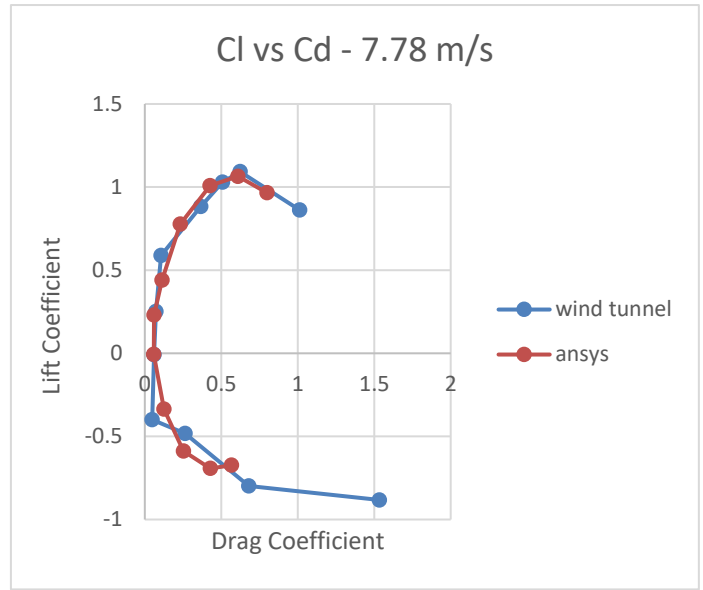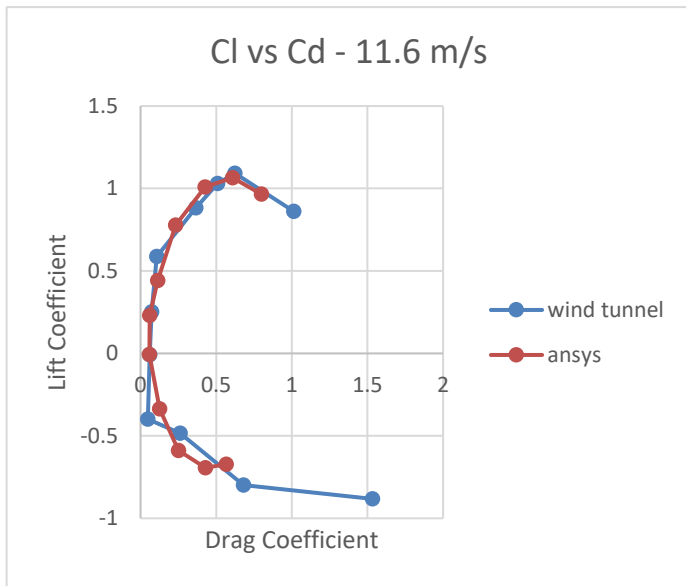

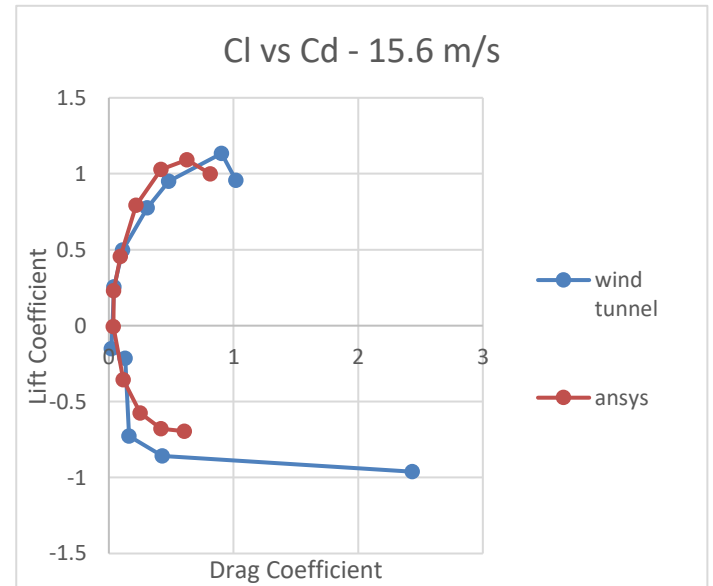*Figure 49 Cl vs Alpha comparison 11.6 m/s scale wing*

Figure 50 Cl vs Alpha comparison 15.6 m/s scale wing

.

Figure 51 Cd vs Alpha comparison 3.7 m/s scale wing

Figure 52 Cd vs Alpha comparison 7.78 m/s scale wing

Figure 53 Cd vs Alpha comparison 11.6 m/s scale wing

Figure 54 Cd vs Alpha comparison 15.6 m/s scale wing

.

Figure 55 Cl vs Cd comparison 3.7 m/s scale wing

Figure 56 Cl vs Cd comparison 7.78 m/s scale wing

Figure 57 Cl vs Cd comparison 11.6 m/s scale wing
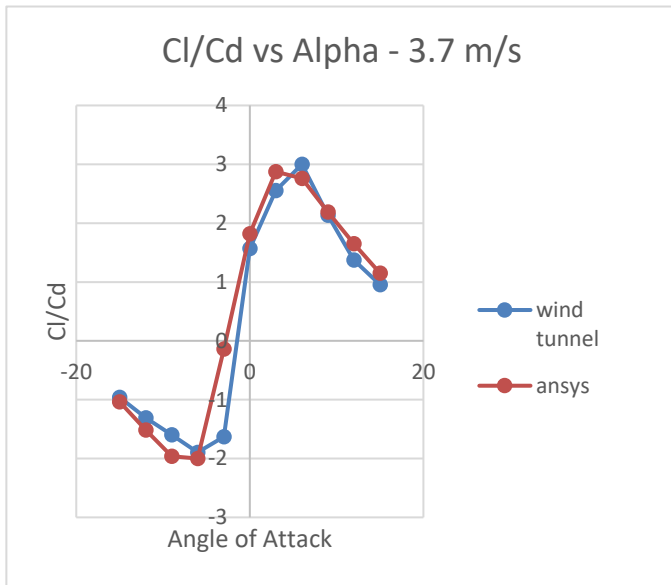

Figure 58 Cl vs Cd comparison 15.6 m/s scale

.

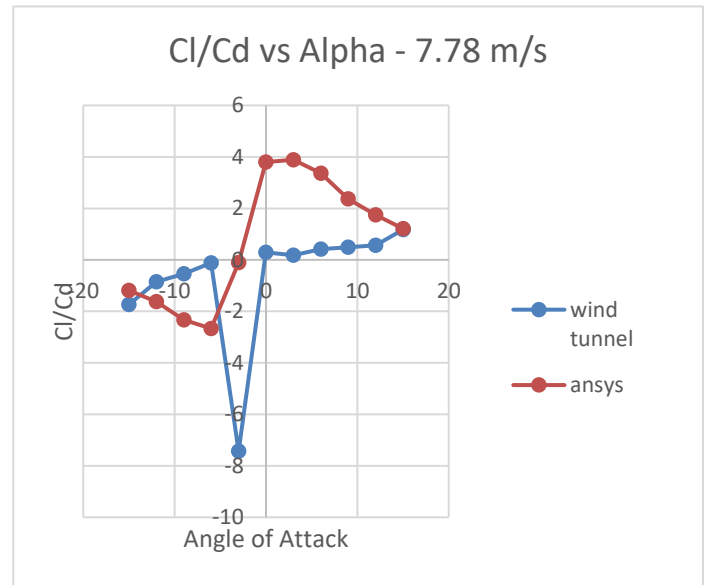*Figure 59 Cl/Cd vs Alpha comparison 3.7 m/s scale wing*
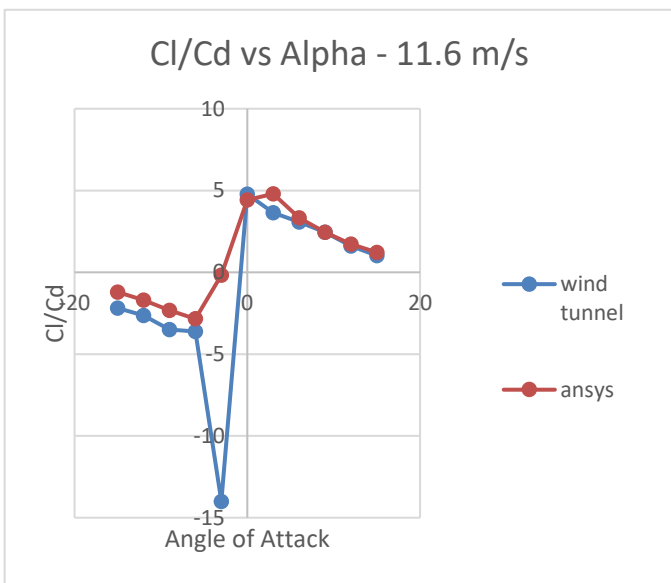

Figure 60 Cl/Cd vs Alpha comparison 7.78 m/s scale wing

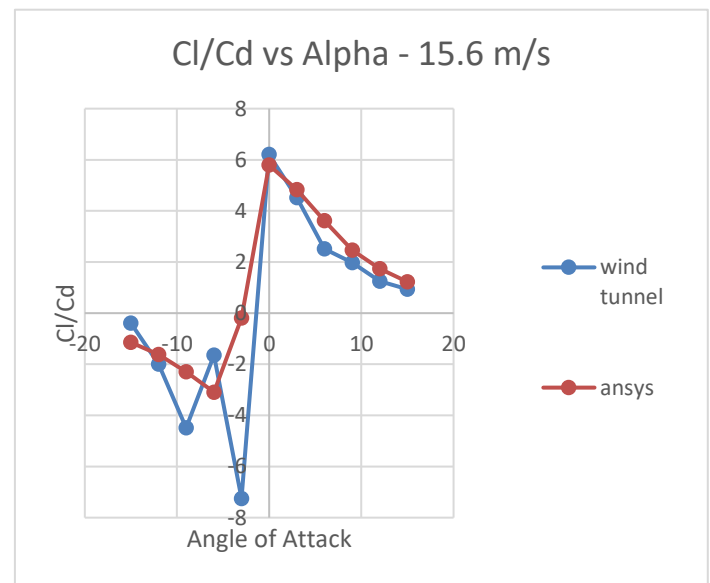*Figure 61 Cl/Cd vs Alpha comparison 11.6 m/s scale wing*

Figure 62 Cl/Cd vs Alpha comparison 15.6 m/s scale wing

Observing the graphs it is clear that the study was successful due to its high lift even though at high angles of attack.

Nevertheless, the comparison between the CFD and wind tunnel are quite similar except from a independent point that the dynamometer has read incorrectly (it is the bad for the dynamometer because the rest of the data in all the graphics are alike).

.

Chapter 9. EXTRAPOLATION FOR AN UAV APPLICATION

To proceed with the UAV design, a study was made about the best UAV in the aviation field. Their properties must count with a wide range, high action ratio and a powerful cruising speed among other qualities.

In continuation, a table has been made with the characteristics of some UAV that already exists and take inspiration and create a UAV with similarities from them.

As most of them are confidential projects, there was no possible to obtain all the data wanted.

MAIN CHARATERISTCS OF THE MOST KNOWN UAVS

	Length (m)	Wing span (m)	Height (m)	Void Weight (kg)	Max Take Off Weight (kg)	Engine configuration	Power (KW)	Cargo
MQ9 Reaper [25]	11	20	3.6	2 223	4 780	Garrett TPE331.	671	215 kg
MQ1 Predator [26]	8,23	14,84	2,1	512	1020	4 cylinder Rotax 912 or Rotax 914.	86	204 kg
Northrop Grumman RQ-4 [27]	13,54	35,41	4,7	3 851	6781	Rolls-Royce AE 3007	13	1 636,6 kg
Avenger (Predator C) [28]	13	20,1	2,7	-	8255	Turbofan Pratt & Whitney 545B.	7,24	1360 kg
EADS Talarion [29]	12	28	4,5	7 000	10 000	Turbojet	-	800 kg
INTA MILANO [30]	8,2	12,5	-	900	1150	Turbocharged four-stroke boxer engine.	-	150 kg

Table 16 Data information about the main characteristics of the most known UAVs

.

PERFORMANCE

	Max operative speed (km/h)	Cruising speed (km/h)	Range (km)	Endurance (hours)	Action ratio (km)	Service ceiling (m)
MQ9 Reaper	482	276-313	1900	28	1 850	15 000
MQ1 Predator	217	130-165	726	24	1100	7620
Northrop Grumman RQ-4	800	650	22 780	36	24 985	19 812
Avenger (Predator C)	740	647	-	18	2 900	15 240
EADS Talarion	630	500	1 700	20	-	3048-15 240 m
INTA MILANO	230	-		7-20	-	7800

Table 17 Data information about performance of the most famous UAVs

As it can be seen from the data collected, the Northrop Grumman aircraft is the one with better performance properties, though more fuel is needed and its dimensions are much than it is needed for the purpose of this project, then the most adequate qualities will be a UAV with some performance and characteristics similar to the MQ9 Reaper and MQ1 Predator.

For the design is concerned, as the study confirms the prototype of UAV is required for the mission proposed, it is proceeded to decide its dimensions and configuration.

.

9.1   UAV preliminar design

Regarding the many parts that conforms the entire design of the aircraft, the principal elements are the tail, fuselage, wing and engine position.

First goes the tail. There are a wide range of options as can be seen below. In this case the best choice is to take the one that corresponds with the example 2. Although the example 2 has more vibrations on the tip than the example 3, the weight is lower because of the intermediate horizontal tape. Also its centre of gravity is located forward than the example 3 and that implies a more stabilized aircraft.
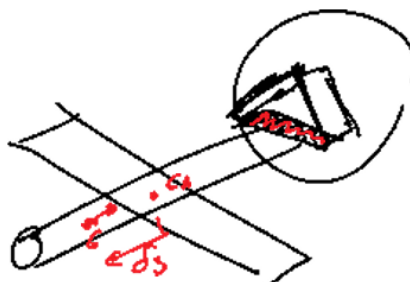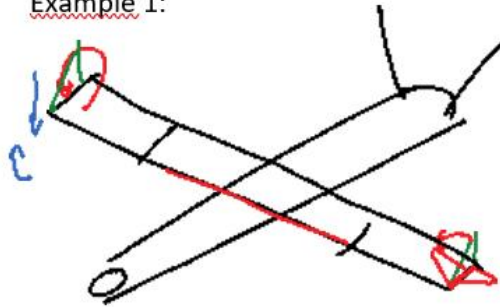
TAIL:

EXAMPLE 1:
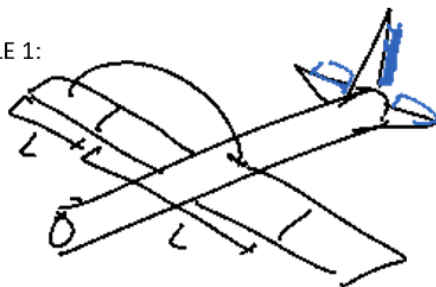
EXAMPLE 2:
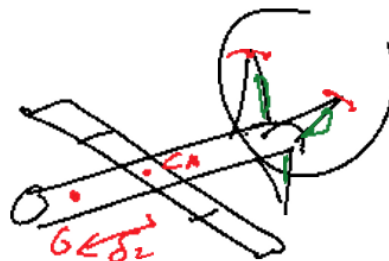
EXAMPLE 3:

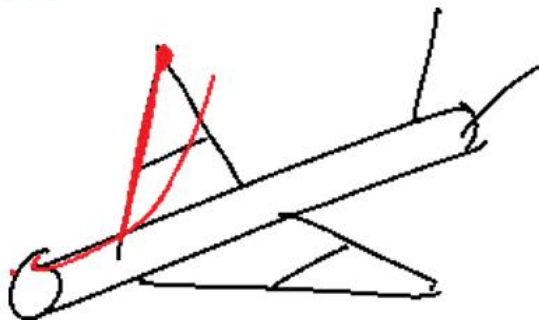*Figure 63 tail options for the UAV design*

.

Concerning the wing, the example 2 implies a complex design and calculation due to its sweep angle. The example 1 and 3 are easier for the running of calculation, but we go for the example 3 as it will have a better lift and less weight.
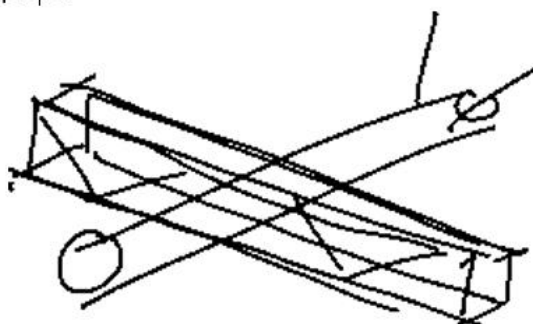
WING:

Example 1:

Example 2:

Example 3:

Figure 64 wing options for the UAV design

.

On one hand for the wing position, the best option is the example 1 due to is light weight and structural simplification. By the other hand the position of the wing at the top of the fuselage also implies a certain asymmetry between the low side of the wing and the up side because of the air contact on the surface will be different.

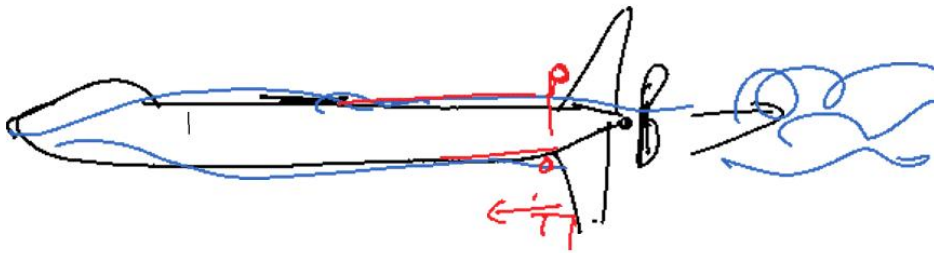FUSELAGE TYPE AND WING POSITION:

Example 1:

Example 2:

Example 3:

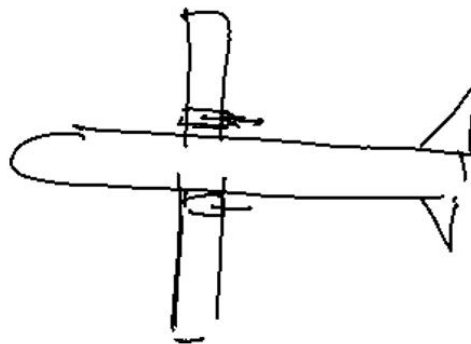*Figure 65 wing position options for the UAV design*

.

Finally the engine position has to be chosen. When the engines goes in the backward part of the aircraft creates more thrust than the engines situated at the front, therefore the best option is the example 1.

Engine postion in the aircraft:

Example 1:

Example 2:

Example 3:

Figure 66 engine position options for the UAV design

.

Now that all the options have been chosen reasonably, the sketch of the final design of the UAV is the next shown in the figure.
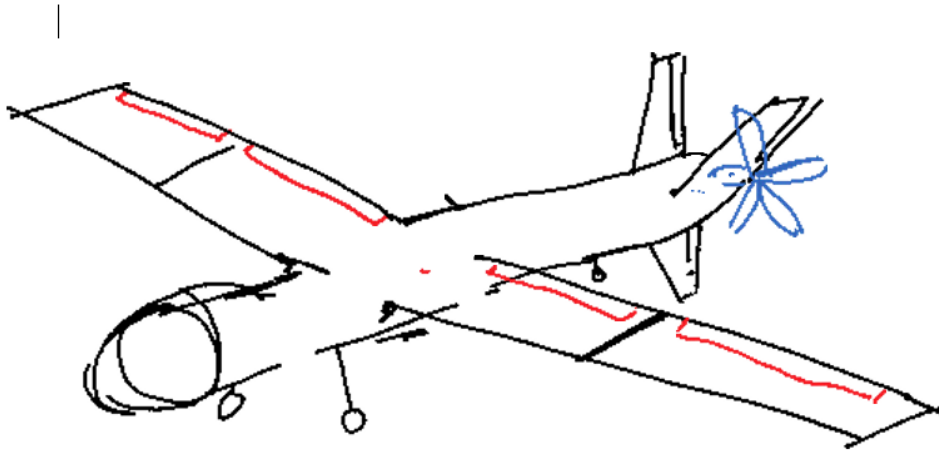
FINAL DESIGN:

Figure 67 final sketch hand drawing of the UAV design

To conclude the UAV design, these options are extrapolated to proceed with the design of the UAV in Catia, to have a professional result plus to later be able to introduce the aircraft in Ansys to run the CFD simulation.

The final measures are described in the table below.

	Length (m)	Wing span (m)	Height (m)	Chord (m)	Max Take Off Weight (kg)	Engine configuration	Power (KW)	Cargo
Final UAV	6,488	7,8	2,446	1,6	2750	Garrett TPE331.	671	122 kg

Table 18 main characteristics of the UAV

.

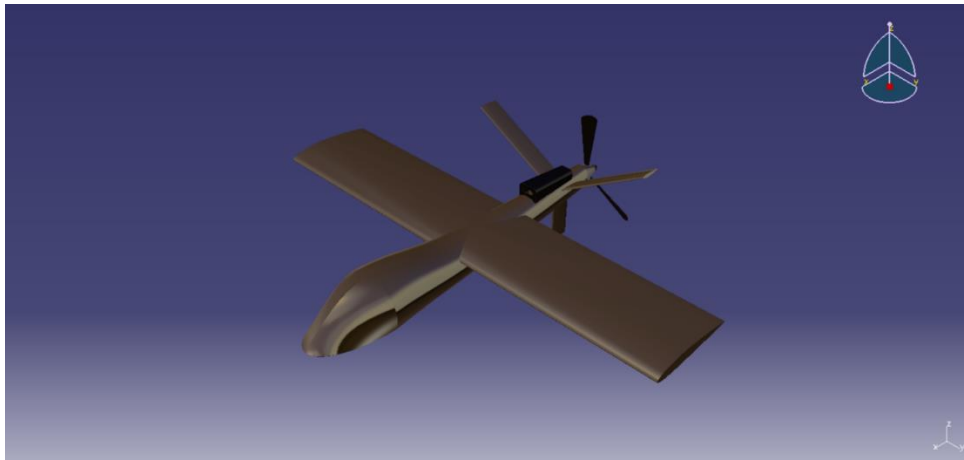Next are shown the final UAV made in Catia from all the different views:

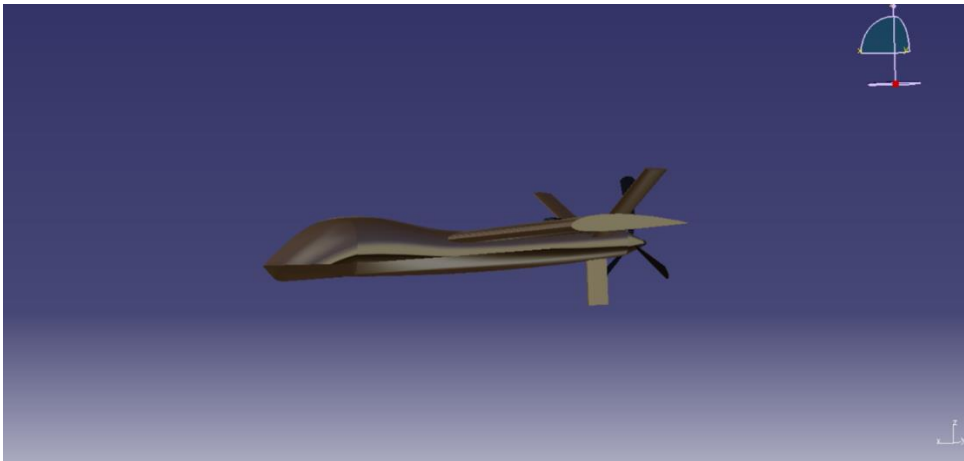*Figure 68 isometrical view of the UAV from Catia*
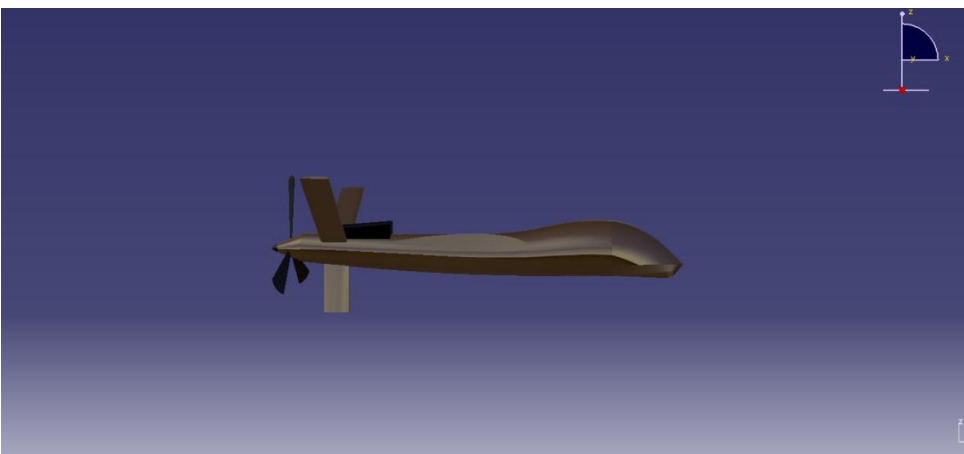

Figure 69 left view of the UAV from Catia

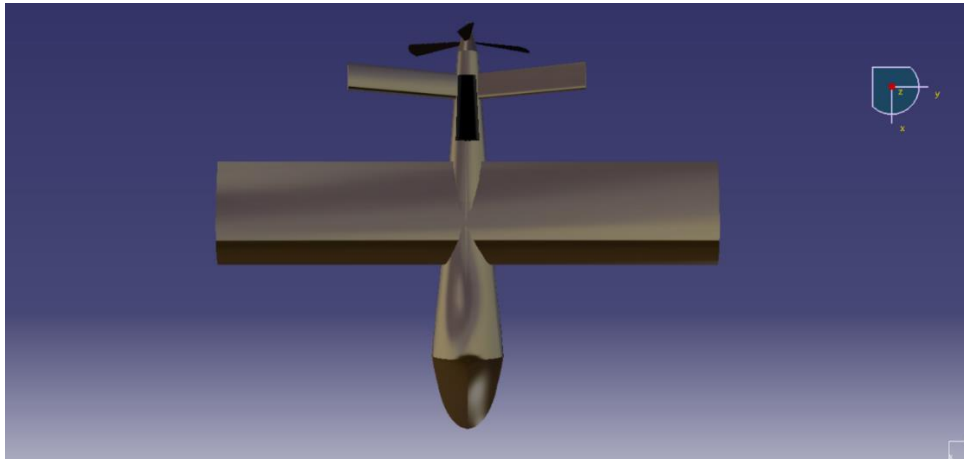*Figure 70 right view of the UAV from Catia*

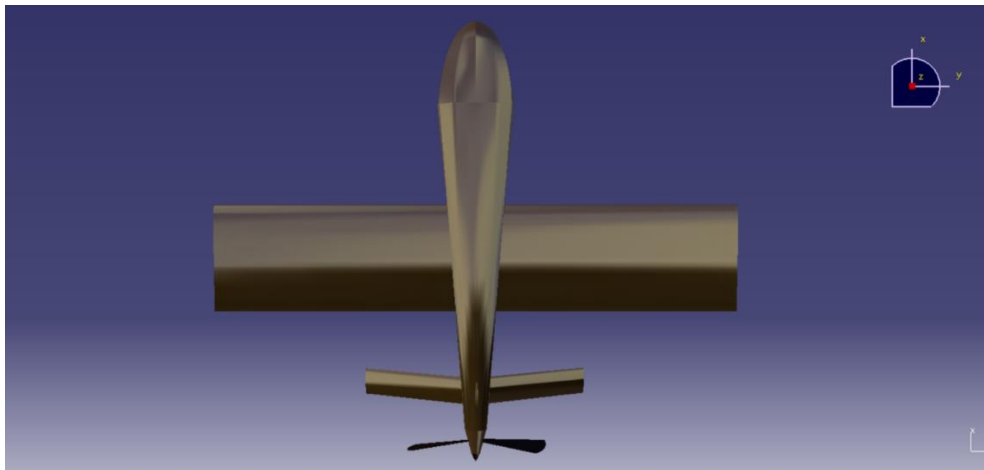*Figure 71 upside view of the UAV from Catia*

Figure 72 downside view of the UAV from Catia
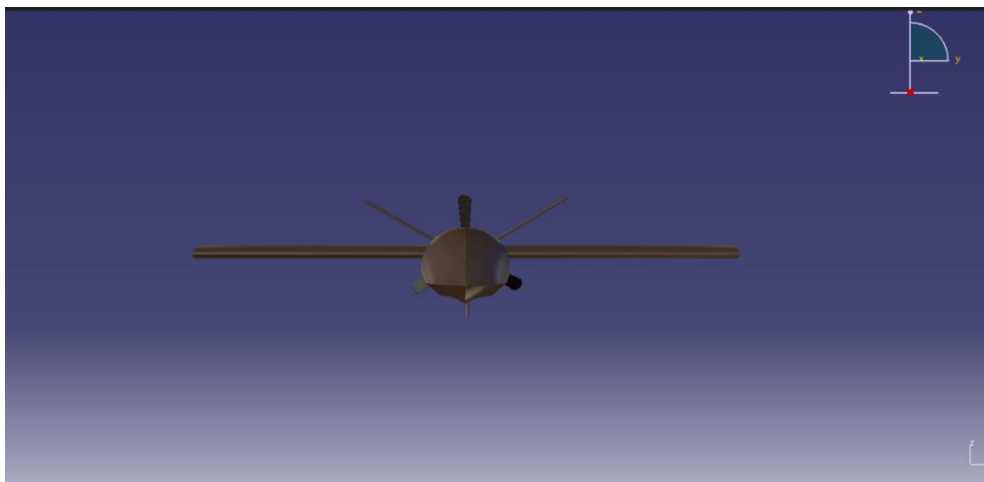
Figure 73 front view of the UAV from Catia

.

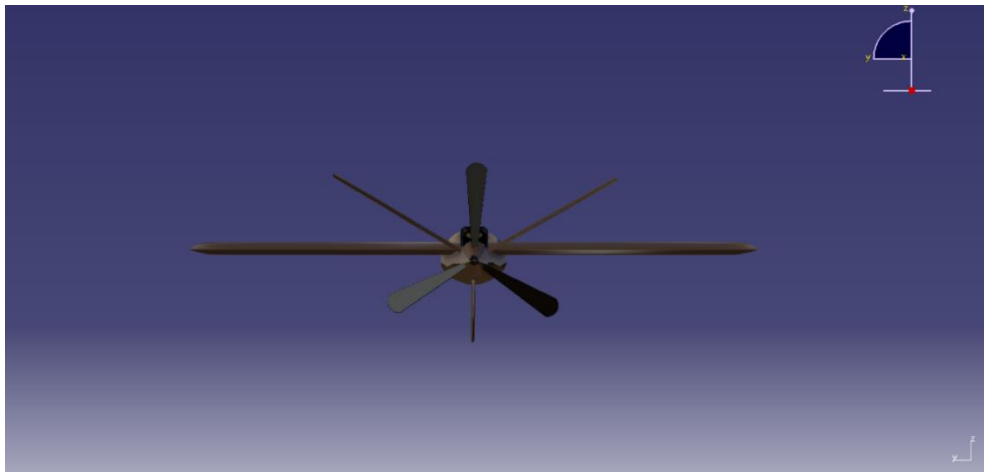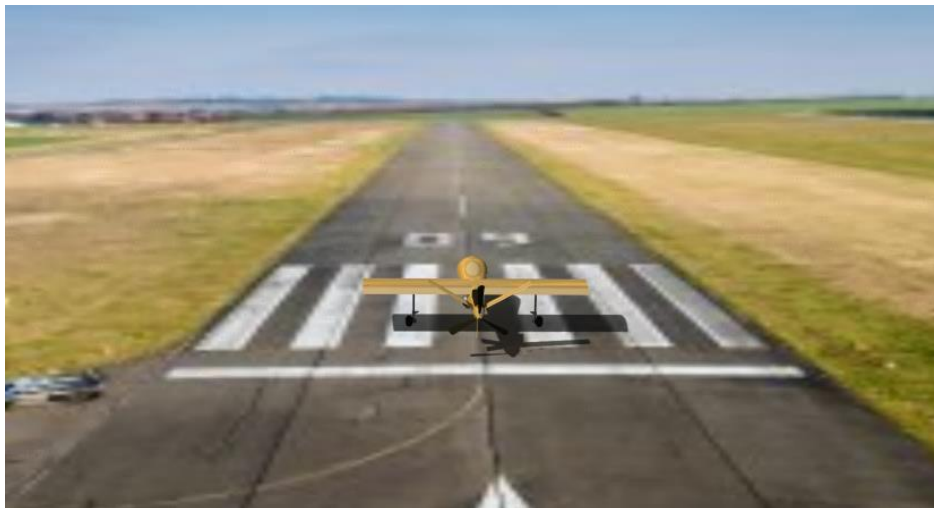*Figure 74 back view of the UAV from Catia*

Figure 75 renderization of the UAV from Catia in a runway

Figure 76 renderization of the UAV from Catia in a hangar and a person part 1

.

Figure 77 renderization of the UAV from Catia in a hangar and a person part 2

Figure 78 renderization of the UAV from Catia flying
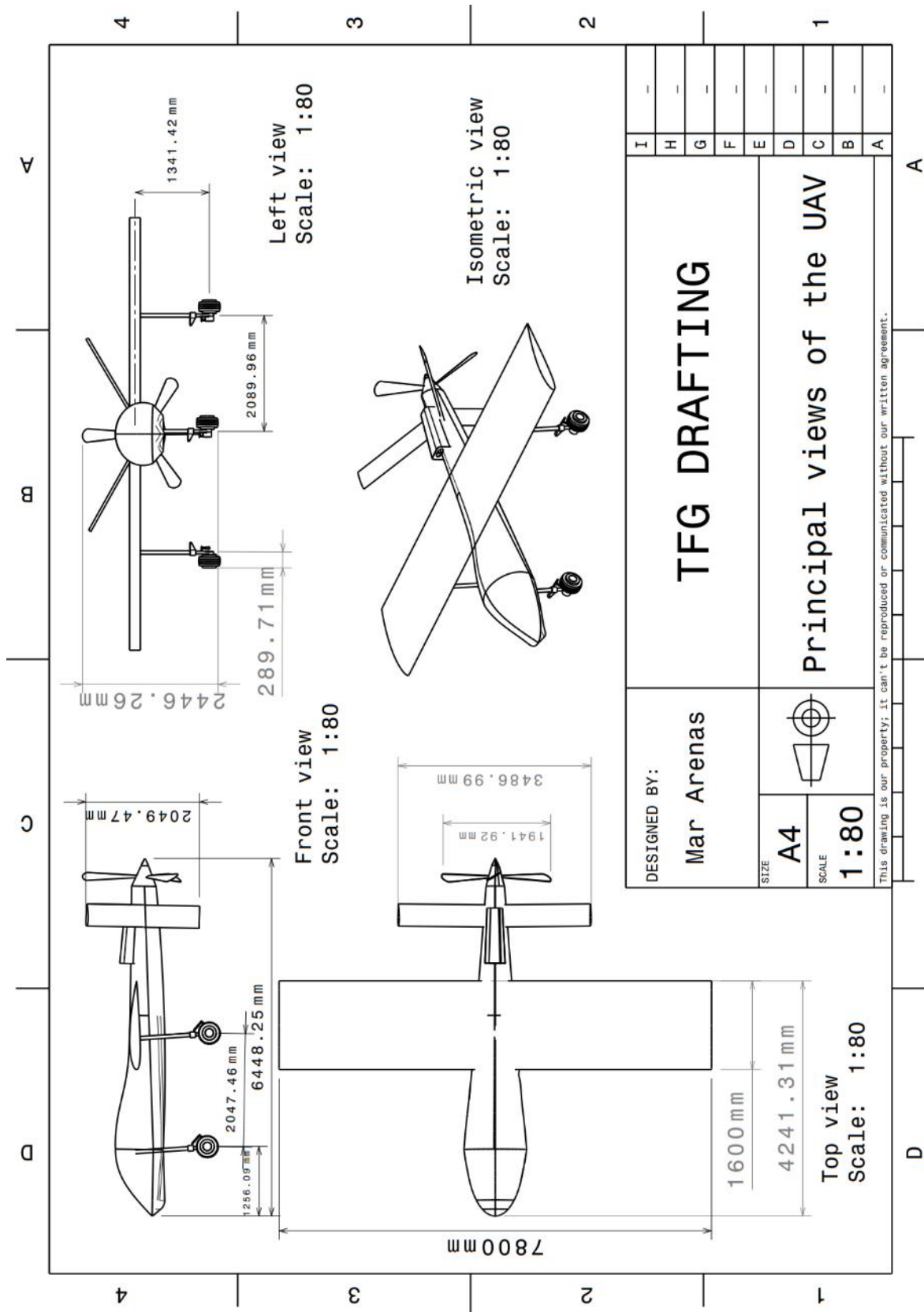
Figure 79 final sketch with measures and their units of the UAV from Catia

.

9.2   UAV CFD simulation in ANSYS

The CFD simulation of the UAV is necessary to prove its efficiency aerodynamically. The simulation was taken in laminar boundaries at its cruise speed of 96,6 m/s at an altitude of 6000 meters for the angles of attack from -5 degrees to 40 degrees.

It takes the same process as did previously with the real wing and scale wing.

First is shown the UAV in its command geometry of approximately 5 meters to be able to run the simulation properly.

Figure 80 UAV exported from Catia to Ansys
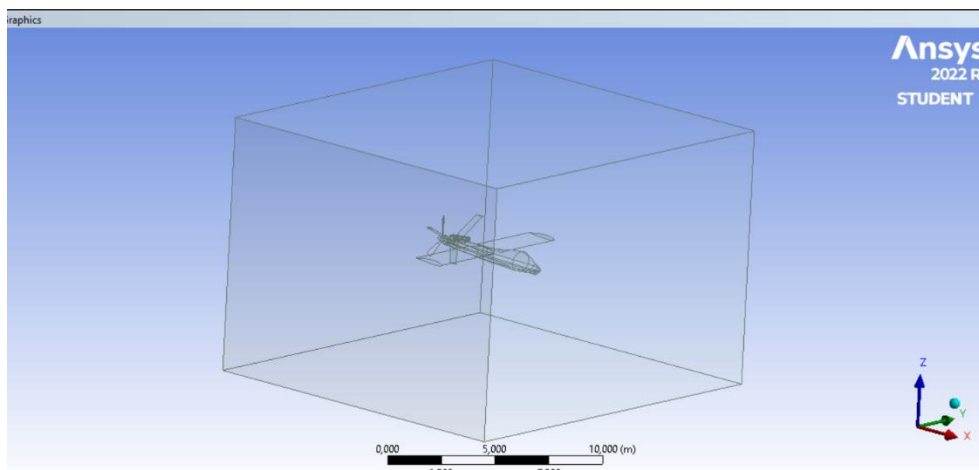
Figure 81 UAV command geometry to run the calculation part 1

.
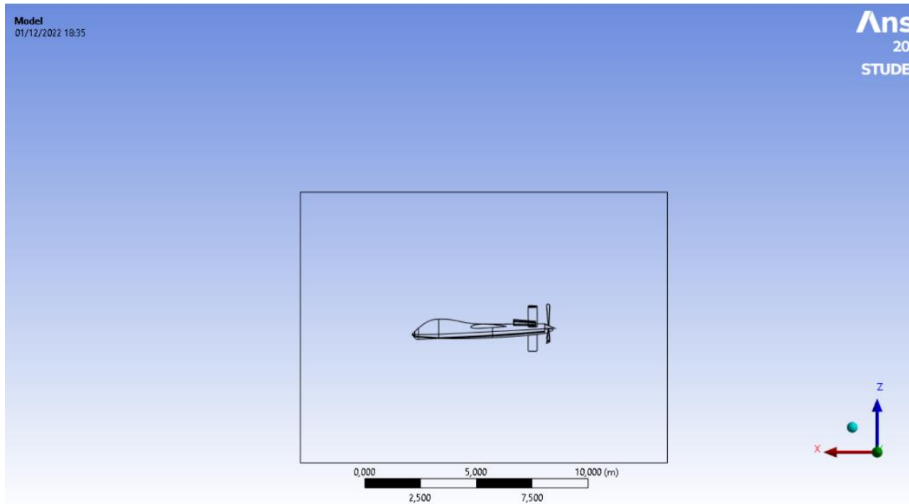
Figure 82 UAV command geometry to run the calculation part 2
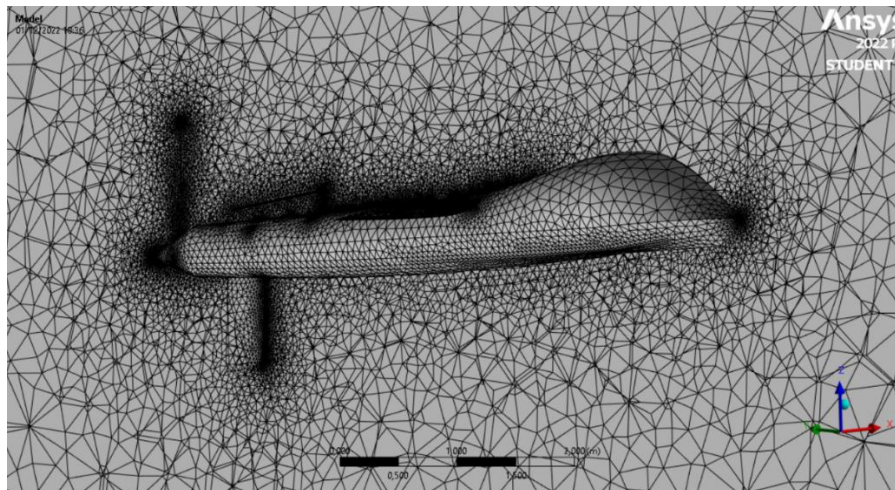
Figure 83 view of mesh from the inside of the UAV in Ansys

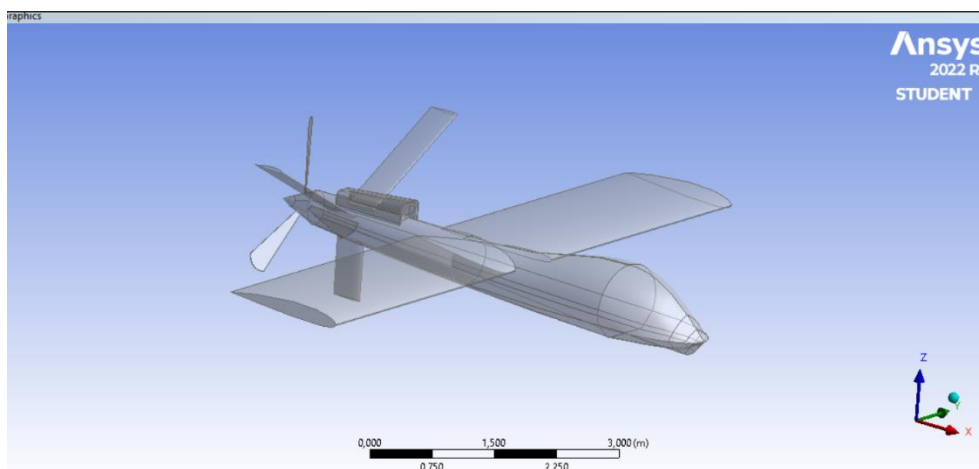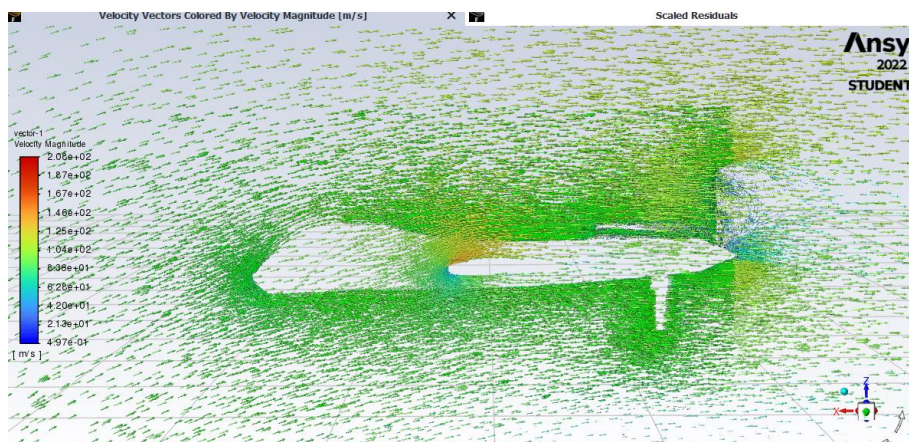*Figure 84 contour of velocity vector at an angle of attack of 15 degrees in Ansys*

.

In the previous images, as well as the preparation of the UAV for the running of the simulation, is found the mesh, the contour of velocity vectors at an angle of attack of 15 degrees as an example. Next images also show part of the process of the CFD in Ansys, as has been run so many simulations these are put in the report as some examples.

Figure 85 contour of static pressure at an angle of attack of 10 degrees in Ansys
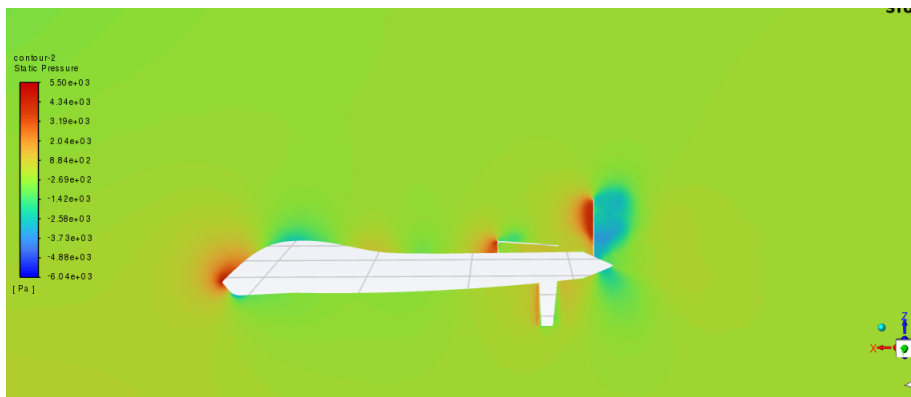
Figure 86 contour of static pressure at an angle of attack of -5 degrees in Ansys
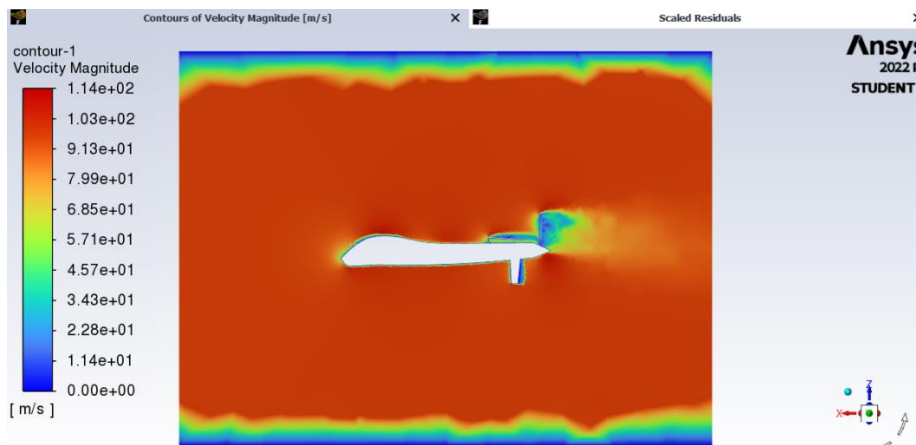
Figure 87 contour of velocity magnitude at an angle of attack of 0 degrees in Ansys

.

Once the run of the simulation is done, the results of the correspondent CL, CD and CL/CD are shown in the next table:

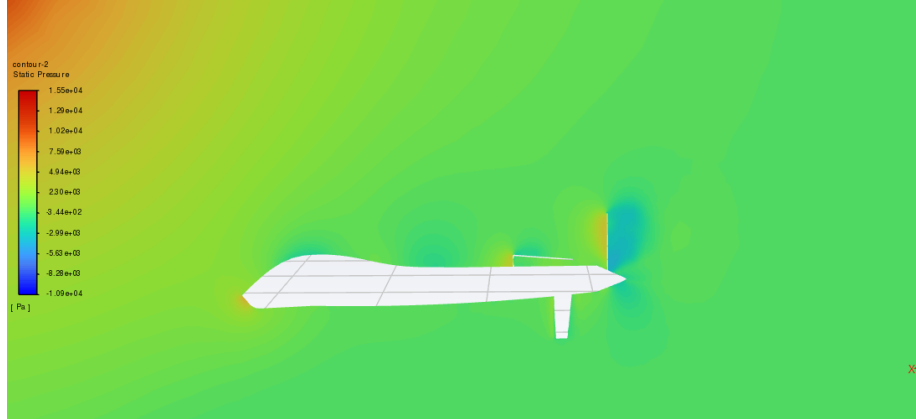| Velocity	Angle	Lift	Drag	Cl	Cd	Cl/Cd
96	-5	2,034.616	6,315.227	0.0542579	0.16841063	0.32217622
	0	4,158.767	6,170.891	0.11090347	0.16456156	0.67393303
	5	9,164.837	6,906.027	0.24440227	0.18416573	1.32707792
	10	14,260.573	8,469.321	0.38029227	0.22585469	1.68379175
	15	19,803.116	11,181.093	0.52809742	0.29817057	1.77112524
	20	27,700.550	15,603.541	0.73870138	0.41610572	1.77527332
	25	35,508.225	21,742.993	0.9469117	0.57982888	1.63308819
	30	47,574.036	31,179.761	1.26867539	0.83148286	1.52579861
	35	48,390.941	36,540.000	1.29046011	0.97442644	1.32432789
	40	46,321.977	40,845.566	1.23528624	1.08924465	1.13407602

Table 19 Data for Cl, Cd and Cl/Cd Ansys for the UAV

Figure 88 Graphic Cl vs Alpha results from Ansys for the UAV

.
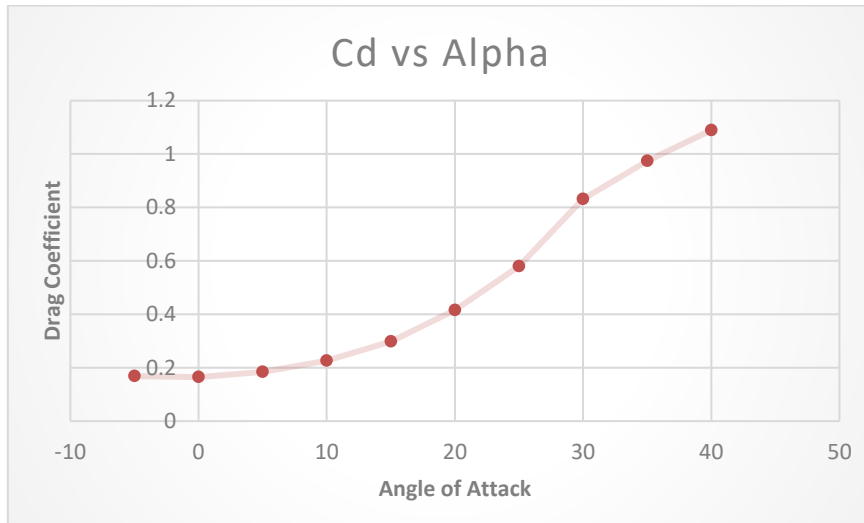
Figure 89 Graphic Cd vs Alpha results from Ansys for the UAV
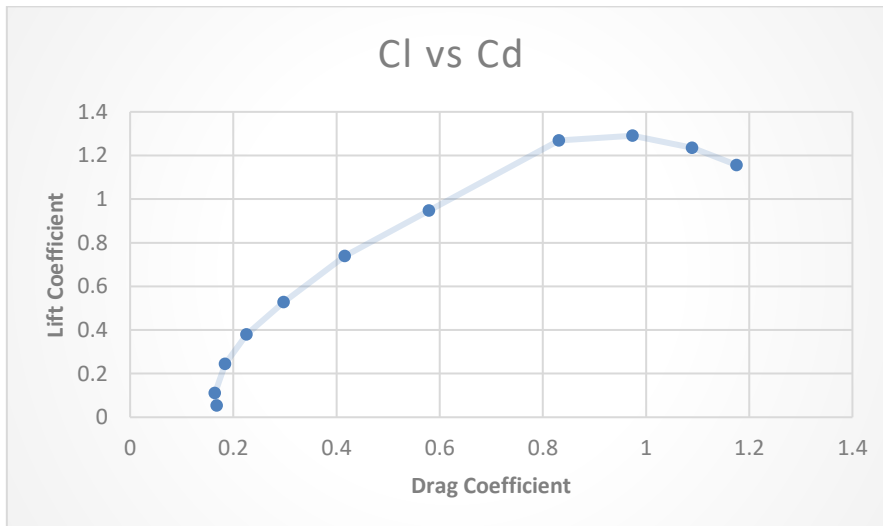
Figure 90 Graphic Cl vs Cd results from Ansys for the UAV
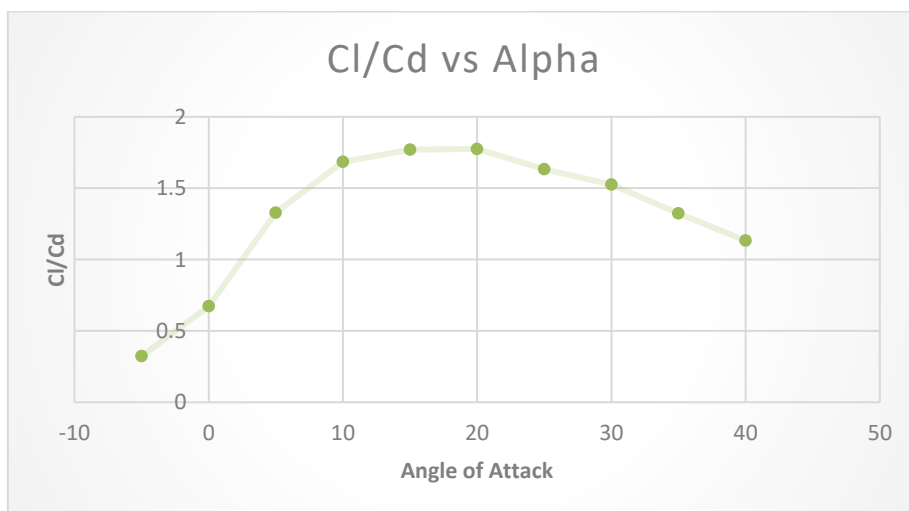
Figure 91 Graphic Cl /Cd vs Alpha results from Ansys for the UAV

.

Chapter 10.   CONCLUSIONS AND FUTURE WORK

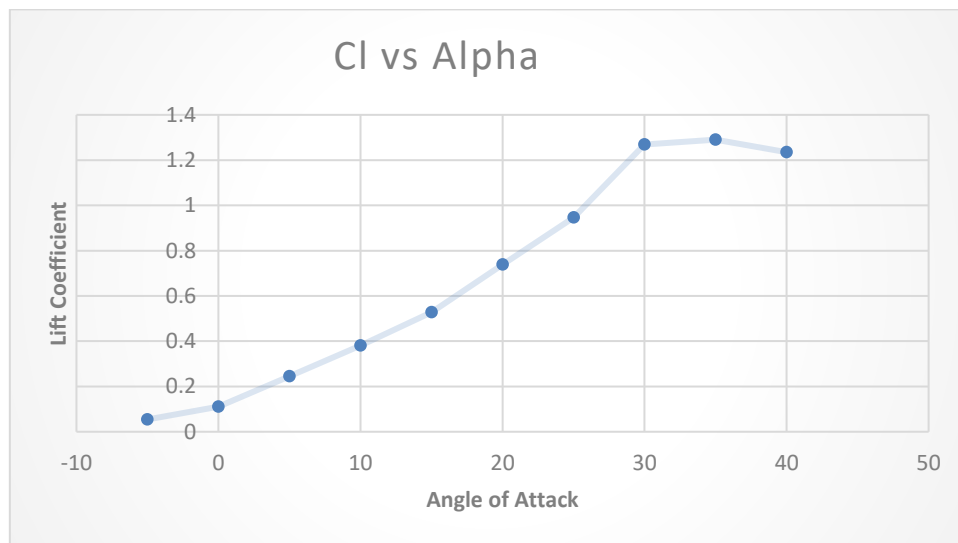Concerning all the CFD simulations run for the scale wing, real wing, wind tunnel test and UAV, their results are favourable to a better lift and stabilization at high angles of attack, even the negative angles of attack. This means the study was successful to keep this project to its further work and achieve its mission.

The next step would be to produce the UAV in scale plus doing the wind tunnel test and corresponding calculation involving its mass estimation of all the different parts that compounds the aircraft., manoeuvre limits, etc.

In the future it is quite probable to see this UAV searching and rescuing people at the stretch of Gibraltar as it was it mainly reason to create it, but also it is possible to see this aircraft in the law enforcement bodies of several countries to do the same task.

In a few years hopefully will be more common to see these types of UAV with electrical engines helping the fight against the climate change. This UAV also has a great capacity for cargo and would be able to fumigate the fire in the forest. This also would reduce the risk of the pilots and firefighter men.

There is a wide range of possibilities of missions and objectives for this UAV to carry us to a better future.

.

REFERENCES AND BIBLIOGRAPHY

1. *Unmanned aerial vehicle*. (s/f). Thefreedictionary.com. *Retrieved December 1, 2022, from* https://www.thefreedictionary.com/Unmanned+Aerial+Vehicle

2. *Wikipedia contributors. (2022, noviembre 28). Unmanned aerial vehicle. Wikipedia, The Free Encyclopedia. Retrieved December 1, 2022, from* https://en.wikipedia.org/w/index.php?title=Unmanned_aerial_vehicle&oldid=1124299112

3. Capacidad de bÃºsqueda Y rescate en tierra o mar para el gran UAV dominator XP. *(2021, October 8). Defensa.com. Retrieved December 1, 2022, from* https://www.defensa.com/industria/capacidad-busqueda-rescate-tierra-mar-para-gran-uav-dominator-xp

4. *De transportar droga a vigilar el Estrecho de Gibraltar: Así es el 'narcodrón' Que quiere la Policía para combatir a los traficantes*. (2021, July 13). *Retrieved December 1, 2022, from sevilla*. https://sevilla.abc.es/andalucia/malaga/sevi-transportar-droga-vigilar-estrecho-gibraltar-policia-quiere-narcodron-para-combatir-traficantes-202107132133_noticia.html

5. *Definición de aerodinámica - Definicion.de. (n.d.). Definición.de. Retrieved December 1, 2022, from* https://definicion.de/aerodinamica/

6. *Wood, A. (2017, August 1). Fundamental forces in flight. AeroToolbox. Retrieved December 1, 2022, from* https://aerotoolbox.com/forces-in-flight/

7. *Aeronautics Guide. (2017, May 17). Forces acting on the aircraft - aerodynamics of flight. Blogger. Retrieved December 1, 2022, from* https://www.aircraftsystemstech.com/2017/05/forces-acting-on-aircraft.html?m=1

.

8. *Irving, F. G. (1966). Preliminary considerations and definitions. In An Introduction to the Longitudinal Static Stability of Low-Speed Aircraft (pp. 6–25). Elsevier. Retrieved December 1, 2022, from*

   Aerodynamic Centre - an overview | ScienceDirect Topics

9. *Irving, F. G. (1966). Preliminary considerations and definitions. In An Introduction to the Longitudinal Static Stability of Low-Speed Aircraft (pp. 6–25). Elsevier. Retrieved December 1, 2022, from*

   Aerodynamic Centre - an overview | ScienceDirect Topics

10. *González, G.-C., & Miguel, L. (n.d.). Centro de presiones, centro aerodinámico y cuerda media aerodinámica. Upv.Es. Retrieved December 1, 2022, from*
    https://riunet.upv.es/bitstream/handle/10251/105209/Garc%c3%ada-Cuevas%3bCarreres%3bTiseira%20-%20Centro%20de%20presiones%2c%20centro%20aerodin%c3%a1mico%20y%20cuerda%20media%20aerodin%c3%a1....pdf?sequence=1&isAllowed=y

11. *Chord (aircraft). (n.d.). Airports-worldwide.com. Retrieved December 6, 2022, from*
    https://www.airports-worldwide.com/articles/article0520.php

12. *Chord (aircraft). (n.d.). Airports-worldwide.com. Retrieved December 6, 2022, from*
    https://www.airports-worldwide.com/articles/article0520.php

13. *Lift coefficient. (2021, July 20). Glenn Research Center | NASA; NASA Glenn Research Center. Retrieved December 6, 2022, from* https://www1.grc.nasa.gov/beginners-guide-to-aeronautics/lift-coefficient/

14. *Wikipedia contributors. (2022, December 4). Drag coefficient. Wikipedia, The Free Encyclopedia. Retrieved December 6, 2022, from*
    https://en.wikipedia.org/w/index.php?title=Drag_coefficient&oldid=1125593343

15. *Perfil NACA. (n.d.). Frwiki.Wiki. Retrieved December 7, 2022, from*
    https://es.frwiki.wiki/wiki/Profil_NACA

.

16. *naca drawing explanation - Bing. (n.d.). Bing.com. Retrieved December 7, 2022, from*

    https://www.bing.com/images/search?view=detailV2&ccid=osysuruV&id=8F86536295
    68361AC661B7EF0DE009EBC3C525D9&thid=OIP.osysuruVcJHt-
    S6O10rgCgHaDF&mediaurl=https%3a%2f%2fmuzamilali.com%2fwp-
    content%2fuploads%2f2020%2f02%2fIMG_6320.jpeg&cdnurl=https%3a%2f%2fth.bi
    ng.com%2fth%2fid%2fR.a2ccacbabb957091edf92e8ed74ae00a%3frik%3d2SXFw%25
    2bsJ4A3vtw%26pid%3dImgRaw%26r%3d0&exph=309&expw=743&q=naca+drawing
    +explanation&simid=608025957854240201&FORM=IRPRST&ck=3F46F620BA4116
    7520E980094EA724F3&selectedIndex=11&mode=overlay

17. *All the formulas has been extracted from Aerodynamic and Aeroelasticity subject
    imparted by the professor Jose Omar Martinez. Retrieved October 14, 2022, from*

18. *NACA 1410 (naca1410-il). (n.d.). Airfoiltools.com. Retrieved December 7, 2022, from*
    http://airfoiltools.com/airfoil/details?airfoil=naca1410-il

19. *Airfoil Tools. (2019). NACA 2412 (naca2412-il). Airfoiltools.com. Retrieved December
    7, 2022, from* http://airfoiltools.com/airfoil/details?airfoil=naca2412-il

20. *NACA 4424 (naca4424-il). (n.d.). Airfoiltools.com. Retrieved December 7, 2022, from*
    http://airfoiltools.com/airfoil/details?airfoil=naca4424-il

21. *NACA 4418 (naca4418-il). (n.d.). Airfoiltools.com. Retrieved December 7, 2022, from*
    http://airfoiltools.com/airfoil/details?airfoil=naca4418-il

22. *NACA 6412 (naca6412-il). (n.d.). Airfoiltools.com. Retrieved December 7, 2022, from*
    http://airfoiltools.com/airfoil/details?airfoil=naca6412-il

23. *NACA 4 digit airfoil generator (NACA 2412 AIRFOIL). (n.d.). Airfoiltools.com.
    Retrieved December 7, 2022, from* http://airfoiltools.com/airfoil/naca4digit

24. *Túnel de Viento. (n.d.). Universidad Europea Retrieved December 7, 2022,
    from.* https://universidadeuropea.com/tu-experiencia/instalaciones/tunel-de-viento-
    madrid/

25. *Wikipedia contributors. (2022, December 7). General Atomics MQ-9 Reaper.
    Wikipedia, The Free Encyclopedia.*

.

https://en.wikipedia.org/w/index.php?title=General_Atomics_MQ-9_Reaper&oldid=1126028426

26. *Wikipedia contributors. (2022c, December 8). General Atomics MQ-1 Predator. Wikipedia, The Free Encyclopedia. Retrieved December 8, 2022, from* https://en.wikipedia.org/w/index.php?title=General_Atomics_MQ-1_Predator&oldid=1126245919

27. *Wikipedia contributors. (2022a, November 9). Northrop Grumman RQ-4 Global Hawk. Wikipedia, The Free Encyclopedia. Retrieved Retrieved December 8, 2022, from* https://en.wikipedia.org/w/index.php?title=Northrop_Grumman_RQ-4_Global_Hawk&oldid=1120909267

28. *Predator C Avenger. (n.d.). General Atomics Aeronautical Systems Inc. Retrieved December 8, 2022, from* https://www.ga-asi.com/remotely-piloted-aircraft/predator-c-avenger

29. *Wikipedia contributors. (2022, October 25). EADS Talarion. Wikipedia, The Free Encyclopedia. Retrieved December 8, 2022, from* https://en.wikipedia.org/w/index.php?title=EADS_Talarion&oldid=1118068623

30. *Wikipedia contributors. (n.d.). INTA Milano. Wikipedia, The Free Encyclopedia. Retrieved December 8, 2022, from* https://es.wikipedia.org/w/index.php?title=INTA_Milano&oldid=144347860

.

ANNEXES

A. Source code for the calculation of the 4 digits NACA airfoil

```
(*Cálculo de un perfil NACA MPT*)
Clear[M]
  borra
Clear[P]
  borra
Clear[T]
  borra
Clear[cc]
  borra
Clear[α]
  borra
M = 2;
P = 4;
T = 12;

cc = 1;
α = 0;




(*Variables auxiliares*)
αrad = α * Pi / 180;
          número pi
(*PASO 1: DEFINIR LAS ECUACIONES*)
(*ecuacion 1*)
eq1 = M / (P^2) * ((2 P / 10) * (x / cc) - (x / cc)^2) // N;
                                          valor numérico

eq1r = M / (P^2) * ((2 P / 10) * (x / c) - (x / c)^2) // N;
                                         valor numérico

eq2 = M / ((10 - P)^2) * ((1 - 2 * P / 10) + (2 * P / 10) * (x / cc) - (x / cc)^2) // N;
                                                                  valor numérico

eq2r = M / ((10 - P)^2) * ((1 - 2 * P / 10) + (2 * P / 10) * (x / c) - (x / c)^2) // N;
                                                                 valor numérico

(*PASO 2: DERIVAR LAS ECUACIONES*)
Deq1 = Expand[D[eq1, x]];
       expand··· deriva
Deq1r = Expand[D[eq1r, x]];
        expand··· deriva
Deq2 = Expand[D[eq2, x]];
       expand··· deriva
Deq2r = Expand[D[eq2r, x]];
        expand··· deriva
```

.

```
(*PASO 3: Cambio de Variable*)
x = cc / 2 * (1 - Cos[θ]);
                |coseno
xres = c / 2 * (1 - Cos[θ]);
                  |coseno
Deq1 = Simplify[cc * Deq1];
        |simplifica
Deq2 = Simplify[cc * Deq2];
        |simplifica
Clear[x]
|borra
```

```
(*PASO4* Limite de integracion^*)

θ1 = ArcCos[1 - P / 5] // N;
     |arco coseno        |valor numérico
```

```
(*PASO 5= Integramos*)

A0 = αrad - 1 / Pi * (Integrate[Deq1, {θ, 0, θ1}] + (Integrate[Deq2, {θ, θ1, Pi}]));
            |n···  |integra                      |integra                |número pi
A1 = 2 / Pi * (Integrate[Deq1 * Cos[θ], {θ, 0, θ1}] + (Integrate[Deq2 * Cos[θ], {θ, θ1, Pi}]));
        |n··· |integra        |coseno              |integra        |coseno          |número pi
A2 = 2 / Pi * (Integrate[Deq1 * Cos[2 θ], {θ, 0, θ1}] + (Integrate[Deq2 * Cos[2 θ], {θ, θ1, Pi}]));
        |n··· |integra        |coseno              |integra        |coseno          |número pi
```

```
(*PASO 6: Obtener los Coeficientes*)
Cl = Simplify[2 * Pi * (A0 + A1 / 2)] // N;
     |simplifica    |número pi            |valor numérico
Cmca = Pi / 4 * (A2 - A1) // N;
       |número pi         |valor numérico
Xcp = cc / 4 * (1 + - (Pi / Cl) * (A1 - A2)) // N;
                     |número pi            |valor numérico
CmLE = - (Cl / 4 + Pi / 4 * (A1 - A2)) // N;
                   |número pi          |valor numérico
```

```
(*PASO FINAL= Interpretación de resultados, y graficos*)

yc = Piecewise [{{eq1, x < P / 10 * cc}, {eq2, x > P / 10 * cc}}];
     |función a trozos
yt = (T / 100) / 0.2 * (0.2969 * Sqrt[x] - 0.1260 * x - 0.3516 * x^2 + 0.2843 * x^3 - 0.1015 * x^4);
                              |raíz cuadrada
ytder = Simplify[D[yc, x]];
        |simplifica |deriva
β = ArcTan[ytder];
    |arco tangente
(*Coordenadas de la cara superior*)

yu = yc + yt * Cos[β];
             |coseno
(*Coordenadas de la cara inferior*)

yl = yc - yt * Cos[β];
             |coseno
(** NO TERMINADO**)

graficoperfil = Plot[{yu, yl, yc}, {x, 0, cc}];
                |representación gráfica
```

.

```
(*RESULTADOS*)

Print["DATOS PARA EL PERFIL NACA ", M, P, T]
escribe
Print["α (Ángulo de Ataque)= ", α, " °"]
escribe
Print["C (cuerda) = ", cc, " m"]
escribe
Print[""]
escribe
Print["Ecuaciones del perfil:"]
escribe
Print["z1/c = ", eq1r]
escribe
Print["z2/c = ", eq2r]
escribe
Print[" "]
escribe
Print["PASO 1: DERIVADAS"]
escribe
Print["d(z1/c)/dx= ", Deq1r]
escribe
Print["d(z2/c)/dx= ", Deq2r]
escribe
Print["PASO 2: CAMBIO DE VARIABLE"]
escribe
Print["x = ", xres]
escribe
Print[""]
escribe
Print["PASO 3: SUSTITUIR EN LAS DERIVADAS, Y ARREGLAR"]
escribe
Print["d(z1)/dx= ", Deq1]
escribe
Print["d(z2)/dx= ", Deq2]
escribe

Print[""]
escribe
Print["PASO 4: LIMITES DE INTEGRACION DE LA VARIABLE θ"]
escribe
Print["I1: θ = [0 ; ", θ1, " ] rad"]
escribe
Print["I2: θ = [ ", θ1, " , ", Pi, " ] rad"]
escribe                          número pi

Print[""]
escribe
```

.

```
Print["PASO 5: INTEGRALES"]
```

$$\text{Print}\left["A0 = \alpha\ -1/\pi\ \cdot\left(\int_0^{\theta_1}\ ("\ ,\ \text{Deq1},\ ")\cdot\ d\theta\ +\ \int_{\theta_1}^{\pi}\ ("\ ,\ \text{Deq2},\ ")\cdot d\theta\ )\ =\ ",\ A0\right]\right.$$

$$\text{Print}\left["A1 = 2/\pi\ \cdot\left(\int_0^{\theta_1}\ ("\ ,\ \text{Deq1},\ ")\cdot\text{Cos}(\theta)\cdot d\theta\ +\ \int_{\theta_1}^{\pi}\ ("\ ,\ \text{Deq2},\ ")\cdot\text{Cos}(\theta)\cdot d\theta\ )\ =\ ",\ A1\right]\right.$$

$$\text{Print}\left["A2 = 2/\pi\ \cdot\left(\int_0^{\theta_1}\ ("\ ,\ \text{Deq1},\ ")\cdot\text{Cos}(2\theta)\cdot d\theta\ +\ \int_{\theta_1}^{\pi}\ ("\ ,\ \text{Deq2},\ ")\cdot\text{Cos}(2\theta)\cdot d\theta\ )\ =\ ",\ A2\right]\right.$$

```
Print["A0 = ", A0]

Print["A1 = ", A1]

Print["A2 = ", A2]


Print[""]

Print["PASO 6: RESULTADOS"]

Print["Cl (coef. sust) = 2·π·(A0+A1/2) = ", Cl]

Print["Cm,ac (coef. momentos centro aerod.) = π/4·(A2-A1) = ", Cmca]

Print["Cm,le (coef. momentos borde ataque) = -[Cl/4 + π/4·(A1-A2)] = ", CmLE]

Print["X,ca (centro aerodinamico) = c/4 = ", cc/4 // N, " m"]

Print["X,cp (centro presiones) = c/4·(1-(π/Cl)*(A1-A2))= ", Xcp, " m"]

Print[""]


graficoperfil
```
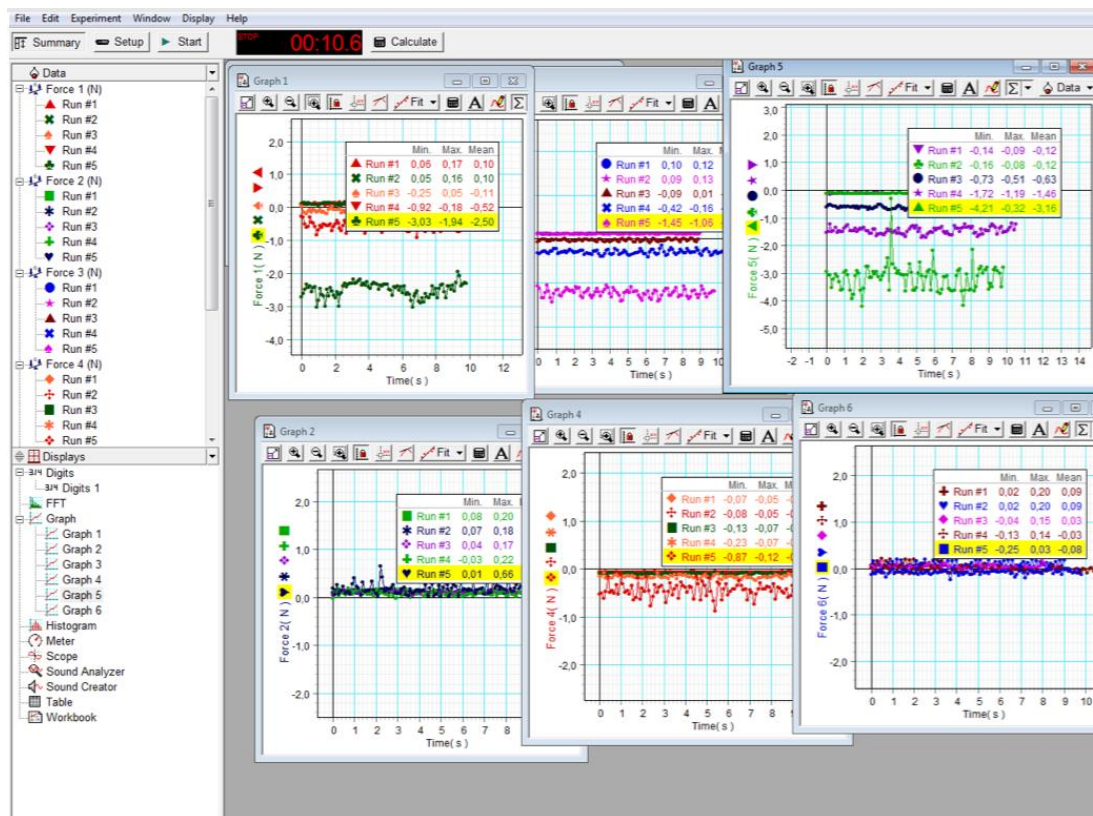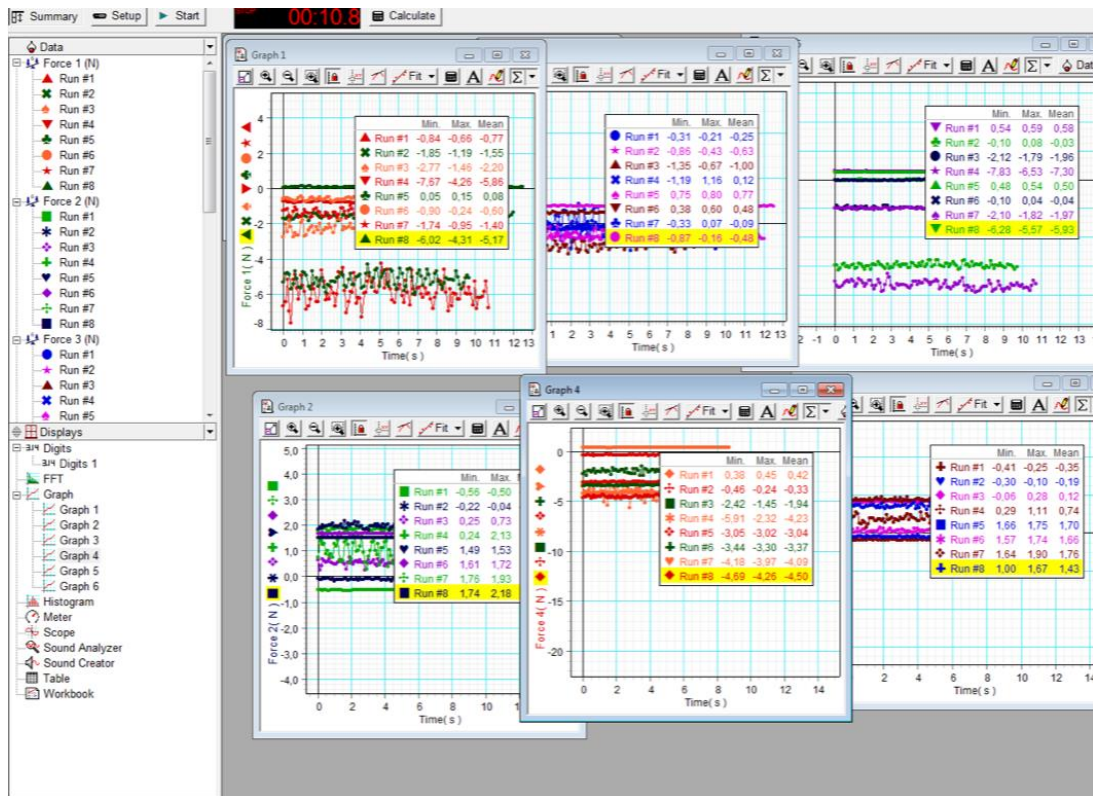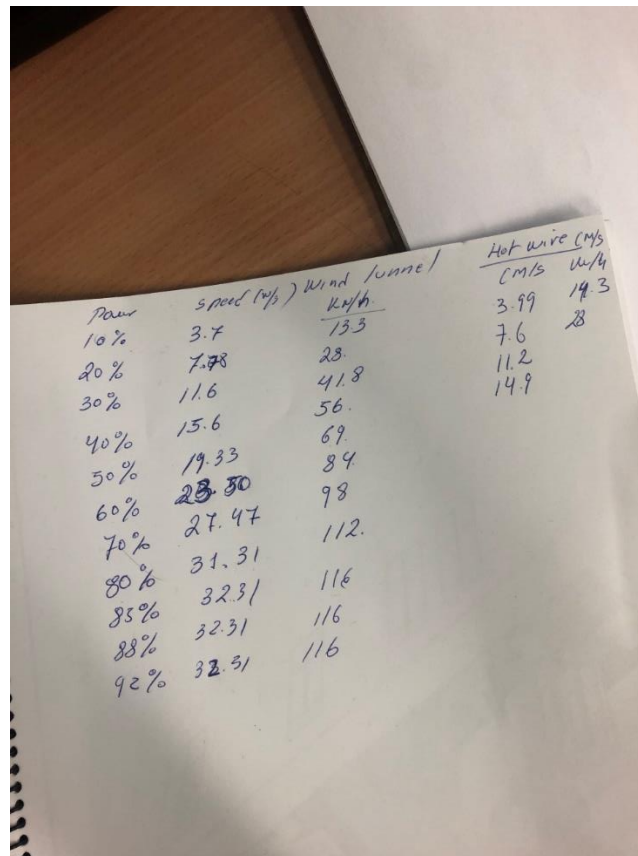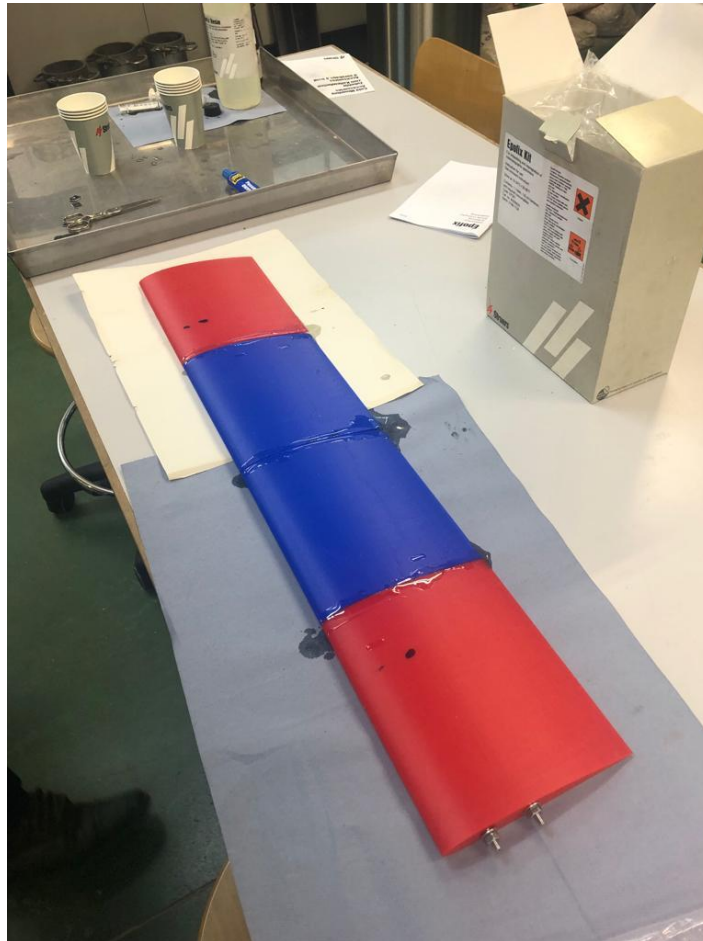
.

B. Wind tunnel test photos of the lift and drag results

.

.

.

.

Information of the speeds of the wind tunnel located in Universidad Europea de Madrid

.

C. First attempt of the printing and sticking the scale wing

C. First attempt of the printing and sticking the scale wing

.
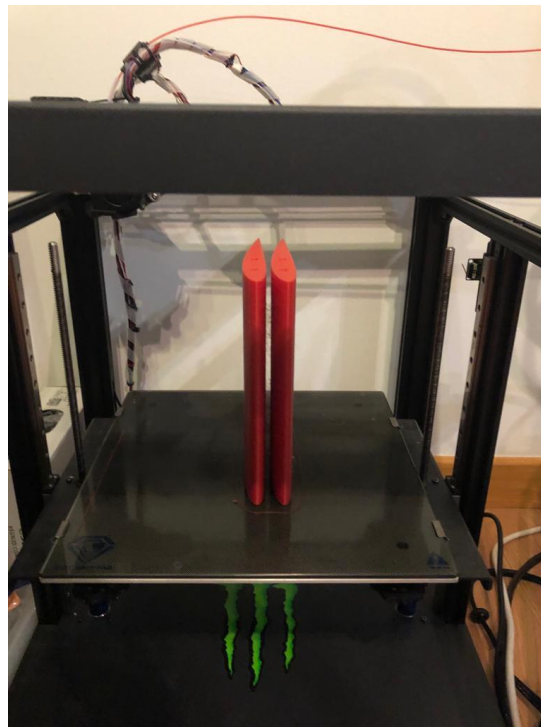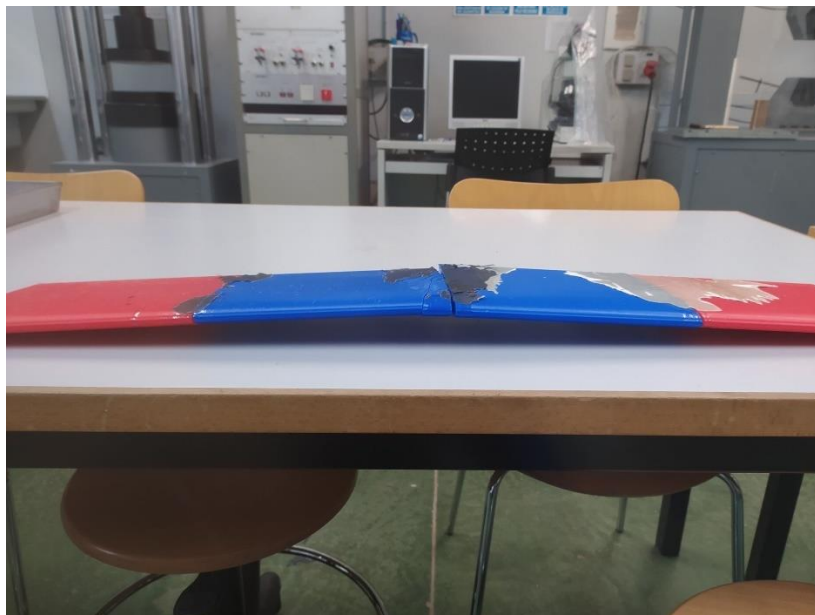
The first attempt in the printing went well, the wing was divided into 4 parts to later sticking it. It went wrong in the process of letting it dry because at the time that was thought that the wing was ready to be tested, in the making of grabbing it stayed the way is shown in the image before. Maybe was due to the bad mixture of the epoxy resin and/or not letting it dry enough time. For the second time the method of sticking was more thoughtful and it went well.